



Doctoral Thesis

ATMOSPHERIC CYCLONE TRACKS AND LARGE SCALE PRECIPITATION UNDER CLIMATE CHANGE CONDITIONS

submitted in satisfaction of the requirements for the degree of
Doctor of Science
of the Vienna University of Technology, Faculty of Civil Engineering

Dissertation

ATMOSPHÄRISCHE ZUGBAHNEN VON TIEFDRUCKGEBIETEN UND GROSSFLÄCHIGER NIEDERSCHLAG IM KLIMAWANDEL

ausgeführt zum Zwecke der Erlangung des akademischen Grades eines
Doktors der technischen Wissenschaften
eingereicht an der Technischen Universität Wien, Fakultät für Bauingenieurwesen
von

Mag. Michael Hofstätter
Matrikelnummer 0300993
Propst-Führer-Str. 42/8, AT-3100 Sankt Pölten

Gutachter: Univ. Prof. Dipl.-Ing. Dr. techn. Günter Blöschl
Institut für Wasserbau und Ingenieurhydrologie
Technische Universität Wien
Karlsplatz 13/222, A-1040 Wien

Gutachter: Univ. Prof. Dr. rer. nat. Bodo Ahrens
Institut für Atmosphäre und Umwelt
Goethe-Universität Frankfurt am Main
Altenhöferallee 1, D-60438 Frankfurt am Main

Gutachter: Univ. Prof. Dr.-Ing. Bruno Merz
Institut für Erd- und Umweltwissenschaften
Universität Potsdam
Telegrafenberg, D-14473 Potsdam

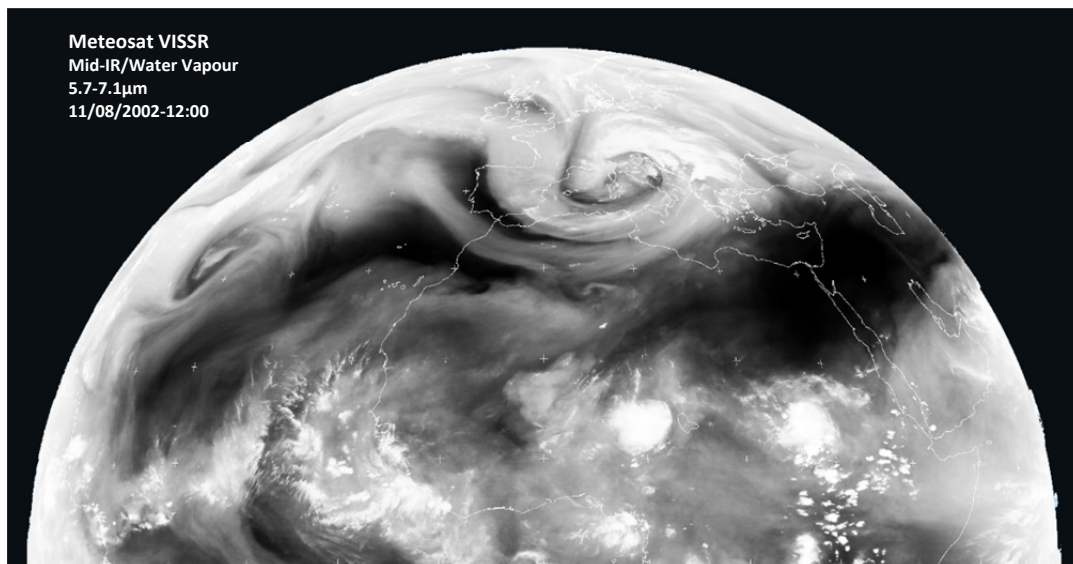
Parts of the present work have been published or are under review in peer reviewed journals:

Hofstätter, M., & Blöschl, G. Vb cyclones synchronized with the North Atlantic-/Arctic Oscillation. *Journal of Geophysical Research: Atmospheres*. (under review).

Hofstätter, M., Lexer, A., Homann, M., & Blöschl, G. (2018). Large-scale heavy precipitation over central Europe and the role of atmospheric cyclone track types. *International Journal of Climatology*, 38, e497–e517. doi.org/10.1002/joc.5386.

Hofstätter, M., Chimani, B., Lexer, A., & Blöschl, G. (2016). A new classification scheme of European cyclone tracks with relevance to precipitation. *Water Resources Research*, 52(9), 7086–7104. doi.org/10.1002/2016WR019146.

Hofstätter, M., & Chimani, B. (2012). Van Bebber’s cyclone tracks at 700 hPa in the Eastern Alps for 1961–2002 and their comparison to Circulation Type Classifications. *Meteorologische Zeitschrift*, 21(5), 459–473. doi.org/10.1127/0941-2948/2012/0473.



On the 11th of August 2002 a major Vb cyclone hit Europe. Excessive large scale precipitation led to devastating floods in many Central European countries.

Satellite image provide by: NERC Satellite Receiving Station, Dundee University, Scotland, <http://www.sat.dundee.ac.uk/>

Kurzfassung

Exzessiver, großflächiger Niederschlag führt zu einem hohen Hochwasserrisiko und ist daher von eminenter Bedeutung für monetäre und infrastrukturelle Schäden sowie die Gefährdung von Leben. Ziel dieser Dissertation ist es, den Zusammenhang zwischen dem Auftreten von Zugbahnen von Tiefdruckgebieten und der Charakteristik von mittleren und extremen Niederschlägen in Mitteleuropa besser zu verstehen. Die Eigenschaften und Variabilität von Vb-Zugbahnen werden insbesondere untersucht.

Zunächst wird eine einfache Tracking-routine auf ERA-40 Daten angewandt, um Vb-artige Zugbahnen im Zeitraum 1961-2002 zu bestimmen. Nach der Erstellung einer einfachen Klimatologie für diese Zugbahnen wird die Eignung von 83 Zirkulationsklassifikationen evaluiert, Vb-Ereignisse durch möglichst wenige Zirkulationsklassen zu erklären. Nachfolgend wird eine komplexere Tracking-routine implementiert und für den Zweck dieser Studie erweitert. Eine neuartige Klassifikation der Zugbahntypen von Tiefdruckgebieten über Europa, samt deren klimatologischen Eigenschaften, wird basierend auf JRA-55 Daten für den Zeitraum 1959-2015 präsentiert. Für diese Zugbahntypen erfolgen eine Auswertung des langjährigen Niederschlages und des Starkniederschlages für Teilgebiete Mitteleuropas, sowie ein Vergleich mit einer Starkniederschlag-Chronologie für Flusseinzugsgebiete. Schließlich wird die zeitliche Variabilität der Vb-Häufigkeit unter dem Gesichtspunkt der Häufungseigenschaften und zeitlichen Änderungen der Ankunftsraten untersucht, sowie ein Zusammenhang mit der großräumigen atmosphärischen Zirkulation hergestellt.

Gemäß der Zugbahnanalyse auf Meeresniveau bzw. 700hPa geopotentieller Höhe erreichen etwa 108 bzw. 76 Tiefdruckgebiete pro Jahr Mitteleuropa. Davon sind 25% Atlantiktiefs, 24% entstehen direkt über Mitteleuropa und 22% südlich der Alpen. Andere Zugbahntypen sind weniger häufig (Mittelmeertiefs 12%, Polare 7%, Vb 5%, Kontinentale 2%, Ostalpine 2% und Subtropische 1%). Die Niederschlagsmengen in den Regionen Mitteleuropas variieren erheblich zwischen den Zugbahntypen, wobei bei den Typen Atlantik und Vb die größten und bei den Typen Kontinental und Polar die geringsten Werte auftreten. Die Saisonalität des Niederschlags kann gut durch die Häufigkeit starker Tiefs der unterschiedlichen Typen erklärt werden. Um Starkniederschläge im Sommer und Herbst vollständig zu erklären, sind aber weitere Faktoren wie die Lufttemperatur und die Temperatur der umliegenden Ozeane, notwendig.

Vb Tiefs ergeben mit Abstand die größten Niederschlagsmengen zu allen Jahreszeiten und sind am häufigsten mit Starkniederschlägen verbunden. Vb zeigt die größte Starkniederschlagsrelevanz in den östlichen Regionen Mitteleuropas, wohingegen winterliche Atlantiktiefs in den westlichen von größerer Bedeutung sind. So konnten 30% der 50 stärksten Niederschlagsereignisse dem Typ Vb zugeordnet werden, aber nur 15% den Typen Atlantik und Mittelmeertief. Bei der Beurteilung des Gesamtrisikos von Starkniederschlägen sind neben dem Typ Vb auch andere Zugbahnen von Bedeutung, die wesentlich häufiger auftreten. So wurden zwischen 60 % (Tschechien) und 88% (W-Deutschland) der 50 stärksten Niederschlagsereignisse (1961-2006) durch andere Zugbahntypen verursacht. An den zehn extremsten Ereignissen in der Region Tschechien/Ostösterreich waren allerdings in acht Fällen Vb Tiefs ursächlich beteiligt.

Die Gründe für die enorme Hochwasserrelevanz von Vb Tiefs sind: Starke Vb Tiefs sind in allen Jahreszeiten gleichmäßig häufig; die Verweildauer in Mitteleuropa ist aufgrund der kreisförmigen Zugbahn im Mittel um einen Tag länger; und die Starkniederschlagsmengen sind um 40% bis 90% größer als bei anderen Typen. Am häufigsten treten Vb Tiefs Anfang April und Ende November auf. In bestimmten Perioden kommen Vb Tiefs gehäuft (in Clustern) vor, bevorzugt wenn die NAO und AO Zirkulationsindices in einer negativen Phase sind. Im Gegensatz dazu war die Vb Häufigkeit zwischen 1988 und 1997, einer ausgeprägt positiven Phase der NAO und AO Indices, besonders niedrig. Während des Auftretens eines Vb Tiefs ist in der Regel ein signifikanter Einbruch der NAO und AO Indices zu sehen, welcher fast drei Wochen andauert. Da dieser Zustand das Entstehen von neuen Vb Tiefs im westlichen Mittelmeer begünstigt, wird dieser Zusammenhang als $NAO^- Vb^+$ Rückkoppelung identifiziert. Abschließend zeigen die Ergebnisse, dass die Häufigkeit von Vb Tiefs in den 1960er Jahren signifikant hoch war, sich aber danach auf einem etwa gleichbleibenden Niveau bewegt hat.

Das in dieser Arbeit geschaffene vertiefte Verständnis des Verhaltens von Tiefdruckgebieten als atmosphärische Auslöser großräumiger Starkniederschlagsereignisse, soll nicht nur den Wissensstand der Hydrometeorologie erweitern, sondern auch Entscheidungsträger des Hochwasser-Risikomanagement in Hinblick auf Klimavariabilität und Klimawandel unterstützen.

Abstract

Excessive large scale precipitation entails a high risk of flooding and is thus of particular significance for infrastructural damage, financial loss and threat to human life. The aim of this thesis is to understand the relationship between European cyclone track types and the characteristics of mean and heavy precipitation in of Central Europe. Specifically, the characteristics and variability of Vb cyclones are investigated in depth.

In a first step, a tracking routine of atmospheric cyclones is used to identify Vb and congeneric track types using ERA-40 data for the period 1961-2002. The climatologic characteristics of these types are analyzed and the ability of 83 circulation type classifications to discriminate between days with and without Vb cyclones is evaluated. Second, a more complex tracking routine is implemented and refined for the purposes of this study. A new classification of Central European track types, including their climatological characteristics, is presented on basis of the JRA-55 data for the period 1959-2015. These track types are related to long term precipitation totals as well as to Central European heavy precipitation records of selected river basins. Finally, the temporal characteristics of Vb cyclone occurrence is analyzed in depth with a focus on dispersion characteristics and temporal changes of the arrival rates as well as on the relationship with the large scale atmospheric circulation.

About 108 and 76 cyclone tracks per year are identified at sea level pressure and 700hPa geopotential height, respectively. About 25% are Atlantic type cyclones, 24% emerge directly over Central Europe and another 22% originate from the lee of the Alps. The other types are less frequent (Mediterranean 12%, Polar 7%, Vb 5%, Continental 2%, Eastern Alpine 2% and Subtropical 1%). Precipitation differs significantly between cyclones, with Atlantic and Vb cyclones producing the highest and Continental and Polar cyclones producing the lowest long-term precipitation totals. The high frequency of strong cyclones was identified as the key factor explaining the seasonality of mean and heavy precipitation at the regional scale within Central Europe. However, to fully explain the contributions of track types to precipitation in summer and autumn, additional drivers such as air temperature and Mediterranean sea surface temperature may be needed.

Vb is identified as the most relevant track type for heavy cyclone precipitation in all seasons, accounting for 30% of the top 50 events in Central Europe, whereas Atlantic and Mediterranean cyclones account for only 15% each. Vb cyclones are most relevant for heavy precipitation in eastern Central Europe whereas Atlantic cyclones in winter are most relevant in the West. In total between 60 % (Czech Republic) to 88% (W-Germany) of the top 50 precipitation events (1961-2006) were triggered by track types other than Vb. Other track types are therefore also important for the overall risk of heavy precipitation, as most of the other types are much more frequent than type Vb. However, out of the 10 most extreme events in the Czech/Austrian region 8 were due to Vb tracks.

The reasons for the enormous flood relevance of Vb cyclones are: Strong Vb cyclones typically occur in all seasons; Vb cyclones remain one day longer over Central Europe than other types because of a circular shape of the cyclone tracks; and precipitation intensities are usually much higher than for all other types.

Vb cyclones are most frequent in early April and in late November. Clusters of high Vb cyclone frequency exist and have occurred when both NAO and AO indices were negative. In contrast, Vb cyclone frequency was particularly low from 1988 to 1997 during a sustained positive phase of both NAO and AO. Vb cyclone occurrence significantly reduces the NAO and AO indices for nearly three weeks, favoring subsequent Vb events, which suggests a $NAO^- Vb^+$ feedback mechanism. Finally, the results show that the frequency of Vb cyclones was high in the 1960s and has remained at a lower level since.

By gaining a deeper understanding of the nature of cyclones as the atmospheric drivers of heavy precipitation this study intends to provide new hydro-meteorological knowledge and to support decision makers in flood management in the context of climate variability and change

Acknowledgements

I would like to show my great appreciation to my supervisor Prof. Günter Blöschl. His vast expertise and straight to the point advices were an important support and guidance for my research. I am truly grateful I had the opportunity to learn from him over the last seven years.

Although I have always been fascinated by heavy rain events, the concrete idea on investigating Vb cyclones emerged after September 2009, when Reinhard Böhm asked me to write a feasibility study on large scale precipitation in relation to Vb cyclones. This feasibility study was the starting point of my dissertation, therefore I am really grateful to Reinhard for asking me of all people at that time. Unfortunately Reinhard passed away in October 2012 when documenting the Alpine glaciers retreat at the Sonnblick mountain, so I dedicate my dissertation to him in particular. Reinhard was one of the most appreciated climate researchers, strictly obligated to objectivity and deeply dedicated to his research.

Above all I would like to thank my wonderful wife Andrea who took over all our obligations when I was spending hours, days and weeks working on this dissertation beside my full-time job. I deeply appreciated your patience and dedication in supporting me throughout the last seven years. I am also grateful to my lovely daughter Carolin for interrupting me from time to time in order to play Lego with her.

I acknowledge financial support from the Austrian Science Funds (FWF) as part of the Vienna Doctoral Programme on Water Resource Systems (DK W1219-N22) and the ERC Advanced Grant “Flood Change”, Project 291152.

Parts of this study have been funded by the Austrian Ministry of Life - Dept. for Water Affairs, and the Bavarian State Ministry of the Environment and Public Health.

Contents

1. Introduction	1
2. Van Bebber's cyclone tracks at 700 hPa in the Eastern Alps for 1961-2002 and their comparison to Circulation Type Classifications	3
Abstract	3
2.1. Introduction	3
2.2. Data	7
2.3. Method	7
2.3.1. Cyclone tracking	7
2.3.2. Categorization of cyclone tracks	9
2.3.3. Comparison of track classes and circulation types	10
2.4. Results and Discussion	12
2.4.1. Verification and comparison with chronicles	12
2.4.2. Verification against Lauscher's manual Vb-record	12
2.4.3. Climatology of cyclone tracks in ERA-40	14
2.4.4. Coherence of Vb with circulation classification schemes	15
2.4.5. Comparison ERA-40 with ERA-Interim	19
2.5. Conclusions	19
3. A new classification scheme of European cyclone tracks with relevance to precipitation	21
Abstract	21
3.1. Introduction	21
3.2. Developing a classification of European cyclone tracks	23
3.2.1. Data	23
3.2.2. Cyclone tracking	24
3.2.3. An illustrative example	27
3.2.4. Synoptically based classification	28
3.3. Track type characteristics	30
3.3.1. A brief climatology of tracks types	30
3.3.2. Intensity characteristics	34
3.4. Precipitation related to track types	36
3.4.1. Long-term precipitation totals	36
3.4.2. Heavy precipitation events from 1961 to 2002	39
3.5. Discussion of classification results	41
3.5.1. Southern Alpine track types in comparison	41
3.5.2. Sensitivity experiment for classifying Vb	42
3.6. Conclusions	42

4. Large scale heavy precipitation over Central Europe and the role of atmospheric cyclone track types	45
Abstract	45
4.1. Introduction	45
4.2. Data and Analysis Procedure	47
4.2.1. Cyclone track types	47
4.2.2. Precipitation data and study region	50
4.2.3. Analysis of mean and heavy precipitation	51
4.2.4. Analysis of outstanding precipitation events	52
4.3. Results	53
4.3.1. Cyclone track types	53
4.3.2. Precipitation stratified by track types	57
4.4. Discussion and Conclusion	67
5. Vb cyclones synchronized with the Arctic-/North Atlantic Oscillation	73
Abstract	73
5.1. Introduction	73
5.2. Data and Methods	75
5.3. Results and Discussion	79
5.3.1. A brief climatology	79
5.3.2. Occurrence rate and temporal changes	80
5.3.3. Dispersion of Vb cyclones	84
5.3.4. Large scale atmospheric circulation	87
5.4. Conclusions and Outlook	96
6. Overall conclusions	99
References	103

1 Introduction

Central Europe (CE) has been hit by several devastating floods, caused by exceptional large scale precipitation events, in recent decades. Examples include the July 1954 flood in Bavaria and Austria, the July 1997 flood in Poland (e.g. Kundzewicz et al., 1999), Germany, the Czech Republic and Austria, the August 2002 flood (e.g. Grazzini and Van der Grijn, 2002) in a number of countries, the August 2005 flood in the Alps (e.g. Godina et al., 2006; Habersack und Krapesch, 2006) and the 2013 flood in Germany and Austria (Blöschl et al., 2013).

Most of these events appear to be related to the occurrence of characteristic patterns of the atmospheric flow, especially when an atmospheric cyclone propagates from the Western Mediterranean or the Adriatic Sea into CE (Kundzewicz et al., 2005; Mudelsee et al., 2004; Ulbrich et al., 2003; Rudolf and Rapp, 2003; Malitz and Schmidt, 1997). Cyclones are organized, counter clockwise (Northern Hemisphere) rotating fluid structures of the atmosphere. Their centers are characterized by a distinct relative minimum of air pressure or geopotential height. The locations of a moving cyclone's path over its life span are known as the cyclone track.

As early as 1882, W.J. van Bebber recognized a causal relationship between heavy large-scale precipitation or winter snowstorms in Austria and the occurrence of certain track types (Van Bebber, 1891). He analyzed surface pressure maps over Europe for the years 1876-1880 and 1875-1890 (van Bebber 1882 and 1891; van Bebber and Köppen 1895) and classified similar paths of isolated pressure minima into five main categories. From this early track classification only track type Vb (pronounced as "five b") is still in use today, as several major CE floods have been associated with Vb cyclones, for example the devastating flood event in August 2002 (Ulbrich et al., 2003). Vb cyclones originate in the Western Mediterranean, propagate to the east across Italy and turn to the northeast over the eastern Alps. A number of studies have attributed Vb cyclones to heavy precipitation or flood events, however, these studies were based on circulation type classifications (CTSs) instead of using cyclone tracks explicitly (e.g. Fricke and Kaminski 2002; Mudelsee et al., 2004; Kundzewicz et al., 2005).

So far, to the best of my knowledge, no studies exist on CE cyclones in relation to heavy precipitation in general and to Vb cyclones in particular. The objective of this thesis therefore is to address the following questions:

1. Are characteristic circulation type classifications or cyclone tracking analyses preferable in capturing Vb events?
2. How are different cyclone track types related to mean and heavy precipitation in different parts of CE?
3. Is track type Vb indeed the most relevant one for CE, large scale heavy precipitation events as suggested by observations?
4. What are the climatological characteristics of Vb cyclones? How do these relate to other track types?
5. Has the frequency of Vb cyclones changed in recent decades given that global temperatures have increased by almost one degree Celsius?

-
6. How are Vb cyclones related to the large scale atmospheric circulation? Is there a prominent atmospheric mode explaining variations in the Vb occurrence rate on a monthly to decadal scale?
 7. Do Vb cyclones occur in clusters, i.e. more frequently than by chance in certain periods, and what are the consequences for flood risk?

This thesis is structured into four main chapters as follows:

Chapter 2 presents a systematic tracking of atmospheric cyclones at the pressure level of 700 hPa by applying an existing, straightforward tracking algorithm (Zahn and van Storch, 2008) using ERA-40 reanalysis data for the period 1961-2002. From this first track catalogue, the climatological characteristics of van Bebber's type V are estimated. In a next step, the ability of eleven selected circulation type classifications to discriminate between days with and without Vb tracks is examined. Circulation type classifications potentially are a cost-effective and well established alternative approach of analyzing large scale heavy precipitation, however, only if circulation types are able to recognize Vb tracks well. Finally, a Vb classification from the Austrian Weather Service (ZAMG) is used to validate the Vb recognition rate of the systematic tracking routine.

Chapter 3 implements a more sophisticated cyclone tracking algorithm using ERA-40 reanalysis data for the period 1961-2002. Developments of the tracking routine include the merging and splitting of cyclones as well as accounting for both open and closed cyclones. Cyclones are tracked at two different atmospheric levels using surface level pressure and geopotential height at the pressure level of 700hPa. A new approach to classifying atmospheric cyclones over Europe is proposed which includes van Bebber's track type Vb. Finally, the resulting track types are briefly analyzed in terms of within-type cyclone characteristics and related to long term precipitation totals as well as to a selected Central European flood records.

Chapter 4 investigates the climatologic characteristics of Central European cyclone tracks in more depth and extends it to the more recent period 1959-2015 using JRA-55 reanalysis data. Characteristic patterns of the upper level atmospheric flow are identified for the track types and a comprehensive analysis of the relation between track types and mean-, as well as heavy precipitation for different parts of Central Europe is presented. The 50 of the largest precipitation events in recent decades are attributed to track types and analyzed in terms of temporal changes additionally.

Chapter 5 specifically explores Vb type cyclones. A less restrictive and more generalized definition of the Vb track is presented and cyclone tracks identified from 700hPa and sea level pressure are considered jointly. Vb tracks are differentiated in terms of their source region in the analysis. First, a short climatology of the Vb subtypes is presented, followed by an analysis of serial clustering and temporal changes of cyclone occurrence for 1959-2015. Second, the relationship between the large scale atmospheric circulation and arrival rates is investigated by selected teleconnection indices, in particular using the Northern Atlantic Oscillation (NAO) index at 500hPa and the Arctic Oscillation (AO) index at sea level pressure.

2 Van Bebber's cyclone tracks at 700 hPa in the Eastern Alps for 1961-2002 and their comparison to Circulation Type Classifications

Abstract

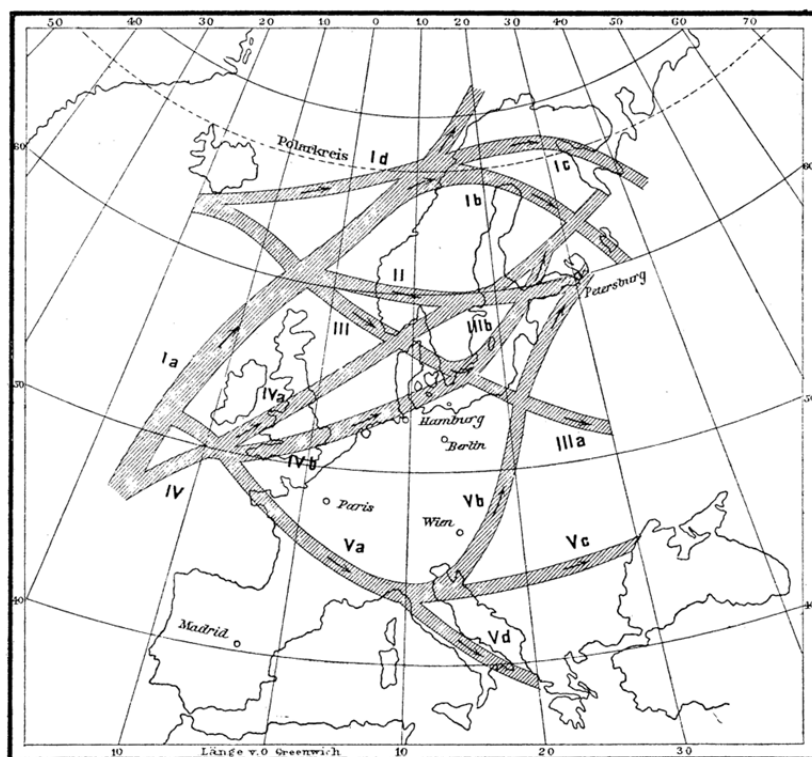
In this study, a systematic tracking of atmospheric cyclones at the pressure level of 700 hPa has been performed to determine three different track types and their climatologic characteristics over Central Europe from 1961 to 2002 by using ERA-40 (ECMWF - European Centre for Medium Range Weather Forecast, 40 year Re-Analysis) and ERA-Interim data. The specific focus is on cyclone tracks of type V as suggested by Van Bebber in 1891 and congeneric types, because of their association with extreme large-scale precipitation amounts and related flooding in Central and Eastern Europe. The tracking procedure consists of detecting isolated minima of the band-pass filtered 700 hPa geopotential height field and combining them over time to continuous tracks by nearest neighbour approach.

Results show that the common Vb cyclone track is a rare event (3.5/year) and the probability of occurrence is largest in April with a secondary maximum in autumn. Furthermore, there is no temporal trend of any of these track types noticeable throughout the 42-years investigation period. The new 700 hPa cyclone track catalogue is used as a reference to verify the hypothesis of a coherence of Vb-tracks with certain circulation types (CTs). Selected objective and subjective circulation type classifications (CTCs) from COST (European Cooperation in Science and Technology) action 733 as well as a manual Vb-classification from the ZAMG (Zentralanstalt für Meteorologie und Geodynamik) are utilized. This study shows both the shortcomings and the potential of CTCs to discriminate Vb cyclone tracks by certain classes of stationary circulation patterns. Subjective CTCs rank higher than objective ones in terms of Brier Skill Score, which demonstrates the power to enhance relevant synoptic phenomena instead of favouring mathematical criteria. For the first time, an objective catalogue with the famous cyclone track Vb and its climatology is now on hand for the period 1961-2002, offering a valuable basis to further improve our knowledge on the issues of Vb and related hydro-meteorological aspects.

2.1 Introduction

Central and Eastern Europe have been hit by several devastating floods, caused by exceptional large scale precipitation events in recent decades. Examples of such major events are the ones in Bavaria and Austria in July 1954, in Poland (e.g. Kundzewicz et al., 1999), Germany, the Czech Republic and Austria in July 1997, in many parts of the Alpine region in August 2005 (e.g. Godina et al., 2006; Habersack und Krapesch, 2006) or the vast flooding in several European countries in August 2002 (e.g. Grazzini and Van der Grijn, 2002). From synoptic observations or post-incident analysis, most of these events appear to be related to a specific pattern of the atmospheric circulation occurring, when low pressure systems (cyclones) are propagating from the Mediterranean Sea or Adriatic Sea northwards (Kundzewicz et al., 2005; Ulbrich et al., 2003; Rudolf and Rapp, 2002).

Besides this kinematic aspect, the available atmospheric water content is another important factor in the generation of large precipitation amounts, which points to the particular relevance of the summer season for this phenomenon. As has been shown for the case of the flooding in Eastern Germany in August 2002, a major contribution of local precipitation originated from sources over the Adriatic Sea or the Mediterranean (Stohl et al., 2004; James et al., 2004). Hence, these regions appear to play an important role for flooding events in Central Europe, either indirectly by the cyclonic advection of water vapour to the European continent through the atmospheric circulation or directly by acting as a local humidity source, when cyclones are moving over open water surfaces, are enriched with water vapour and then move over the European continent (Řezáčová et al., 2005; Rudari et al., 2004; Zängl, 2004). As a consequence, this specific propagation path of low pressure systems is an important risk factor for heavy large scale precipitation and potential flooding in Central and Eastern Europe (e.g. Mudelsee et al., 2004; Malitz and Schmidt, 1997).



Zugstraßen der Minima in Europa nach W. J. v. Bebber und W. Köppen.

Figure 1: Cyclone tracks over Europe by Van Bebber and W. Köppen (in Umlauf, 1891), showing track type Vb, Vc as well as Vd as determined from surface level pressure minima.

As early as 1882 W.J. van Bebber recognized this causal relationship, when he analysed surface pressure maps over Europe for the years 1876-1880 and 1875-1890 (van Bebber 1882 and 1891; van Bebber and Köppen 1895) and classified the respective tracks of isolated pressure minima into five main categories. Especially the track type V is still being used until this day, since many of the major European floods have been associated either with Vb-tracks in Central Europe like in August 2002 (Ulbrich et al., 2003) or with Vc-tracks in Eastern Europe (Apostol, 2008). As shown in Figure 1, cyclones on the path Vb, for instance, propagate from the northern Mediterranean or from the Adriatic Sea northwards over the Eastern Alps into the Baltic region. Although the relevance of certain cyclone tracks

for the risk of major floods in Europe is well known in the scientific community, not least because of the 2002 event, only few studies exist up to now focusing on Vb-events. Cyclone tracks of type Vb under future climate conditions have previously been investigated by Muskulus and Jacob (2005), who used climate simulations with emission scenario B2 from the regional climate model REMO. Another study, investigating future climate simulations from the global climate model ECHAM5 (Nissen et al., 2011), has shown that the total number of cyclones of type Vb will decrease in the summer half year (Apr-Sep). Kundzewicz et al. (2005) analysed Vb-tracks in the simulations of the global climate model ECHAM4 and found that the track density will decrease by 20-30% until 2070-2099 compared to 1961-1990 in scenario A2 in summer. All of these authors assume that this decrease of Vb-events might go along with increasing precipitation amounts in individual cases.

- The first aim of this study is to track atmospheric cyclones at the pressure level of 700 hPa to determine track types and their climatologic characteristics especially for the study region of Central Europe (2.25°W-23.63°E and 37.57°N-58.88°N) in the period 1961-2003 by using ERA-40 (ECMWF) and ERA-Interim data with focus on Van Bebbers type V.

Whereas many cyclone tracking studies focused on the winter season only, the described relevance of atmospheric water content for Vb-related precipitation events, calls for the investigation of the summer season as well. The focus there is on cyclone tracks of type V as suggested by van Bebber and congeneric types because of their probable causality for the risk of flooding in the study region.

- As the second aim of this study the ability of selected circulation type classifications (CTCs) to discriminate between days with a Vb track and such without is verified.

The calculation of CTC's appears more straightforward and computationally faster than in case of atmospheric cyclone tracking, so might be a cost-effective alternative if circulation types are able to recognize Vb tracks sufficiently. Therefore, selected objective and subjective CT-classifications (CTCs) from the COST action 733 (European Cooperation in Science and Technology; "Harmonisation and Applications of Weather Type Classifications for European Regions"; Phillip et al. 2010) are used, as well as the manual classification from ZAMG-Lauscher (Lauscher 1972) in which a Vb-like weather pattern has been classified explicitly on a daily base by hand since 1948 (see Table 1 for all 83 CTC-variants used herein). Generally, subjective (manual) classifications are based on the expert knowledge about the effect of certain circulation patterns on various surface climate parameters whereas objective (automatic) classifications are reproducible by computer based methods (Phillip et al., 2010). The term "Vb track" will be used hereafter for all cyclone tracks following Van Bebber's cyclone path - which has originally been defined for pressure minima at the surface level - although the following results are strictly based on cyclone tracks determined from 700 hPa geopotential height (Z700).

Table 1: Circulation type classifications used in this study. (Notations on CTC 1-10 as listed in COST733cat). Parameters used as input fields for classifications are abbreviated: SP (surface level pressure), Z (geopotential height), U/V (zonal/meridional wind component), TW (total water column), Y (relative vorticity), K (Thickness 500/850). Suffixing numbers denote levels of constant pressure in hundreds of hPa.
All CTCs are derived over cost733 domain no. 6 (D06; Alps; 41°N-52°N, 3°E-20°E).

id	Abbr.	Circulation type classification (CTC)	number of CT's	base period (Yr., year, SE...seasonal)	4-day sequencing without (S01)	with (S04)	parameters	total number	reference
1	CAP	Cluster Analysis of Principal components (PCACAC)	9;18 28 27	YR SE YR	x x x	x x x	SP; SP-Z5 SP; SP-Z5; SP-K5; SP-Y5; SP-Z5-Y5-K5 SP; SP-Z5; SP-K5; SP-Y5; SP-Z5-Y5-K5	8 5 10	Yarnal (1993)
2	GWT	GrossWetterTypes	8; 18; 26	YR	x	x	SP	3	Beck (2000)
3	GWLo	„Hess-Brezowsky GrossWetterLagen“	11;30	YR	x	x	not specified	2	Hess and Brezowsky (1952)
4	LND	Lund classical leader algorithm	9;18;27	YR	x	x	SP; SP-Z5	12	Lund (1963)
5	OGWo	Objectivised Hess-Brezowsky „GrossWetterLagen“	29	YR	x	x	SP	1	James (2007)
6	PERo	Perret alpine weather statistics	31	YR	x	x	SP	1	Perret (1987)
7	SAN	Simulated ANeilling clustering (SANDRA)	9;18;27 28	YR SE	x x	x	SP; SP-Z5; SP-K5; SP-Y5; SP-Z5-Y5-K5 SP; SP-Z5; SP-K5; SP-Y5; SP-Z5-Y5-K5	30 5	Philipp et al. (2007)
8	SUEo	Schuepp alpine weather statistics	40	YR	x	x	SP, Z5, U5, V5, U10, V10	1	Schüepp (1979)
9	WLKo	„Objektive Wetterlagenklassifikation“	9 18 28 40	YR YR YR YR	x x x x	x x x x	U7-V7 U7-V7-Z9 U7-V7-Z9-Z5 U7-V7-Z9-Z5-TW	1 1 1 1	Dittmann et al. (1995)
10	ZMGo	„ZAMG Wetterlagenklassifikation“	43	YR	x	x	not specified	1	Lauscher (1985); ZAMG
11	LAU	„Ostalpine Wetterlagenklassifikation“	18	YR	not specified	not specified	not specified	1	Lauscher (1972)

2.2 Data

The reanalysis of geopotential height at the constant pressure level of 700 hPa (Z700) from the ECMWF was used to investigate Van Bebber's cyclone tracks and their climatologic characteristics over Europe. ERA-40 (Uppala et al., 2005) provides 6-hourly atmospheric data from 1957-2002 with a spatial resolution of 1.125°, whereas for this study only the years from January 1961 to August 2002 were analyzed. Additionally, the tracking procedure was applied to ERA-Interim data (Dee et al. 2011) at the same spatial resolution for the years from 1989 to 2001 to evaluate basic differences. Apart from the initial spatial resolution, there are other important differences between ERA-40 and ERA-Interim as the use of a different data assimilation scheme (including improved model physics) and consideration of additional observational data in the latter. As this is the first catalogue with van Bebbers cyclone tracks type V, determined by objective means and published for the years 1961-2002, an appropriate database for verification or comparison is not on hand. However, to examine the validity of the results, well documented historical Vb-events are available for comparison. The circulation type classifications (CTCs) used herein have been retrieved from the COST733 database (catalogue version 2.0, domain 06 – Alps), except for the classification by Lauscher, which originates from the ZAMG. All 83 variants of CTCs tested herein are summarized in Table 1. For a more detailed description of these CTCs, including technical references and descriptions of the method, see Phillip et al. (2010) or COST733 online (<http://cost733.met.no/>).

2.3 Method

2.3.1 Cyclone tracking

In his work, van Bebber analysed cyclone tracks on the basis of surface level pressure (SLP) maps. Unfortunately, this attempt appears inadequate for the implementation of a systematic tracking procedure in or around the complex topography of mountain regions like the Alps. A major reason for this are inhomogeneities that might appear in the trace, when cyclones are only indicated by a weak or fairly disturbed pressure signal on the surface, which is frequently observed in the summer season. The analysis is therefore based on the atmospheric level of 700 hPa (approx. 3000m above mean sea level). Consequently, the exact position of tracks identified herein is not necessarily identical with the ones which would result from SLP. For a comprehensive review of different cyclone tracking procedures and studies see, for example, Ulbrich et al. (2009) or Raible et al. (2008).

Data preparation

As ERA-40 is used on regular grid points and provided at a coarser spatial resolution than ERA-Interim, the latter had to be transformed from spectral coefficients to the Gaussian grid first. This was done by means of the routine "sp2gp" as well as by the bilinear interpolation method "remapbil" using the software package CDO (Climate Data Operators, <http://code.zmaw.de/projects/cdo>). Thereafter both datasets were handled in the same way:

In order to avoid the recognition of small-scale, secondary low-pressure centres among one main cyclone or any other spurious systems, a spatial filtering of the input fields was done. Such systems occur mainly on the edge of major depression systems or in weak gradient situations, potentially leading to erratic and/or very short cyclone tracks. For this purpose, a two-dimensional discrete spatial low pass filter (Freser and von Storch, 2005) was applied to the Z700 anomaly field. This filter width of 550-970km was chosen in accordance with the distance criterion in the detection algorithm (see next section for the distance criterion). The effect of this filter can be seen in figure 2, where very small low pressure centres are removed and only two main centres are left, that are clearly identifiable as distinct low pressure centres.

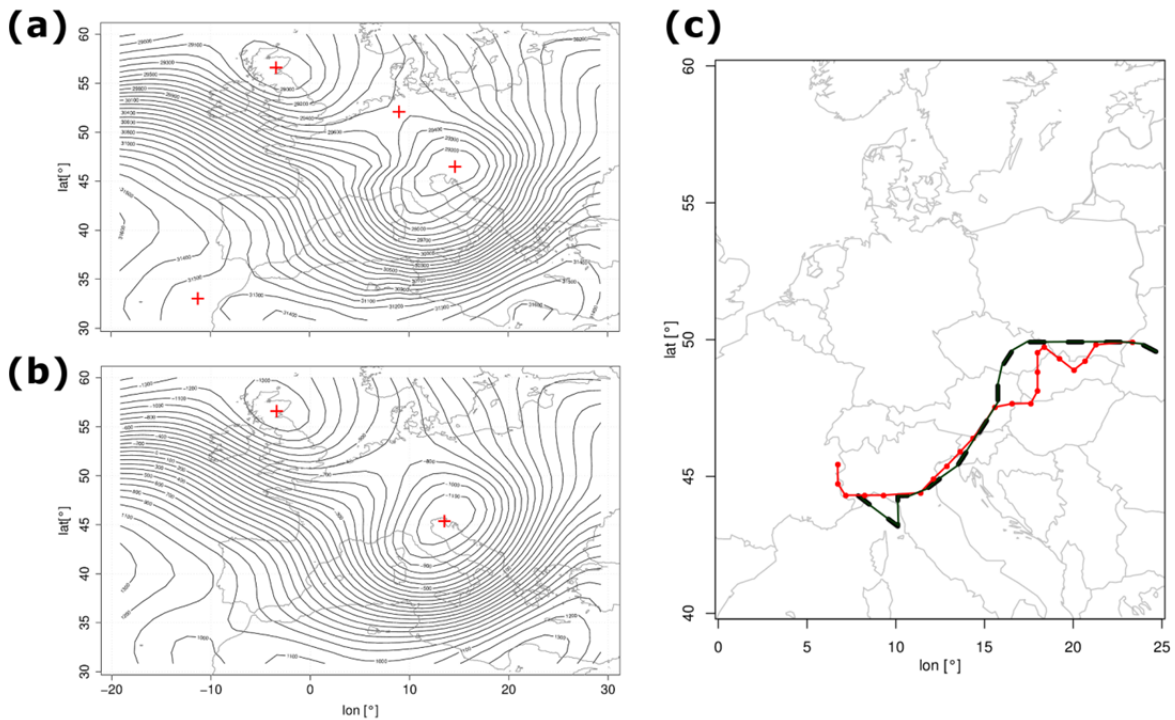


Figure 2: Cyclone track analysis from 11th of August 2002 - 18UTC. (a-b): Geopotential height at 700 hPa with raw (a) and filtered (b) data. Troughs are indicated by the red crosses. (c): Tracks from filtered (black) and unfiltered (red) fields for the Vb-event from 10.-13. August 2002.

Detection and tracking procedure

A simple approach was chosen for the detection of separated cyclone centres or low pressure centres (LPs). For each grid-point i , the first derivative of geopotential height ϕ in both x- and y-directions to the neighbouring grid points was calculated by Equation 1, leading to four gradients.

Those grid-points, showing a positive value for all the four gradients, were detected as an isolated minimum.

$$\begin{aligned}
 & \frac{(\phi_{xi+1} - \phi_{xi})}{\Delta x} > 0 \quad \text{and} \quad \frac{(\phi_{xi-1} - \phi_{xi})}{\Delta x} > 0 \\
 \text{and} & \\
 & \frac{(\phi_{yi+1} - \phi_{yi})}{\Delta y} > 0 \quad \text{and} \quad \frac{(\phi_{yi-1} - \phi_{yi})}{\Delta y} > 0
 \end{aligned} \tag{1}$$

Next, a minimum distance of 500km between two adjacent LPs was set to discriminate between very close centres. In such cases, only the grid-point with the lower GPH value was considered, and the other was skipped from thereon. The detection algorithm has been applied time-independently, disregarding any information from previous or subsequent time steps. Then the tracking algorithms from Zahn and van Storch (2008) were applied, combining LPs from different time steps by nearest neighbour approach and hence tracking the propagation path of the systems. Thereby, LPs from a certain time step are combined with the nearest LPs from adjacent time steps, assuming a minimum propagation ahead. The maximal distance between LPs from one track between two time steps (6 hours) is set to 600km. In the case of a cyclone splitting, only one minimum is assigned to the initial track, the other one builds the starting point for an additional track. All tracks must be present for at least 12 hours in order to be considered. The tracking routine was applied to the study region 2.25°W-23.63°E and 37.57°N-58.88°N.

2.3.2 Categorisation of cyclone tracks

The following subjective criteria have been set to discriminate between three track types (1) Vb, (2) Vcd (either Vc or Vd) and (3) NST (no specific type). The criteria for track type Vb are:

- i. The track has to be within the area "O" for at least one time step (4°E-16°E; 42°N-46°N).
- ii. The track has to be located beyond 14° East at any time step.
- iii. The track must have an overall movement from west to east.
- iv. From the area "O", the track crosses area "E" (14°E-20°E; 47°N-60°N) at any time step.

This categorisation also allowed for the separation of track types Vcd. Those had to fulfil all criteria for Vb except the last one. The third category of track types NST refers to a group of miscellaneous tracks which could not be attributed to types 1 or 2, but appear within the core study region "R" for at least one time step (10°E-20°E, 44°N-50°N, see rectangle R in figure 3). This inner domain covers the Eastern Alps and has been chosen as an additional region of interest from the meteorological standpoint, but also with reference to the predefined position of van Bebber's track V near Austria in this regard. However, in the following the term "study region" always refers to the larger domain covering most parts of Europe for which the cyclones have been tracked initially. If not marked otherwise, results refer to this outer domain.

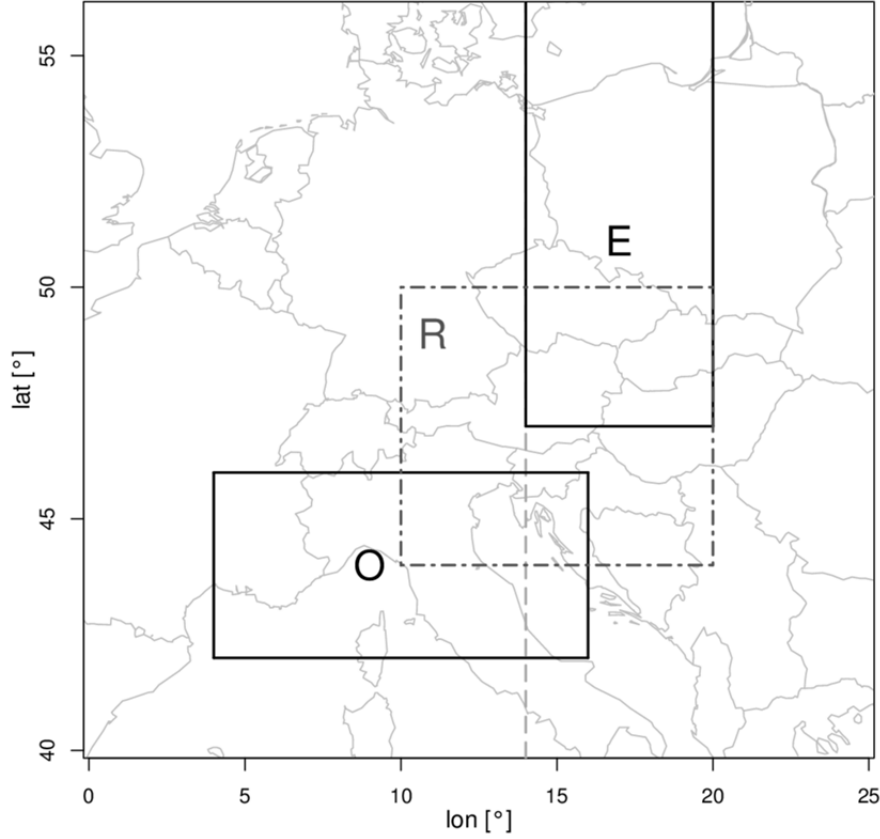


Figure 3: Study region for tracking analysis (2.25°W-23.63°E and 37.57°N-58.88°N) and areas for the categorisation of Vb-like 700 hPa cyclone tracks: "O" stands for the area of origin for Vb- and Vcd-tracks, "E" ..exit area for Vb, dashed gray line at 14°East for Vb and Vcd, "R"...core study region for the detection of all remaining tracks.

2.3.3 Comparison of track classes and circulation types

To test the hypothesis as to Vb events can be investigated by just using certain classes of circulation types instead of Vb-tracks or vice versa, we compared the new catalogue of Vb-tracks developed in the present study with 10 of the existing CTCs from the COST733 catalogue in different variants, which resulted in a total of 83 cases for evaluation (see Table 1 for selected schemes).

The climatological probability of Vb to occur on any day is given by

$$Vb_{clim} = \left(\frac{\text{days with Vb}}{\text{all days}} \right) = \left(\frac{585}{15218} \right) = 3.84 \text{ (\%)} \quad (2)$$

equivalent to a typical occurrence of Vb on 14 days per year in Central Europe (3.5 events per year). As CTCs can be viewed as probabilistic binary predictions (Schiemann and Frei, 2010), the conditional probability $\text{prb}_{\{Vb | CT_k\}}$ of a Vb-event to be observed within a certain circulation class k is hence determined by

$$\text{prb}_{\{Vb | CT_k\}} = \left(\frac{\text{Vb days in } CT_k}{\text{all days in } CT_k} \right)_k \quad (3)$$

whereas the conditional probability $\text{prb}_{\{CT_k | Vb_{obs}\}}$ for any CT_k to occur if Vb occurs is determined by the observed Vb characteristics and given through

$$\text{prb}_{\{CT_k | Vb_{obs}\}} = \left(\frac{Vb \text{ days in } CT_k}{\text{all } Vb \text{ days}} \right)_k \quad (4)$$

The unconditional probability $\text{prb}_{\{CT_k\}}$ for the occurrence of any day within a certain CT_k is calculated by simply dividing the number of days in CT_k by all days. This probability equals the climatologic probability of occurrence of Vb-events in each CT $\text{prb}_{\{CT_k | Vb_{clim}\}}$ when Vb-days are spread over CTCs just by chance.

$$\text{prb}_{\{CT_k | Vb_{clim}\}} \equiv \text{prb}_{\{CT_k\}} = \left(\frac{\text{all days in } CT_k}{\text{all days}} \right) \quad (5)$$

The difference between (4) and (5) will be defined as “excess probability” ε for all cases where $\text{prb}_{\{CT_k | Vb_{obs}\}} > \text{prb}_{\{CT_k | Vb_{clim}\}}$. Excess probability is a measure for the power of a certain CTC to discriminate - or not - between Vb events by means of CTs. Hence, if we would like to use a CTC instead of certain cyclone tracks, the sum of ε should be as large as possible and be concentrated on the lowest possible number of CTs.

As a second measure to assess the ability of the different CTCs to distinguish between certain track types by CT-classes, the Brier Skill Score for CTC-evaluation (*BSS) as proposed by Schiemann and Frei (2010) is used. The *BSS is always a number between 0 and 1, shows largest skill at higher values and is defined by Equation 6 for this purpose:

$$*BSS = \left(\frac{N^{-1} \sum_{k=1}^K N_k * (\text{prb}_{\{Vb | CT_k\}} - Vb_{clim})^2}{Vb_{clim} * (1 - Vb_{clim})} \right) \quad (6)$$

where N_k is the number of days with circulation type k and N is the total number of days from all classes K. This variant of the Brier Skill Score is showing larger values if the conditional empirical event frequencies $\text{prb}_{\{Vb | CT_k\}}$ differ from the unconditional (climatological) event frequency. Unfortunately, the BSS has a general tendency to converge towards very low values, when dealing with rare events as in the case of Vb-tracks. As this does not have any consequence for the overall meaning of the BSS itself, all CTCs have been ranked by the magnitude of the BSS for comparison (shown in Figure 6 and 7).

The Hit Rate (also named as probability of detection POD) as a classical score from forecast verification (Donaldson et al., 1975) is used to test results against Lauscher’s CTC. By this classification, days with Vb-like synoptic features have been determined manually since 1948 at the ZAMG. HR is the ratio of correct forecasts to the number of times this forecasted event is observed (Wilks, 2006).

2.4 Results and Discussion

2.4.1 Verification and comparison with chronicles

Despite an exhaustive review of relevant literature, only three major events could be found in recent history that are attributed to cyclones propagating on track Vb. These are:

- i. 1977, 31. Jul – 3. Aug (Malitz u. Schmidt, 1997).
- ii. 2001, 15. – 17. Jul (Ulbrich et al., 2003; Kundzewicz et al., 2005).
- iii. 2002, 10. – 14. Aug (Steinacker, 2002; Rudolf and Rapp, 2003; Ulbrich et al., 2003).

From our results, we are able to confirm that all these events are indeed cyclones on track Vb. However, it appears that only those events have been documented that are accompanied by extensive precipitation or massive flooding, leading to the assumption that highly subjective notions and preconception prevail regarding Vb-events. In fact as much as 146 tracks could be attributed to type Vb (Vcd 801; NST 507) from this study for the years 1961-2002 using ERA-40. Another study by Nissen et al. (2011) identified a total of 37 Vb-events, as compared to 56 Vb-tracks detected in this study, for the summer half years (April-September) 1971-2000. The underestimation of Nissen et al. (2011) may have been caused by tracking at SLP and missing those events where cyclones only appear at higher atmospheric levels, which is often the case during the summer season as already mentioned before.

When considering those 16 historic precipitation events that are listed as the highest daily areal-precipitation amounts found in the neighbouring country of Czech Republic between 1961 and 2002 (Kaspar and Müller, 2008), it appears that 13 of them are perfectly congruent with track-dates found in the present study (7 Vb, 2 Vcd, 4 NST), although a totally different approach is used. For two of the other cases, a track could be found, but only one day subsequent to the precipitation record, indicating that the precipitation had probably been triggered well before the arrival of the main synoptic system. In the last remaining case, the tracking procedure identified a cyclone track over Europe, but missed to identify it correctly as Vb. In this particular case an extreme tilt of the system was obvious, with the upper level trough (500 hPa) located over the North Sea whereas the corresponding surface pressure minimum was to be found over the Central Alps (7-8 August 1978). This example is of special interest as it points to the limits of the tracking approach used in this study. From an extensive analysis of daily weather maps at 500 hPa and on SLP manual for the period 1989-2002, we estimate that about 9% of Vb-events appear to be missing in the current catalogue. These events would only be detected if an additional tracking on the surface level were included.

2.4.2 Verification against Lauscher's manual Vb-record

Being aware that Lauscher and subsequent colleagues mainly focused on stationary atmospheric patterns in their classification and only decided for Vb when a cyclone was located close to or within the study region, a Vb-track was set to be recognized by Lauscher (a hit), if Vb was ruled at least once during the whole lifetime of the track.

Results (Table 2) show that only 15% of all Vb-tracks are identified as such by Lauschers CTC, 64% are classified as Tk or Ts (low pressure over Central Europe; low pressure in the Northern Adriatic Sea) and 21% are not captured by any of these classes. Tk and Ts have been chosen as these are the only ones that indicate an LP system located in or near the study region and should thus be able to contain synoptic situations of the Vb-family. In 3 % (Vcd) and 6% (NST track type) of the remaining track types Lauscher ruled Vb. The large Hit Rate in the CT-class Tk and Ts demonstrates the affinity of these circulation types with the track types identified in this study, especially in the case of Vb (64% Hit Rate).

Table 2: Hit Rate (HR) for certain track types as classified from objective analysis and three related circulation types taken from Lauscher’s manual classification: (i) Vb...”low pressure systems following Vb-path”, (ii) Tk...”low pressure over central Europe” and (iii) Ts...”low pressure in the south (Northern Adriatic Sea)”

objective track type	total number of tracks	days	HR for Lauscher’s manual CT		
			Vb	Tk or Ts	other CT
Vb	146	585	15 %	64 %	21 %
Vcd	801	2513	3 %	39 %	58 %
NST	507	1372	6 %	38 %	56 %
total	1454	4470			

When analysing Lauscher’s CTC from the perspective of which track type was observed when Lauscher and colleagues issued Vb, Tk, or Ts (Table 3), it appears that only 23% of these match with a Vb-track from the objective analysis, even if the number of Vb-days from tracking is four times larger (585 vs 145 in Lauscher). The remaining days can be attributed to type Vcd (17%), type NST (24%) and for 28% not a single track could be detected in the Alpine Region. It should be noted that the large discrepancy between the study results and Lauscher’s CTC may be due to a tendency to rule Vb only if any significant precipitation occurred along with a potential Vb-cyclone, as became clear in a personal communication at ZAMG in the course of the study.

Table 3: Hit Rate (HR) for three circulation types from Lauscher’s manual classification and track types classified by objective means. (see Table 2 for Lauscher’s CT acronyms). “either” means that more than one track type occurred on a given day due higher temporal resolution of tracks (6-hourly).

Lauscher’s manual CT	number of CTs (days)	HR for track types from objective analysis				
		Vb	Vcd	NST	either	none
Vb	145	23 %	17 %	24 %	8 %	28 %
Tk	740	12 %	39 %	13 %	4 %	32 %
Ts	1048	11 %	17 %	19 %	5 %	48 %
total	1933					

2.4.3 Climatology of cyclone tracks in ERA-40

In this section the climatology of cyclone tracks Vb, Vcd and NST based on ERA-40 are presented. On average, 3.5 Vb-events (19.2 Vcd and 12.2 NST) could be detected over Central Europe per year. The total number of Vb-events for the period 1961-2002 is 146 (Vcd 801; NST 507), with a typical occurrence of about 12 days per year (Vcd 47; NST 25). For none of these track types could a temporal trend be identified over the last 42 years. However, when looking at the time series of the occurrence of Vb-, Vcd- and NST tracks (not shown), a very high inter-annual variability is obvious for each type, as the annual number of tracks ranges between 0 and 7 for Vb, 11 and 29 for Vcd and 5 and 25 for NST.

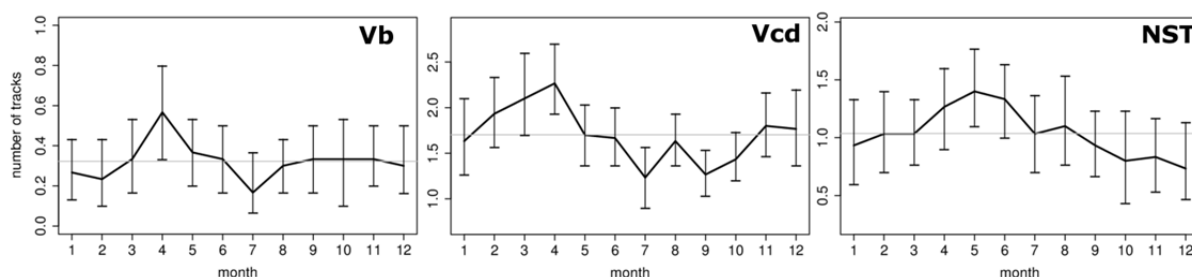


Figure 4: Mean seasonal cycle of the number of 700 hPa cyclone tracks over Central Europe (2.25°W-23.63°E, 37.57°N-58.88°N) from ERA-40 (1961-2002). Vertical bars show the 5th and 95th percentile from 500 bootstrap simulations (random 30-year means) indicating sampling uncertainty.

The seasonal cycle for the number of each track type (Figure 4) was obtained using the whole period of 1961-2002. The uncertainties were calculated using bootstrapping. In this process 30 years were randomly chosen out of the period 1961-2002 to determine the seasonal cycle repeatedly (500 times). Shown are the 5th and the 95th percentile of those bootstrap simulations as the upper and lower end of the whiskers. As shown in Figure 4 the uncertainties are quite large due to the large year-year variability. Nevertheless, a pronounced maximum in April and a minimum in July is obvious in case of Vb-tracks. Vcd-tracks, however, show a broader maximum peak in April, activity generally starting earlier in the year. The maximum of NST tracks spans from April to June whereas for this type a clear minimum appears in early winter. In another study by Flocas et al. (1988), an enhanced activity of cyclones which originate from N-Italy or the Northern Adriatic Sea was found especially in autumn, but this cannot be seen from our study. On the contrary, the results from our objective approach show a primary maximum in spring (April or May) for all track types and only a very weak secondary one in autumn for types Vb and Vcd (Figure 4).

Track density maps (Figure 5) are given by the sum of time steps for which a track passed the single grid points during the years 1961-2001. As per the predetermined criteria, the main path of Vb-cyclones is orientated to the northeast and shows a second major maximum in the region between Austria, Slovakia and the Czech Republic. Vcd tracks move on to the south east, with a second major maximum in the Central Adriatic Sea. NST-cyclones have no specific track to follow by definition, but it seems that these cyclones preferably propagate around the Eastern Alpine Region instead of moving straight ahead. The pronounced maximum near the Gulf of Genoa can be seen for all track types, emphasizing the importance of this region in the genesis of cyclones and their propagation path. This region could be identified as the starting point for a majority of cyclones following tracks Vb, Vcd or NST (not shown). This region is one of the major cyclogenesis regions

around Genoa in the NE of the Mediterranean Basin, which has been identified by Trigo et al. (1999), Trigo (2006), Lionello et al. (2002) and Pinto et al. (2005) for example. In the case of the Vb-tracks, a second track density maximum can be seen over the Northern Adriatic Sea, despite the fairly coarse spatial resolution of the ERA-40. Only recently has this region been identified as a second important cyclogenesis region for Mediterranean cyclones by Muskulus and Jacob (2005), when investigating cyclone tracks in high resolution, regional climate model simulations for the years 1961-2009.

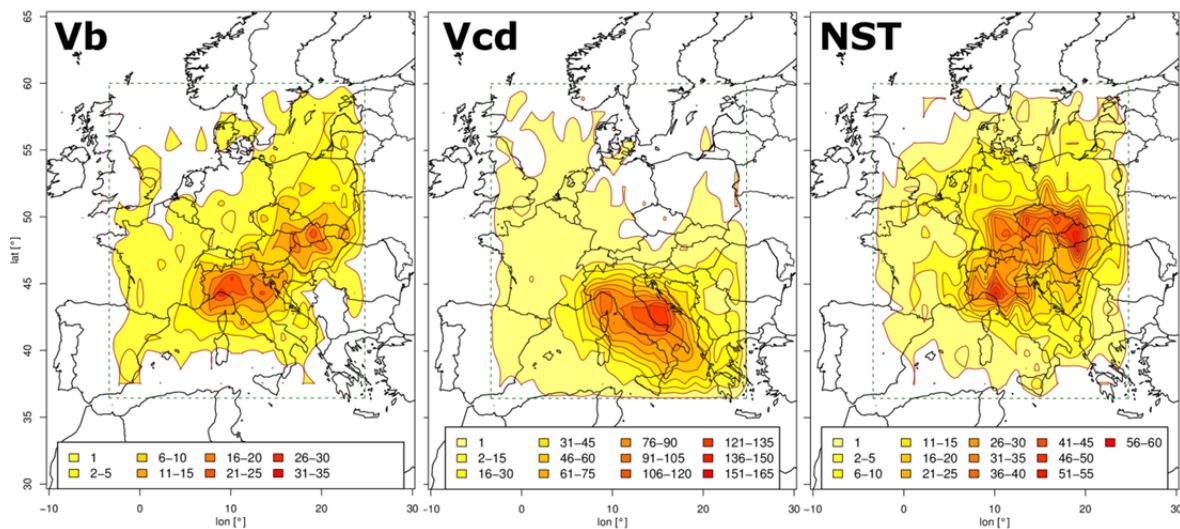


Figure 5: Track density (track count on grid points) for all track types from ERA-40 over Central Europe for 1961-2001. The broken line marks the investigation area for all tracks.

2.4.4 Coherence of Vb with circulation classification schemes

To verify the hypothesis of coherence between cyclone track Vb and certain circulation types from circulation type classifications using stationary atmospheric patterns (e.g. Fricke and Kaminsky, 2002; Mudelsee et al., 2004; Kundzewicz et al., 2005), the new catalogue of Vb-tracks is used as a reference and compared to selected CTCs from the COST733 catalogue for the cost733-domain “Alps” (D06; 41°N-52°N, 3°E-20°E). For this only days on which a Vb track was located within the Alpine domain were considered as a Vb-day. In doing so, the conditional probability $\text{prb}_{\{CT_k | Vb_{\text{obs}}\}}$ of CT_k to occur along with Vb (Vb as observed), is compared to the conditional probability $\text{prb}_{\{CT_k | Vb_{\text{clim}}\}}$ of CT_k in case of a climatologic occurrence of Vb (by chance) in figure 6 a-b and figure 7 a-b in the upper panel. The best performing CTC in this respect is ZMGo43 (Figure 6a), with a large total excess probability ε of 48%. Almost all of this excess probability comes from four CTs only (33, 36, 39 and 42), which indicates a strong ability to distinguish Vb-days. The conditional probability of Vb $\text{prb}_{\{Vb | CT_k\}}$ to occur in CT36 or CT33 is nearly five times larger than expected from climatology. All four CTs mentioned look very similar with a low pressure system or large scale trough located over Central Europe.

As Fricke and Kaminski (2002) and Kundzewics et al. (2005) postulated, this ability can also be seen in the classical classification scheme GWLo30, ranking as 2nd of 83 CTCs, where ε is 43% (Figure 6b). But in addition to CT17 (TRM – trough over Central Europe) as mentioned in Fricke and Kaminski, our results demonstrate that CT11 (TM – low pressure over Central Europe) is of similar or even higher importance. As shown in figure 6b (lower panel), the conditional probability of Vb to occur in CT11 is even larger than in CT17. Rank three of 83 belongs to CTC SUEo, again a manual/subjective scheme. CT-Classification SAN27_YR_S01_SP-Y5 is the best performing, fully objective scheme tested in the present study (Figure 7a) and ranked fifth among 83 with an ε of 47%. For this scheme, most of the excess probability is contributed by seven circulation types only, which is rather convincing. Most of the other fully objective schemes do not perform so well, as it is shown for LND27_YR_S04_SP for example (Figure 7b). The excess probability is as low as 0.22 and *BSS only leads to rank 76 for this CTC. As can be seen in figure 7b in the lower panel, Vb-events are not captured by any CT in specific and the conditional probabilities almost equal climatology.

When the results of all 83 CTCs tested in this study are compared, it follows that manual/subjective schemes outperform objective ones as long as the latter are not optimized with respect to the Vb-issue. The skill of objective schemes depends on the input fields which were used to derive a CTC. A combination of SLP with GPH or relative vorticity at 500 hPa appears as the best choice in this respect. Sequencing does not add any skill therein, on the contrary, for some schemes the results get even worse. Thus, including information from ongoing time steps for the classification does not lead to a higher recognition rate, despite the kinematic nature of the cyclone tracks. Finally the number of CTCs should be sufficiently large (~18-27), but this depends on the specific characteristics of the CTCs.

All in all, the hypothesis of Fricke and Kaminsky can definitely be supported by this work: Vb-tracks are included in one or the other stationary circulation pattern to some extent, depending on the specific characteristics of a CTC.

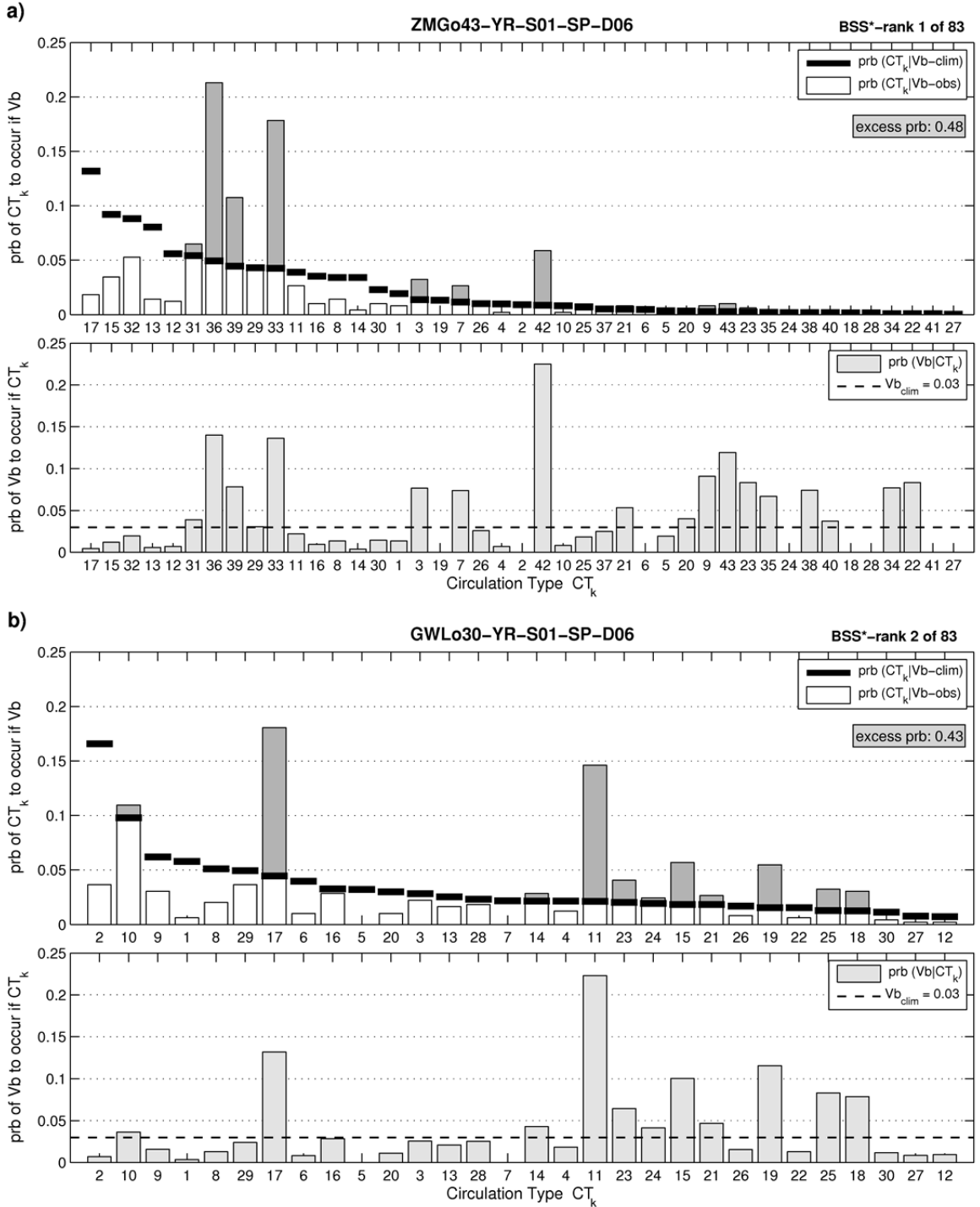


Figure 6: Ability of selected circulation classification schemes to discriminate Vb-days. a) ZMGo, b) GWLo (please see Table 1 for abbreviations). Upper panel: Conditional probability of occurrence of CT_k for detected Vb-events (Vb-obs) and for Vb-climatology (Vb-clim). Probability above climatology is summed up to excess probability. Lower panel: Conditional probability of the occurrence of Vb for a given CT_k . (see section 3.3. for more details)

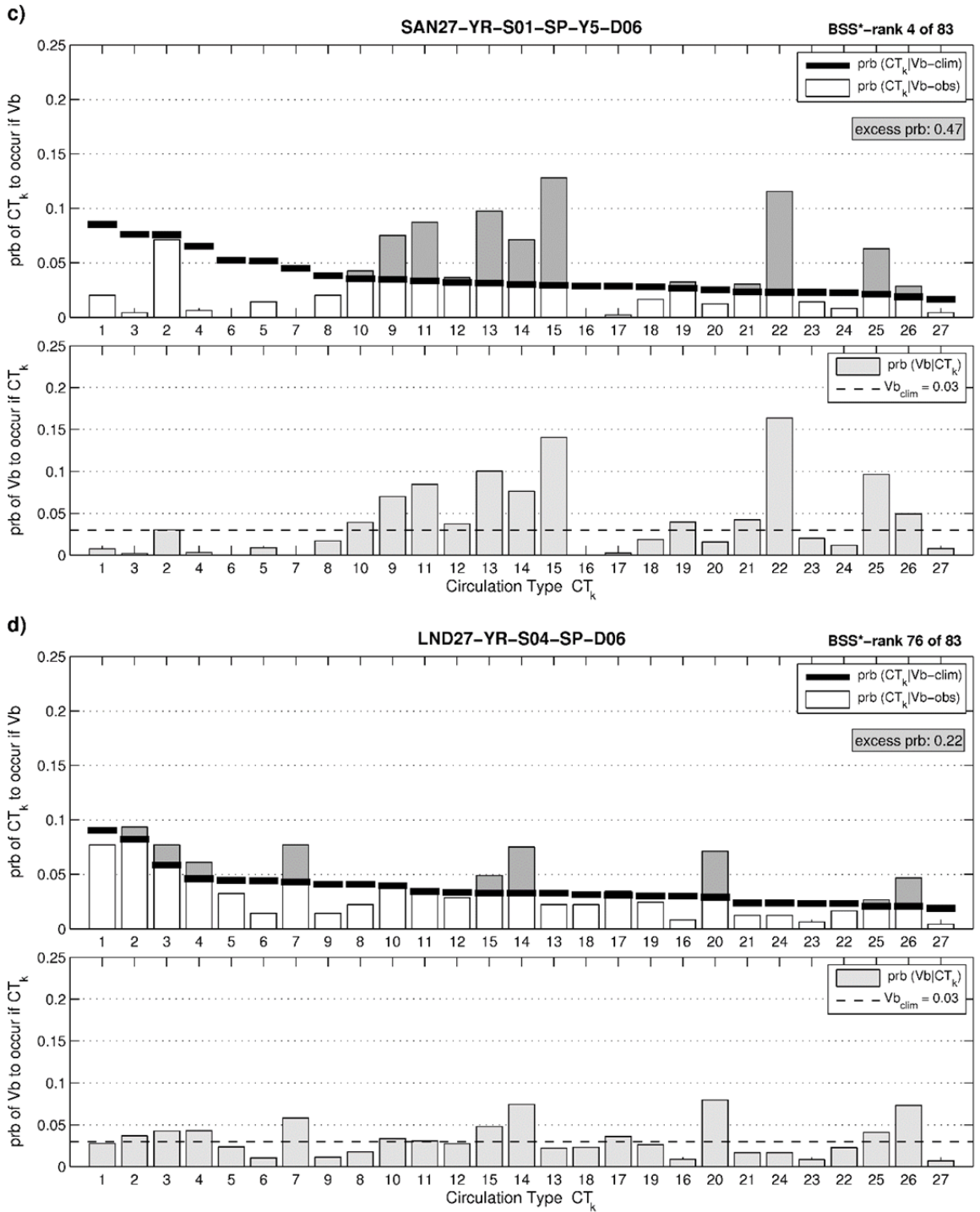


Figure 7: Same as figure 6 but for c) SAN and d) LND.

2.4.5 Comparison ERA-40 with ERA-Interim

For the years 1989 to 2001, a comparison of main climatologic characteristics of Vb, Vcd and NST tracks between ERA-40 and ERA-Interim has been done and will be described in the following without showing any figures. The annual number of Vb-tracks is very similar in both reanalyses and only differs for individual tracks that could not be found in one or the other data. Similar results are obtained when analysing Vcd- and NST tracks which is mainly due to using ERA-Interim and ERA-40 at the same spatial resolution. In another study by Akperov and Mokhov (2010), where cyclones had been tracked in both reanalyses at their initial resolution, more cyclones were detected in ERA-Interim than in ERA-40 for example. The track densities of all track types are also similar in both reanalyses. The biggest difference between both data sets appears to lie in the mean seasonal cycle of Vb-tracks where ERA-Interim shows a lower number of tracks occurring from May to July (-30%). Another interesting feature is the underestimation of the inter-annual variability of Vcd-tracks in ERA-Interim (3.4/y compared to 4.4/y), for which no profound assessment could be done.

2.5 Conclusion

In this study, an automatic cyclone tracking procedure has been applied and a systematic approach has been developed to classify three major cyclone track types over Central Europe from ERA-40 and ERA-Interim. These track types are based on the early work of Van Bebber from 1891: Vb, Vc or Vd (“Vcd”) and the new NST-type referring to cyclones which were detected in the study region (Figure 3), but for which no specific or unique propagation path could be assigned. The analysis is based on tracking isolated minima of the geopotential height on the pressure level at 700 hPa in time, contrary to the approach of Van Bebber where the focus was on tracking isolated minima at surface level pressure (SLP). This new approach was chosen to avoid erratic or even discontinuous tracks which may arise from weak or fairly disturbed pressure signals when using SLP in a region with complex topography, especially in the summer season. Of all seasons it is exactly the summer season when cyclones on Vb track are of greater relevance for flood risk in Central Europe due to the higher atmospheric water content.

Results show that especially track type Vb is quite a rare event in Europe, as only 3.5 events (12 days) per year with a lifetime of 3.4 days could be detected. However this corresponds to a total of 146 cases, only very few events could be found in literature. This leads to the assumption of highly subjective notions and preconception in connection with the issue of Vb-tracks, when only those events are recorded that go along with extensive precipitation or massive flooding. Regarding the seasonal cycle, a primary maximum can be seen in spring (April-May) for all types, with a secondary maximum in autumn for types Vb and Vcd (Figure 4a). The track density analysis shows a region with enhanced activity near the Gulf of Genoa for all track types, emphasizing the importance of this region in the genesis of cyclones and their propagation path (Figure 5).

From the comparison of Vb-tracks with 83 CTCs, the hypothesis of Fricke and Kaminsky (2002) can definitely be supported: Vb-tracks are included in one or the other stationary circulation pattern, but to which extent this is the case depends on the specific characteristics of any CTC. Schemes with the largest skill in this regard are subjective/manual ones (e.g. ZAMGo43, GWLo30 or SUEo; see Table 1 for acronyms),

demonstrating the ability to enhance relevant synoptic phenomena instead of emphasizing mathematic criteria for classification.

Objective CTCs appear to perform better when a larger number of classes (27 or 18 vs. 9) is used and sequencing seems to result in loss of discrimination power due to blurring. In accordance with the findings of Beck et al. (2010), we also conclude that the position and extent of the region where the CTC has been derived is of major importance and should be calibrated to the spatial/temporal characteristics of the phenomenon under investigation. When using geopotential height or relative vorticity at 500 hPa (Z5 or Y5) additionally to SLP in the CTC, a clear improvement could be seen for SAN in case of Z5 as well as for LND and CAP in case of Y5. However, this advantage is totally missing when 4-day sequencing is used.

Lauscher's manual/subjective Vb classification showed somewhat sobering results, although the criteria for this verification were set on a rather low level. Only 15% of all Vb-tracks were detected by the classification and only 23% of all Vb-days in Lauscher's record could be confirmed from the relevant tracking procedure. Reasons for that may be the lack of objective criteria, the focus on extreme precipitation events, inhomogenities in time due to switching observers or the mixing of kinematic and stationary aspects in the classification itself.

For the first time, an objective catalogue with the famous cyclone track Vb and its climatology is now on hand for the period 1961-2002 based on ERA-40. These events have been determined by tracking minima of the geopotential height at 700 hPa. Although this approach signifies a considerable improvement in the recognition of systems with a weak or disturbed surface signal especially in the summer season, it possibly fails for developing cyclones with a large tilt in vertical structure so that the track does not match the criteria for Vb at 700 hPa. We conclude that a combined tracking on different levels would be beneficial for the Vb-issue, possibly leading to the recognition of some additional events (~9%). We also address the need for a more thorough definition of what exactly is meant by a Vb-event in one or the other study, to allow for comparability of the results. Nevertheless, this new cyclone track catalogue will serve as an essential and valuable basis to further improve our knowledge about the issue of Vb. Especially the Vb cyclone track catalogue may be used as an information source for, inter alia, climatologists, synoptic meteorologists or the hydrologic community.

3 A new classification scheme of European cyclone tracks with relevance to precipitation

Abstract

This paper proposes a new classification scheme of atmospheric cyclone tracks over Europe. The cyclones are classified into nine types, based on the geographic regions the cyclones traverse before entering Central Europe. The method is applied to ERA-40 data for the period 1961-2002, considering all significant cyclones above a relative vorticity threshold. About 120 and 80 cyclone tracks per year are identified at sea level pressure and 700hPa geopotential height, respectively. About 25% are Atlantic type cyclones, 25% emerge directly over Central Europe and another 25% originate from the lee of the Alps. The other types are less frequent (Mediterranean 12%, Polar 7%, Continental 2% and Vb 4%). The track types show distinct characteristics in terms of cyclone intensity and cyclone life stage when entering Central Europe. Cyclones of type Vb are, on average, the most intense cyclones over Central Europe and even more intense than Atlantic cyclones in summer, pointing to their potential for generating extreme precipitation. The identified cyclones account for 46% to 76% of long-term precipitation in a focus region in Central Europe. Precipitation differs significantly between cyclones, with Atlantic and Vb cyclones producing the highest and Continental and Polar cyclones producing the lowest long-term precipitation totals. The contributions of cyclone types to total precipitation show distinct spatial patterns within Central Europe. The new cyclone type catalog will be useful for identifying the relevance of specific track types for precipitation extremes in Central Europe and analyze their temporal behavior in the context of climate change.

3.1 Introduction

Mid-latitude cyclones play an essential role in maintaining the global atmospheric energy balance by the exchange, transport and transformation of mass, energy and momentum. The cyclones are associated with a range of local weather phenomena including extreme windstorms and precipitation. As early as 1891 van Bebber recognized the role of a specific cyclone track type in generating heavy, large-scale precipitation and winter snowstorms in Central Europe (*van Bebber*, 1891). He attributed several of these events to cyclones that propagate from northern Italy to Poland, leaving the Alps on the left (type Vb, read “five b”). His analysis was based on manually tracking barometric minima over time from surface weather maps for the years 1876-1890, resulting in one of the first subjective classifications of cyclone tracks in the Atlantic-European region. Some of the most devastating European floods have indeed been associated with Vb or similar type cyclones such as the August 2002 flood (Ulbrich et al., 2003) and the June 2013 flood (Kummler, 2014; Schröter et al., 2014; Blöschl et al., 2013), as well as with Vc-type cyclones in eastern Europe (Apostol, 2008). The Vc type is less well known and represents all cyclones propagating from south of the Alpine ridge straight to the east. Renard and Lall (2014) related floods in Mediterranean France to geopotential heights and found the temporal flood variability to be associated with a particular spatial pattern in the geopotential heights. On the other hand, gale-force winds in western-Continental Europe are usually caused by cyclones that propagate from the north-eastern Atlantic into Europe (Hanley and Caballero, 2012; Donat et al., 2010), such

as storm Kyrill in January 2007 and storm Lothar and Martin in December 1999 (Roberts et al., 2014). Clearly, the geographical region from where a cyclone enters Europe plays an important role in generating specific weather extremes.

One of the earliest classification studies (apart from van Bebber's) focusing on dominant paths of cyclones in the northern Hemisphere was carried out by Klein (1957). In a more recent study, Davis et al. (1993) classified cyclones over the north-western Atlantic Ocean into distinct types, based on the depression's origin, track and intensification during the storm's lifetime. They defined eight types and analyzed them with regard to their potential for coastal damages. This was probably the first study that directly related the occurrence of hazardous weather events to specific classes of cyclones by considering the source regions and tracks as input information for separating types.

A more objective analysis of track types in the Atlantic-European region was performed by Blender et al. (1997), using a clustering approach to classify North-Atlantic cyclones into three groups depending on the average direction of movement of the storm ("stationary", "zonally" and "north-eastward"). Mediterranean storm tracks may also be important as pointed out by Bengtsson et al. (2006) and Hoskins and Hodges (2002), who identified a dominant cluster of intense winter cyclones ranging from the western to the eastern Mediterranean. A similar track type emerging from the North-Mediterranean and propagating to the east was identified by Dacre and Gray (2009) and Trigo et al. (1999). Horvath et al. (2008) classified North-Mediterranean cyclone tracks into four types ("Genoa", "Adriatic", "twin", "others") depending on the region of origin, and Wernli and Schwierz (2006) found most Central European winter cyclones to emerge either in the north-eastern or the northern Atlantic region.

Thus cyclones appear to occur along preferred atmospheric "streams", with distinct thermodynamic and dynamic characteristics. For example, cyclones emerging from the Genoa region are mainly deep depressions at the most intense stage (Campins et al., 2006) with a large fraction of cold-core type cyclones (Campins et al., 2011).

Notwithstanding the large number of tracking studies in the literature, we are unaware of any study that focused on different types of cyclones propagating to Central Europe. Such a stratified analysis would be very useful for better understanding the role of cyclone tracks in generating high impact weather extremes such as precipitation.

- The aim of this study is to present a new approach to classifying atmospheric cyclones over Europe and relate it to long-term precipitation totals.

The precipitation analysis focuses on Central Europe. Cyclone tracks are determined by the tracking procedure of Murray and Simmonds (1991) and Simmonds et al. (1999) with some refinements for the purpose of this study. Inspired by the early work of van Bebber (1891), the identification of track types is based on the geographic regions the cyclones traverse before entering Central Europe. The identification by region is motivated by the expectation of preferred pathways of cyclones over Europe, so called atmospheric streams. The resulting track types are analyzed in terms of within-type cyclone characteristics, including precipitation.

3.2 Developing a classification of European cyclone tracks

3.2.1 Data

In this study, ERA-40 data (Uppala et al., 2005) are used (Table 4), covering the time period January 1961 to August 2002 and with a temporal (spatial) resolution of six hours (1.125°).

Table 4: Overview of data used in this study.

data set	parameters	spatial coverage	resolution	temporal extent	source
ERA-40	Gopotential height and relative vorticity at 700hPa and 500hPa	Global	Six-hourly, T159 (~125km)	1 Sep 1957 to 31 Aug 2002	European Centre for Medium Range Weather Forecasting (Uppala et al. 2005)
WETRAX precipitation	Daily precipitation totals <i>RR</i>	Germany, Austria (Switzerland and Czech Republic in parts, see Figure 17)	Daily, 6km x 6km regular grid	1 Sep 1961 to 31 Dec 2006	Hofstätter et al. (2015)
Flood-related precipitation events	Significant precipitation: date and rank	Major Central European rivers	River catchments	1 Jan 1951 to 31 Dec 2002	Müller et al. (2009)

As atmospheric cyclones do not necessarily extend through the entire depth of the atmosphere and the vertical axis of troughs can be tilted, cyclone tracks at different atmospheric levels may be different despite being related to the same main trough. Tracks of Vb-type cyclones have traditionally been identified from sea level pressure (SLP) using hand-drawn synoptic maps. However, surface pressure patterns are strongly influenced by surface topography or boundary layer processes and may therefore contain short lived and highly variable low pressure systems, which are not relevant for significant weather events. At higher atmospheric levels, the fields tend to be smoother, so tracks are more clearly defined. To better understand the differences between levels, cyclones are investigated independently at two levels in this paper: at sea level (using sea level pressure fields, SLP) and at the constant pressure level of 700hPa (using geopotential heights Z700).

The ERA-40 data are interpolated to an equidistant 80km grid by polynomials (Akima, 1978; Akima, 1996). The final grid is centered on 5°E and 50°N, ranging from about 40°W to 50°E at 65°N, and 20°W to 40°E at 30°N. In order to exclude small-scale or spurious systems the data are filtered by a discrete spatial low-pass filter (Freser and von Storch, 2005) that removes any structures smaller than 400 km, relaxes smoothly up to 1000 km and lets all large scales pass through (see Hofstätter and Chimani, 2012). To understand the relevance of the cyclone classification for precipitation, a focus region within Central Europe is selected for precipitation analysis (Germany, Austria, parts of Switzerland and the Czech Republic). The focus region is embedded in a larger region, denoted as "Track Recognition Zone" (TRZ), to analyze precipitation with respect to the cyclone types for all cyclones moving through TRZ. Daily precipitation data on a 6km grid are used (see Table 4) which, in

case of Austria have been obtained from the Austrian Weather Service (ZAMG) (the GPARD-6 data set, Hofstätter et al., 2015) and for the remaining parts of the focus region from the German Weather Service (DWD) (the HYRAS dataset, Rauthe et al., 2013).

3.2.2 Cyclone tracking

The detection and tracking of cyclones in this paper is based on the concept of Murray and Simmonds (1991) and Simmonds et al. (1999), and modifications suggested by Pinto et al. (2005). The tracking procedure consists of four basic elements: (a) identification of significant cyclones at time t_n , (b) prediction of a subsequent cyclone position at time t_{n+1} , (c) association of cyclones between times t_n and t_{n+1} by scoring the difference between the predicted (first guess, “FG”) and all present cyclone positions (candidate points, “CP”) from the data at time t_{n+1} , and (d) removal of spurious tracks. Similar to the authors mentioned above, both closed and open depressions are considered. Additionally, the following refinements have been made in the tracking procedure: (i) The association procedure not only considers the distance between *FG* and *CP* but also the angle between the propagation vectors to *FG* and *CP*. (ii) Splitting and merging of cyclone tracks is permitted, which is of importance in the classification where the tracks are investigated with regard to their source region.

First, cyclones are identified by detecting local minima of geopotential height ϕ or air pressure p . We identify closed cyclones where pressure or geopotential height is lower than at the four surrounding grid points and open cyclones where it is lower at three grid points and equal or higher at the fourth point. As a measure of intensity, geostrophic relative vorticity ξ is used for SLP and Z700

$$\xi_{SLP} = \left(\frac{1}{\rho f} * \nabla^2 p \right) \text{ or } \xi_{GPH} = \left(\frac{1}{f} * \nabla^2 \phi \right) \quad (7)$$

where f is the Coriolis parameter and ρ is the air density. All cyclones below a minimum intensity ξ_{\min} are disregarded. This threshold is set to $3.8 \times 10^{-5} \text{ s}^{-1}$ for open and $2.9 \times 10^{-5} \text{ s}^{-1}$ for closed systems in the case of SLP, and $3.5 \times 10^{-5} \text{ s}^{-1}$ and $2.6 \times 10^{-5} \text{ s}^{-1}$ in the case of Z700. The intensity thresholds are slightly higher than those of Pinto et al. (2005) and Lim and Simmonds (2007) which is consistent with the calculation of $\nabla^2 p$ and $\nabla^2 \phi$ within a comparatively small radius of 160 km. Only the most intense open system along the same trough axis is considered in this study, whereas several systems have been considered by Pinto et al. (2005). Second, the subsequent position (first guess, “FG”) of a cyclone at time t_{n+1} is predicted through a propagation vector \mathbf{U}_{pred} , calculated as two components. The first component, \mathbf{U}_{pst} , takes into account continuity in cyclone propagation (Murray and Simmonds, 1991). For existing tracks, \mathbf{U}_{pst} is therefore set to the previous displacement vector, and for new tracks the climatological cyclone propagation at the respective grid point \mathbf{U}_{pst} is used. The climatological cyclone propagation is derived from an existing track catalog for the period 1961-2002 (Hofstätter and Chimani, 2011) and updated here by the analysis of SLP. The second component uses steering winds \mathbf{U}_{low} from the level of interest (700hPa or SLP) as well as \mathbf{U}_{upp} from the respective upper level (500hPa or 700hPa) referring to Simmonds et al. (1999). $\mathbf{U}_{\text{upp,low}}$ is estimated as the associated averaged gradient of p calculated within a radius of 320 km around the cyclone

center in case of SLP and is approximated by the geostrophic wind vector $\mathbf{U}_{\text{grd}} = f^{-1}(\hat{\mathbf{e}}_3 \times \nabla Z)$ elsewhere. The two components are weighted to obtain the predicted propagation vector \mathbf{U}_{pred} as given by Equation 8:

$$\mathbf{U}_{\text{pred}} = (1 - w_1) \cdot \mathbf{U}_{\text{pst}} + w_1 \cdot \{w_2 \cdot \mathbf{U}_{\text{low}} + (1 - w_2) \cdot (f_{\text{red}} \cdot \mathbf{U}_{\text{upp}})\} \quad (8)$$

The weight w_1 was set to 0.60 following Simmonds et al. (1999), and w_2 to 0.33 respectively, to put more emphasis on upper level winds for the latter. The reduction factor f_{red} accounts for the decrease of wind speed from upper to lower atmospheric levels (Simmonds and Murray, 1999). ERA-40 data over Europe suggest a typical ratio of 0.65 between \mathbf{U}_{grd} at GPH500 and Z700 (0.80 for Z700 and SLP). For clarity, f_{red} is set to 0.7 at both levels.

Third, cyclones are connected between adjacent time steps t_n and t_{n+1} , if the association score C is larger than a threshold. This score is a measure of consistency between the candidate cyclone positions (“CP”) and the predicted (first guess, “FG”) position at time t_{n+1} (see Figure 8).

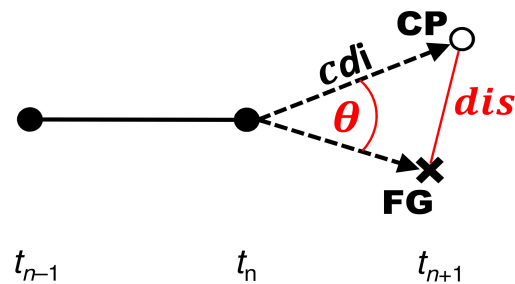


Figure 8: Schematic showing the concept of cyclone association between times t_n and t_{n+1} by assessing the distance (dis) between the predicted cyclone position (FG) and a candidate cyclone (CP), the angle (θ) between the propagation vectors (dashed) of CP and FG as well as the distance (cdi) between the cyclone position at time t_n and a CP at time t_{n+1} .

The concept of cyclone association using scores is similar to that of Murray and Simmonds (1991) and Pinto et al. (2005), with the difference that here not only the best candidate is selected to form a track, but all candidates with scores above the threshold are selected. This entails the formation of cyclone splits and/or mergers for some tracks. As another refinement, the score C is not simply the Euclidian distance between CP and FG but consists of two parts

$$C = C_{dis} + C_{dir} \quad (9)$$

where C_{dis} is related to the distance (dis) between CP and FG and varies between 0 and 1. C_{dir} is related to the angle (θ) between the propagation vectors to FG and CP and varies between -0.15 and +0.25. To avoid poorly defined angle scores for slowly moving cyclones, C_{dir} is reduced to zero if the distance between CP and the cyclone location at time t_n (see Figure 8) approaches zero (Equation 12). In this work C_{dir} is introduced to put more weight on a correct prediction of the propagation direction, to avoid cases where a similar distance would lead to the same result although the direction might be very different. The threshold of C , above which CPs are accepted to be connected to form a track, was set to 0.5 as a

result of extensive testing and comparison of tracks with well documented case studies. The scores are calculated by Equation 10-12:

$$C_{dis} = \begin{cases} \left[1 - \left(\frac{dis}{d_{max}} \right)^2 \right]^{2.5} & (0 \leq dis \leq d_{max}) \\ 0 & (\text{otherwise}) \end{cases} \quad (10)$$

$$\text{with } d_{max} = 450\text{km} + \left[255\text{km} * \tanh \left(\pi * \frac{\phi}{360} \right) \right] \quad (0^\circ \leq \phi \leq 90^\circ) \quad (11)$$

$$C_{dir} = \left[0.25 - \left(\frac{\theta}{450} \right) \right] * \tanh \left(\pi * \frac{cdi}{450} \right) \quad (0^\circ \leq \theta \leq 180^\circ) \quad (12)$$

where the units of d_{max} , dis and cdi are km. Other studies used a constant value of the maximum association radius d_{max} such as 420 km (Zahn and Storch, 2008). In Equation 11, however, the maximum distance depends on the latitude ϕ , with values between 515 km and 604 km (at 30°N and 80°N resp.), to account for faster moving cyclones at higher latitudes (e.g. Hewson and Titley, 2010) as higher velocities usually imply larger prediction errors of FG. In Equation 10-12, a distance error of, say, 160 km for a cyclone at latitude of 50°N ($d_{max} = 555$ km) gives $C_{dis}=0.8$, and a directional error of, say, $\theta = 45^\circ$ and $cdi=450$ km gives $C_{dir} = 0.15$. This would result in an overall association score of $C = 0.95$, which is above the minimum threshold of 0.5, so the candidate point would be connected. Although Equation 10-12 is adapted to the ERA-40 data, it can be readily applied to other data at different spatial resolutions by changing the intercept parameter in Equation 11 from 450 km to 550 km for the NCAR-NCEP1 data (Kalnay et al., 1996), and to 350 km for the ECMWF-ERA Interim data (Dee et al., 2011) as has been tested in this study (not shown).

In a last step, all tracks are screened to identify and remove very unlikely tracks. Such tracks may be the result of weak gradient situations with several ill-defined cyclone centers moving around slowly and/or erratically. A second type of spurious tracks occurs at SLP near major orographic features when a strong flow aloft generates quasi-stationary troughs. Other studies (e.g. Sinclair, 1994, 1997) removed all “non mobile cyclones”. However, as the region over northern Italy is one of the most important cyclogenesis regions in Europe (Trigo et al., 2002; Campins et al., 2011), in this study such tracks are detected and excluded in a more selective way. A track is considered as spurious if all of the following criteria apply: (i) short living (≤ 48 h), (ii) weak intensity (ξ smaller than 33th percentile of all cyclones at the respective level), (iii) a short total track length (<1000 km), (iv) low average cyclone velocity (<38 km h⁻¹), (v) frequent large changes of propagation direction (>60° on average per track), (vi) track endpoint located close to the starting point (<500 km). This method eliminated 17% of all tracks at SLP (11% at 700hPa). Almost all of them are located within well-defined regions south of the Alpine ridge over the Ligurian Sea, north of the Alps over southern Germany or in the vicinity of the Carpathian Mountains in Romania (not shown).

3.2.3 An illustrative example

To illustrate the cyclone detection and tracking procedure, Figure 9 shows the tracks associated with a major Central European flood event in August 2002, with the day and time in UTC (ddhh) indicated.

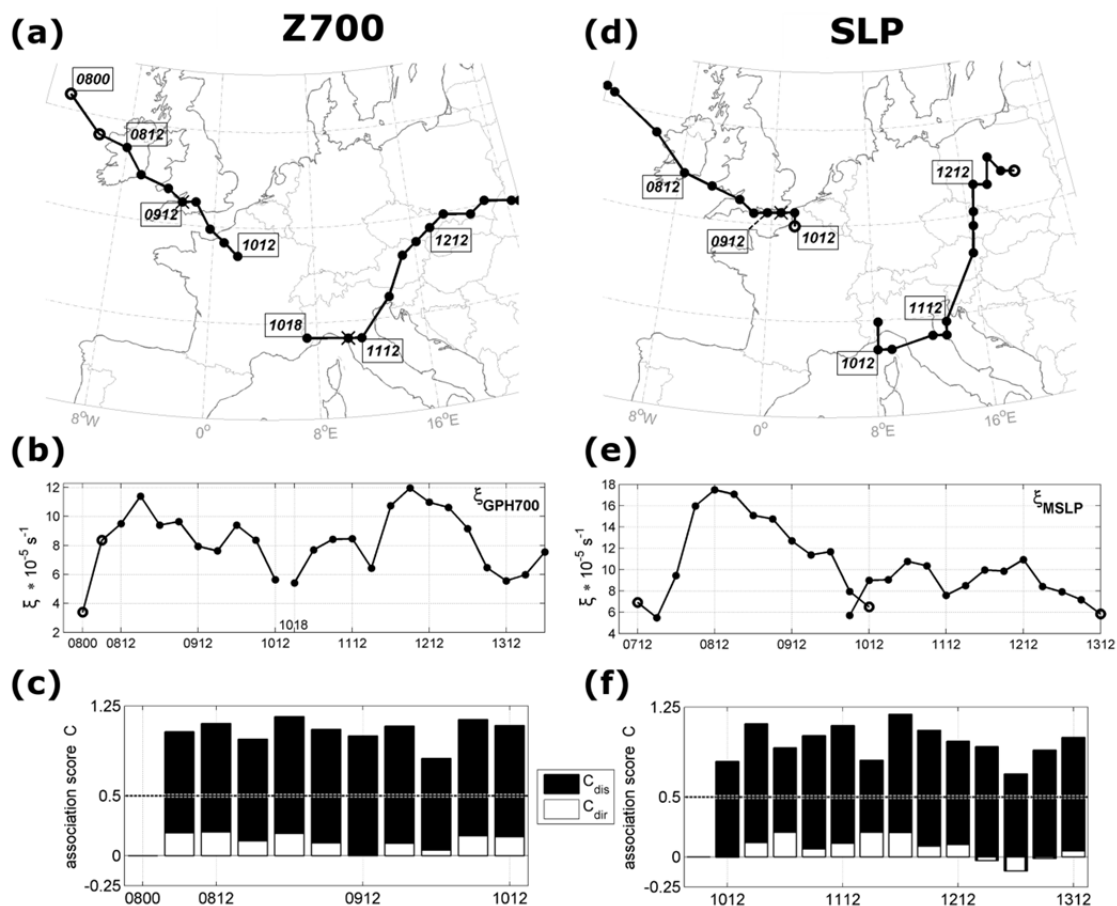


Figure 9: Cyclone track analysis for the devastating Central European flood event in August 2002 at Z700 (a)–(c) and SLP (d)–(f).

(a) and (d) Individual tracks with corresponding day and time in UTC (ddhh). Full and open circles indicate closed and open depressions, respectively. Positions where cyclones were found at two time steps are indicated by crosses. (b) and (e) Time series of relative vorticity (Equation 7). (c) and (f) Association score C (Equation 9) for the tracking of the first track at 700hPa and the second track at SLP. The score is partitioned into directional (white) and distance (black) components. Dotted line indicates threshold $C_{min} = 0.5$ for connecting candidate points.

The event is characterized by two individual tracks at both levels (top panels) interrupted at 12 UTC on the 10th of August. For SLP (Figure 9(d)) this finding is consistent with Ulbrich et al. (2003) who also identified two separate cyclones. At the level of 700hPa (Figure 9(a)) the tracking routine also appears correct in providing two separate tracks, as the cyclone approaching from the Atlantic had weakened over the British Islands and was followed by a secondary cyclone developing in the lee of the Alps (Figure 9(b)). A further interesting case is point 00 UTC on the 13th of August at SLP (Figure 9(f)) where the distance is well predicted ($C_{dis} = 0.78$) but the direction is more than 120° off, as the cyclone changes its direction sharply. This results in a negative directional association score ($C_{dir} = -0.14$), reducing the total score considerably although CP and FG are close to each other. Clearly, direction adds

important information to the total score, even though the total score is still above the threshold in this particular case.

3.2.4 Synoptically based classification

In this section, all cyclones reaching Central Europe (CE) are classified into nine types, motivated by the expectation of preferred pathways of cyclone movement over Europe (Table 5).

Table 5: Cyclone track types.

Priority	Acronym	Type
1	Vb	van Bebber's type "five-b"
2	X-N	Northward propagation, emerging from <i>nas*</i> or <i>med*</i>
3	X-S	Southward propagation, emerging from <i>nas*</i> or <i>med*</i>
4	MED	Mediterranean
5	STR	Subtropical
6	ATL	Atlantic
7	POL	Polar
8	CON	Continental
9	TRZ	"track recognition zone" All tracks emerging within TRZ (except Vb, X-N, X-S)

Separate geographical regions are defined and it is then checked whether a cyclone traverses a certain region just before moving over CE. In this study, CE is represented by a "Track Recognition Zone" (TRZ) which is set to 0.5°E to 23.9°E and 42.3°N to 56.2°N. Only those cyclones are considered in the following that are located in TRZ for at least 18 hours. The main idea of this geographical separation is the definition of reasonably homogeneous areas with distinct climatic features, such as surface characteristics (ocean, land, major mountain ridges) and latitude. The separation of cyclones approaching from such different regions should therefore allow the identification of track types that are systematically linked to high impact weather events. Vb-type cyclones, for example, often develop over Genoa, very close to TRZ, and should therefore exhibit a higher relative vorticity than other track types when crossing CE

The regions used in the classification (Figure 10) consist of the Subtropical, Atlantic, Polar, Continental and Mediterranean regions defining five track types (STR, ATL, POL, CON and MED) which all enter TRZ from outside. Another two track types, X-N and X-S, include cyclones emerging from one of the major source regions "*nas**" or "*med**" (northern Adriatic Sea or Mediterranean Sea) located inside TRZ. These rather small regions are important in terms of preferred Alpine lee-side cyclogenesis (Buzzi and Tibaldi, 1978, Pichler and Steinacker, 1987, Trigo et al., 1999; Trigo et al., 2002; Campins et al., 2011). Type X-N cyclones move to the north over the first 24 hours in contrast to X-S cyclones moving to the south during the initial phase. The eighth class includes Vb cyclones which propagate from

the region around northern Italy towards Poland, leaving the Alpine mountain range on the left (Figure 10b). Based on van Bebber's definition, three areas, " $x_{(t_0)}$ ", " $x_{(t_n)}$ ", and "in" are defined (Figure 10(b)), and the criteria for tracks to be classified as type Vb are chosen as follows (all criteria must apply):

- i. The track is within area " $x_{(t_0)}$ " for at least one time step (4°E to 17°E; 42° to 46°N).
- ii. At any later time step, the track appears in area " $x_{(t_n)}$ " (14°E to 20°E; 47°N to 55°N).
- iii. Any time between located in " $x_{(t_0)}$ " and " $x_{(t_n)}$ " the track appears in area "in" (12°E to 22°E; 46°N to 52°N).
- iv. There is an overall movement from west to east between " $x_{(t_0)}$ " and " $x_{(t_n)}$ ".

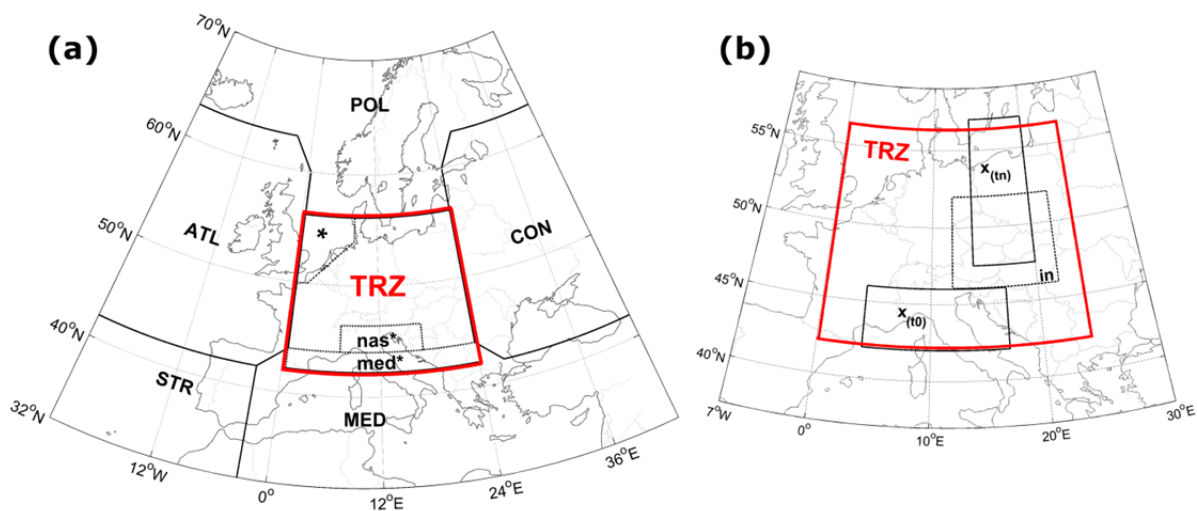


Figure 10: Regions used for the classification of cyclone tracks: (a) Geographical regions determining nine different track types. TRZ (Track Recognition Zone). The small area (*) in the northwest of TRZ indicates a region where newly emerging cyclones are assigned to POL or ATL, depending on the initial propagation direction. (b) Regions defining track type Vb following the original route of van Bebber (see main text for details).

The ninth class, TRZ, includes all tracks originating inside region TRZ which cannot be attributed to any other type. An exception are cyclones emerging in the small area (*) in the northwest of TRZ (Figure 10a) which are assigned to POL or ATL, if the average propagation direction in the first 18 hours is between 145° and 235° or 45° and 135°, respectively.

The nine track types are assigned according to priority. Because of their relevance for flooding in Central Europe, Vb is set as the highest priority. Therefore, the tracks are first tested whether they qualify for type Vb. If not, the track is subsequently tested for the other types (see Table 5). Track types X-N and X-S are set as priorities two and three, respectively, because they originate from important cyclogenesis regions close to CE.

In case of a track-complex, including cyclone mergers and/or splits, only the branch with the highest priority (Table 5) is considered. For example, if a track T_i includes a single split, the track type is assessed for each of the two sub-tracks T_{i1} and T_{i2} (Figure 11) independently, followed by identifying the primary track type by priority and only retaining the primary branch. Hence, all tracks considered in the following are single paths without branches.

Finally, due to their very low number, STR tracks are not considered further in the statistics of this paper.

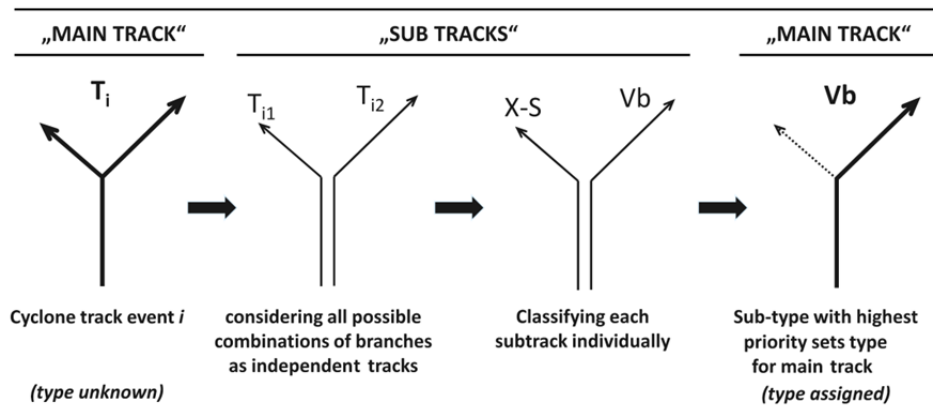


Figure 11: Procedure for identifying track type for split tracks (analogously for merge tracks).

3.3 Track type characteristics

The new track type catalogue offers a range of opportunities for investigating track type processes and impacts. In this section, the analysis focuses on selected climatological characteristics of the track types.

3.3.1 A brief climatology of tracks types

The climatological track frequency and mean propagation direction for each track type at 700hPa are shown in Figure 12 and 13. Track frequency (shown as colors) is calculated as the number of cyclones that have been recognized at each grid point during the period 1961-2002 for each track type. Yellow and red cells refer to areas with a particularly large number of track passages, i.e. hot spots. Arrows, indicating the mean direction of cyclone propagation, have only been plotted for track frequencies above a threshold. ATL-type cyclones usually approach directly from the north-eastern Atlantic turning to the northeast over CE, with a pronounced frequency maximum over the southern parts of the North Sea. In contrast, Polar tracks (POL) have their maximum over Denmark with a clear propagation from northwest to southeast. For track type TRZ there is no clear hot spot apparent, unlike most other types. A closer look at the synoptic situation during several major TRZ track events revealed that many of these cyclones originate over CE at SLP, induced by a major upper level trough located over western Europe. This also explains the strong northward component in the propagation of type TRZ cyclones.

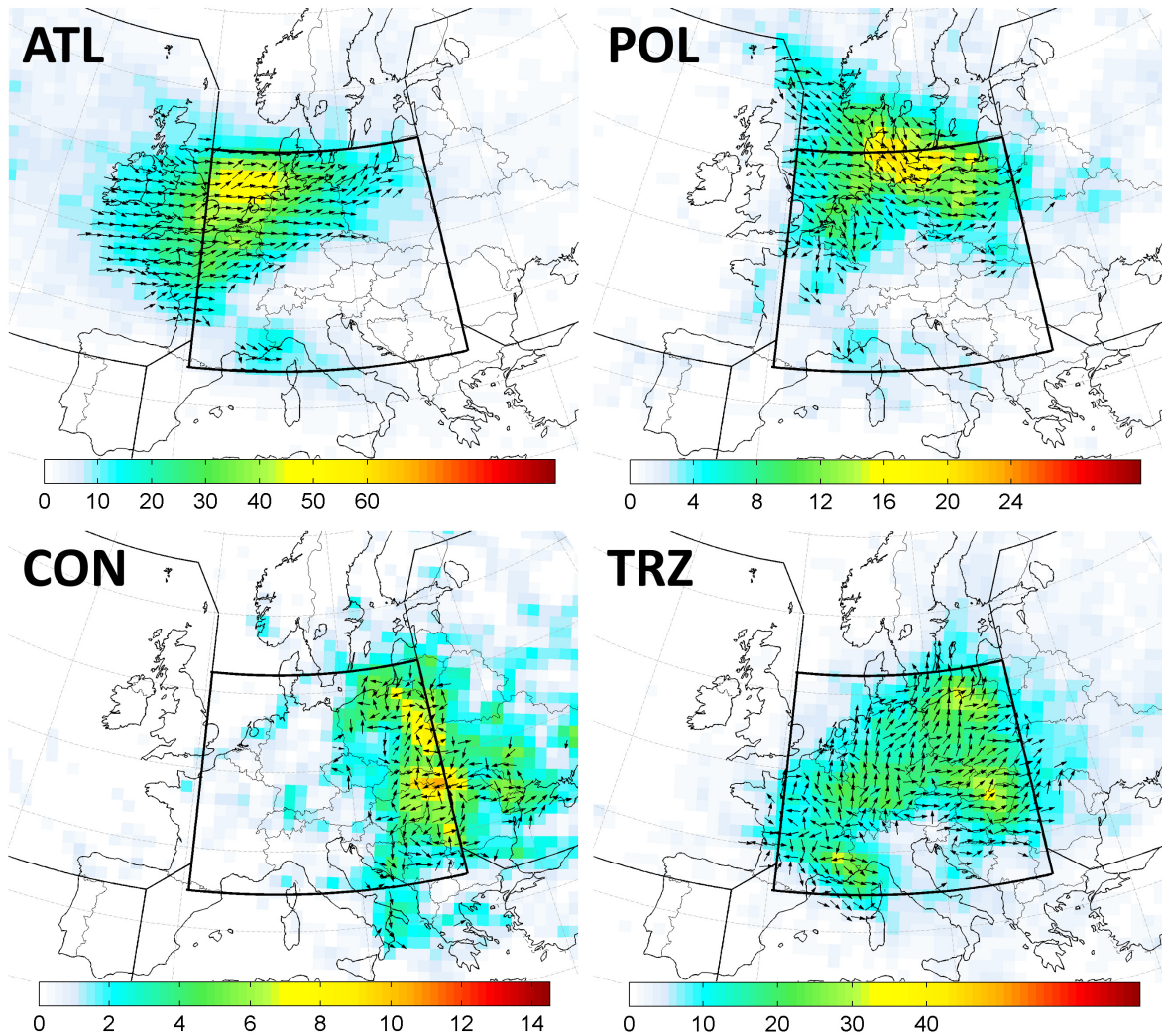


Figure 12: Track frequency (colors) for cyclone track types ATL, POL, CON and TRZ at 700 (ERA-40, 1961-2002). Arrows indicate the mean direction of cyclone propagation. Numbers next to color bars indicate total number of cyclones recognized at a respective grid point for each track type in the analysis period.

The frequency map for Vb-type cyclones (Figure 13 top left) demonstrates that the current classification is very close to the original Vb path as defined by van Bebber in 1891. These cyclones emerge between the first frequency maximum near the Gulf of Lion and northern Italy and propagate to the northeast bypassing the eastern Alps, as intended by the classification (Figure 10b). Interestingly, there is a second maximum of cyclone frequency to the lee of the eastern Alps (western Hungary/ Slovakia). This maximum might be related to a secondary cyclogenesis region in the eastward lee of the Alps, which has not been mentioned by other authors so far, presumably because this feature can only be seen when focusing on Vb-type tracks alone.

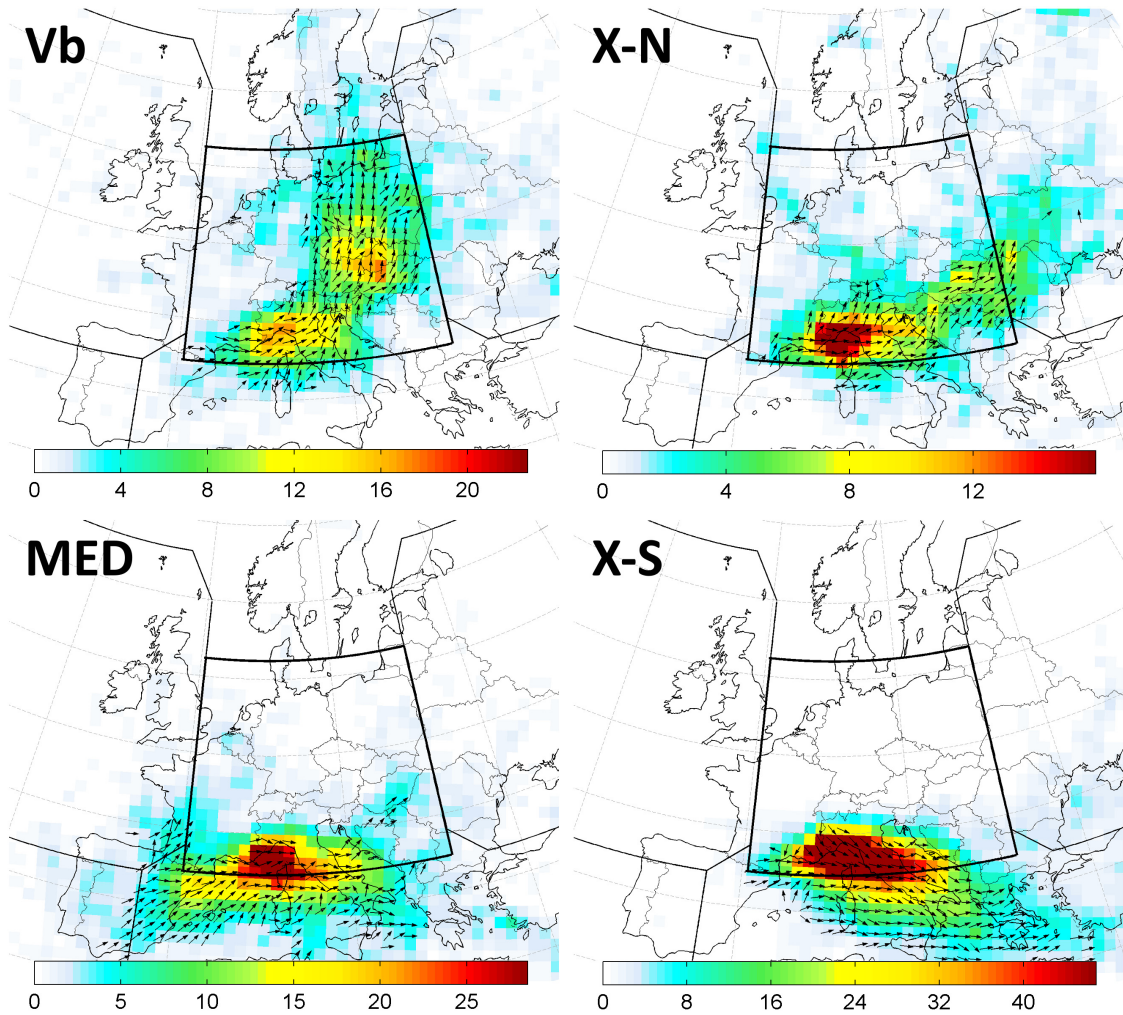


Figure 13: As Figure 12 but for cyclone track type Vb, X-N, X-S and MED at Z700 (1961-2002).

The frequency map for type X-S (Figure 13 bottom right) shows a very distinct region with numerous cyclone tracks over north-western Italy. These cyclones directly emerge on the leeside of the European Alps and propagate to the east into Eastern Europe or to the southeast into the eastern Mediterranean Sea (see also Figure 14). The general propagation of X-S tracks is very different from that of type X-N. This is worth noting as these types are separated only by their mean propagation direction during the first 24 hours, with no restrictions related to the subsequent movement. Overall, the typical propagation directions shown in Figure 13 correspond very well with a manual composite of propagation vectors for the western Mediterranean (Campins et al., 2011) as well as with those presented by Trigo et al. (1999). Track frequency maps for SLP (not shown) are similar to those at 700hPa with the main difference that cyclones tend to move around major orographic features such as the Alps. Figure 14 shows the tracks of all cyclones by track type.

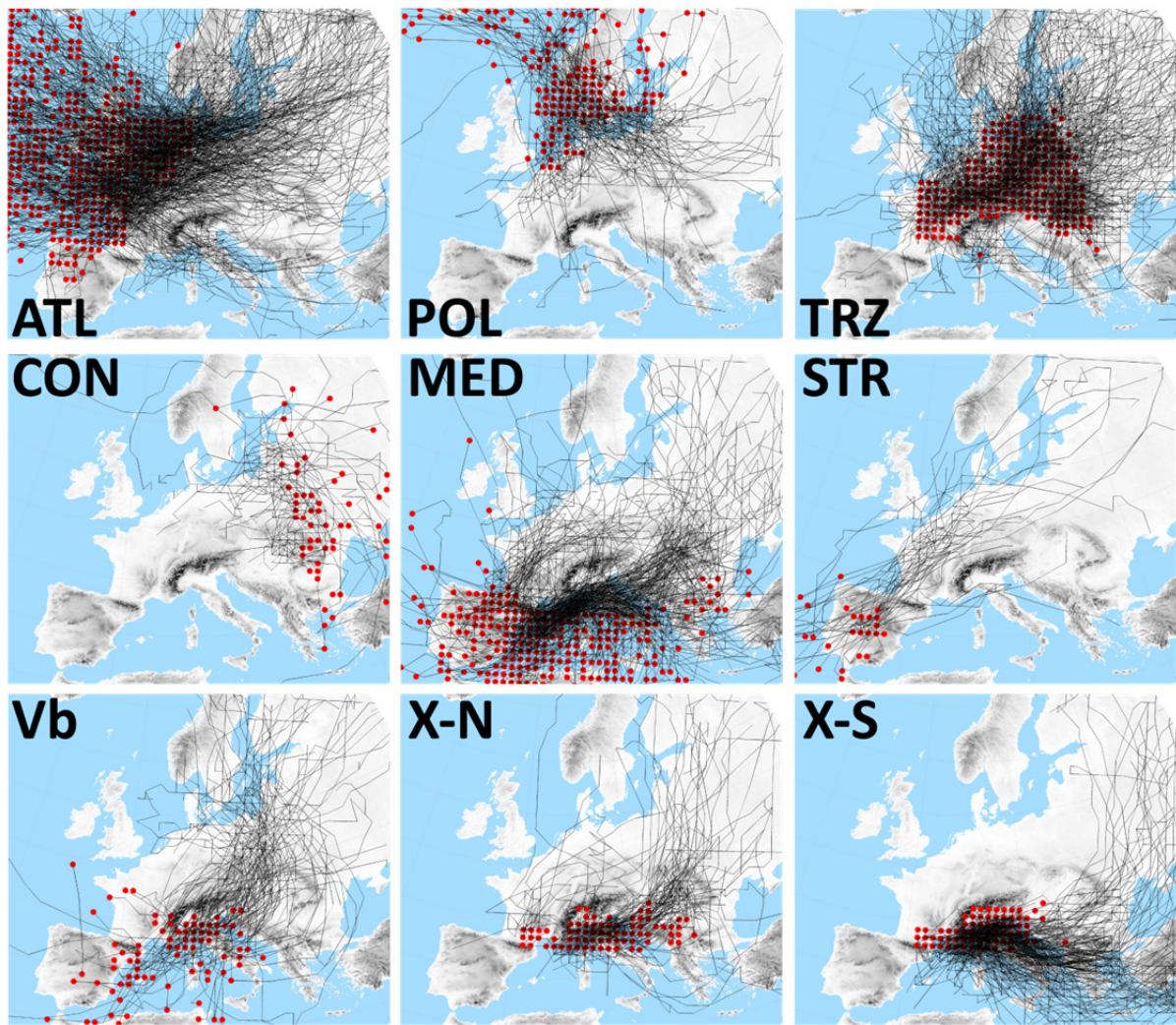


Figure 14: Members of the cyclone track types (SLP, 1961-2002). Red dots indicate the point of first detection of individual tracks.

The mean annual number of cyclones per track type is presented in Table 6. On average, about 122 tracks per year are found at SLP and 83 tracks per year at Z700 over CE. The smaller number of tracks at Z700 is due to the smoother pressure patterns, despite the same spatial resolution and the pre-filtering. Mountain ranges such as the Alps, Pyrenees and Dinaric Alps, have a significant impact on the atmospheric flow, particularly at low levels (Smith 1979), affecting the number and track locations of cyclones over Europe (Egger and Hoinka, 2008). As regards the different track types, about 50% of all cyclones approach from the Atlantic to CE (type ATL, about 25%) or emerge directly over CE (type TRZ, about 25%). A substantial number of cyclones is of type X-S (about 20%), which are usually inside CE only during the first few time steps, i.e., in the initial phase. The remaining 30% of Central European cyclones consist of the other types X-N, MED, Vb, CON and POL. The number of SLP cyclone tracks originating within the region nas* or med* (type X-N, X-S and Vb) south of the Alpine ridge is about 36 tracks per year, which corresponds very well with the number of cyclogenesis events found by Campins et al. (2011) around the Genoa region with about 37 events per year. Table 6 also gives the frequencies of the strongest 10% of the cyclones (intensity $\xi > 90^{\text{th}}$ percentile). About 40% to 55% of strong cyclones follow ATL-type tracks, which corresponds well with synoptic observations. For almost all of the other track types,

the frequency is much lower (POL, MED, CON, X-N, X-S), except for Vb where the relative frequency of strong cyclones is significantly higher than for all cyclones (7% as opposed to 3% at SLP, and 13% as opposed to 5% at Z700).

Table 6: Cyclone track frequency^a.

	Mean annual number		Frequency			
	Z700	SLP	Z700		SLP	
			all	strong	all	strong
ATL	21.8	27.7	26%	40%	23%	54%
POL	7.2	6.5	9%	10%	5%	7%
CON	2.5	1.6	3%	4%	1%	2%
TRZ	20.2	32.6	24%	14%	27%	7%
Vb	4.1	3.1	5%	13%	3%	7%
X-N	4.6	7.7	6%	4%	6%	2%
X-S	14.8	25.2	18%	10%	21%	9%
MED	7.4	17.3	9%	5%	14%	12%
Total	82.6	121.7	100%	100%	100%	100%

^aFrequencies (number of tracks for a type per total number of tracks) are given for all cyclones (all) and for strong cyclones (intensity $\xi > 90^{\text{th}}$ percentile) separately, rounded to percent integers. ERA-40 data (1961-2002).

3.3.2 Intensity characteristics

Here, selected climatological characteristics of cyclone intensity in terms of central air pressure and relative geostrophic vorticity are presented. The track types are investigated with respect to their life-cycle stage when entering CE. For all cyclones, six-hourly tendencies of vorticity and pressure are averaged over the first 24-hours after a cyclone has entered TRZ. All cyclones with a significant ($>75^{\text{th}}$ percentile) change, in both tendencies, are grouped into either “intensifying” or “decaying”. To be classified into the former group, both falling pressure and increasing vorticity must occur, and vice versa for the latter group. About 10% of all cyclones at each level are classified as significantly changing. The results (Figure 15) show that cyclones of type Vb, X-N, X-S or TRZ are usually intensifying when entering CE. Cyclones of type Vb, X-N and X-S (i) strongly intensify over, and (ii) originate from around the western Mediterranean Coast between the Rhône Valley and the Gulf of Genoa (not shown). As X-N and Vb cyclones move straight through or close by CE right after their intensification, they are expected to be closely related to high-impact weather events in CE. In contrast, most significantly changing cyclones of track types ATL, CON and POL are already at a decay stage over CE, which is related to their genesis outside CE (e.g., Wernli and Schwierz, 2006). The relative frequencies of the life cycle stages (intensification, decay) do not depend very much on the season, but appear to be an overall characteristic feature of the individual track type (not shown).

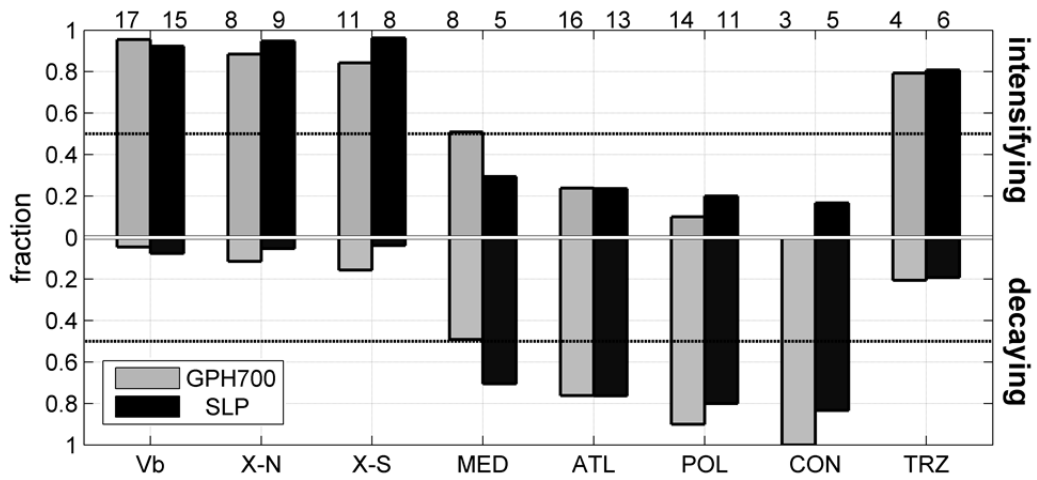


Figure 15: Fraction of cyclones that significantly intensify (upward bars) and decay (downward bars) during the first 24 hours after entering Central Europe (region TRZ) of all tracks with a strong change in both central pressure and relative vorticity. Numbers on top indicate the sample size as percentage for each track type.

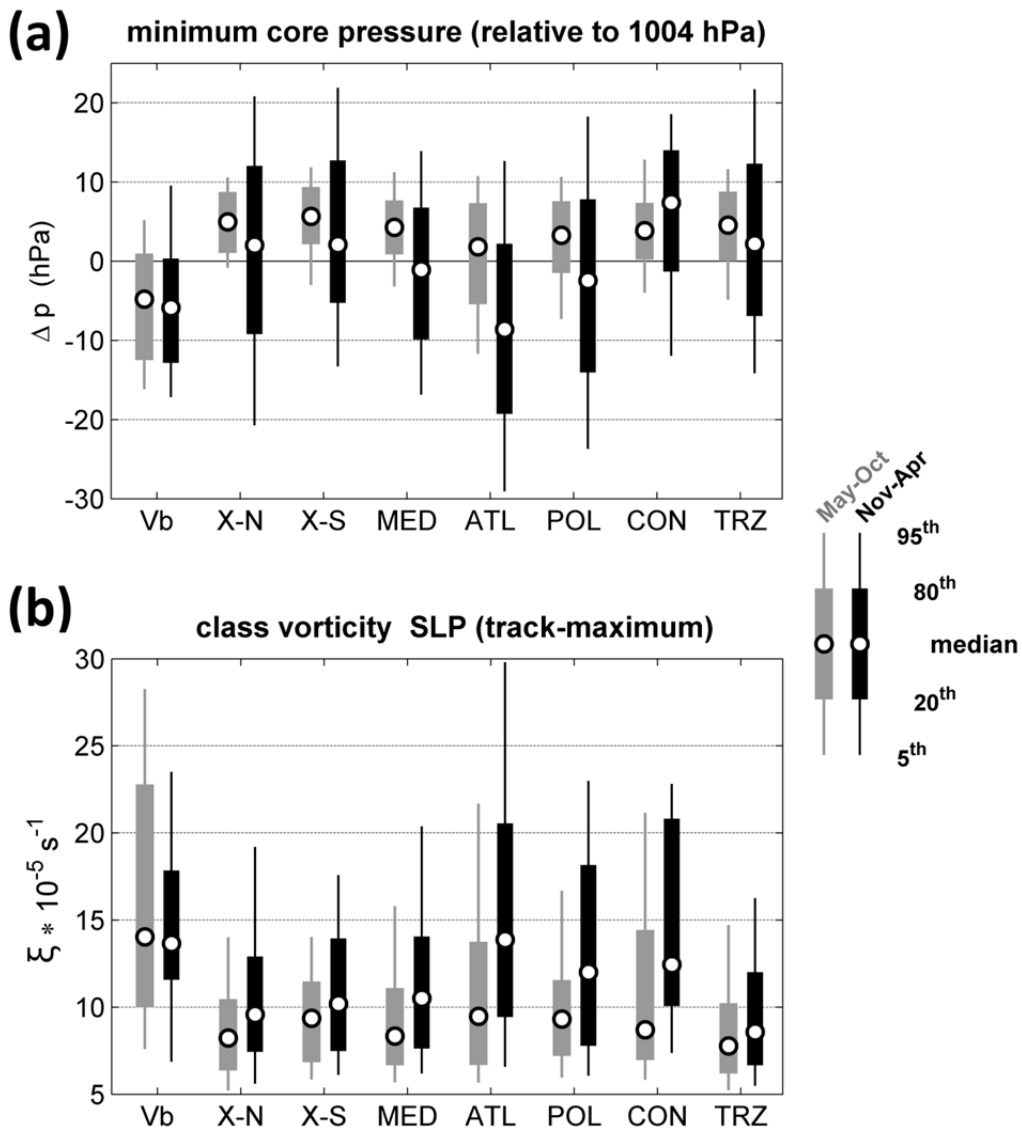


Figure 16: Climatological characteristics of cyclone track types at SLP in region TRZ (grey: May-Oct, black: Nov-Apr). (a) minimum core pressure and (b) maximum relative vorticity.

The fraction of intense cyclones is remarkably high for certain track types as shown before (Table 6), suggesting systematic differences in cyclone intensity between the types. Therefore minimum central pressure and maximum relative vorticity of the cyclones during their location within TRZ are investigated in more depth for SLP (Figure 16). In winter (Nov-Apr, black bars) Atlantic and Vb-type cyclones are the most intense ones on average (low pressure, high vorticity), followed by CON and POL. However, ATL cyclones are usually stronger over the Atlantic Ocean than over Central Europe (not shown). The most striking finding is the exceptionally high intensity of track type Vb during the summer half-year (May-Oct, gray bars). The 80th percentile of the relative geostrophic vorticity in summer is even above the corresponding value of ATL winter cyclones. Clearly, Vb-type cyclones are not only among the most intense and deepest Central European cyclones, but particularly strong in the summer season. This may explain why Vb-type cyclones have been related to the most devastating floods in CE in recent decades, all of them occurring in the summer season, when equivalent-potential temperatures are usually high. However the processes causing Vb cyclones to develop so strongly in the warm season are not fully clear, as the upper level steering flow over CE is significantly stronger in winter. Interestingly, Trigo et al. (2002) found that cyclones evolving from the region of Genoa, such as the Vb type, are more intense in winter mainly due to dynamic forcing between the Alps and the atmospheric flow, whereas low level baroclinity plays a secondary role. They also observed a large number of significant summer cyclogenesis events in the region of Genoa, often when the upper level dynamic forcing acted at the time of the local thermal daily maximum in the late afternoon, especially in August (Trigo et al., 2002). This corresponds with the findings of Aebischer and Schär (1998), with latent heating at low to intermediate levels, resulting from water vapor condensation, contributing significantly to frontogenesis and cyclogenesis on the lee-side of the Alps over northern Italy. High equivalent potential temperatures over northern Italy over the Po Plain may therefore be an essential prerequisite for the formation of exceptionally strong cyclones evolving in the summer season over northern Italy.

3.4 Precipitation related to track types

The classification scheme of cyclone tracks can be used for a range of analyses relevant to regional hydrology. Here, for space reasons, only a brief analysis with respect to long-term precipitation totals as well as selected flood events is presented as a proof of concept. More detailed analyses will be presented in future publications.

3.4.1 Long-term precipitation totals

In a first analysis we examine the effect of the cyclones on precipitation totals in the focus region (Germany, Austria, parts of Switzerland and the Czech Republic). During the time a cyclone was within TRZ, daily precipitation from the HYRAS and GPARD-6 data at a given grid point was assigned to that track type and accumulated over all cyclones of the same type, irrespective of the level. Precipitation of less than 1mm per grid-point and day has been disregarded. If a cyclone was located within TRZ only for a part of a day on a given date (6, 12 or 18 hours), daily precipitation was weighted according to the fraction of time (0.25, 0.5 or 0.75). The results of this analysis are eight maps of precipitation totals during 1961-2002 associated with the nine track types. As indicated earlier (Table 6) an average of 83 and 122 cyclones per year have crossed Central Europe as identified from the levels of 700hPa and SLP. These cyclones (all types, both levels) account for a total of 46% to 76% of

observed precipitation in the focus region (Figure 17), depending on the location, with an average of 62%. If the pressure levels are analyzed solely, the percentages are 54% and 37% for SLP and 700hPa, respectively. This difference arises from the larger number of cyclones at SLP as well as from the enhanced lifting of low-level moist air associated with cyclones extending down to the surface. The identified cyclones capture a large part of the rainfall in the area (62%), although the percentage of days, where a cyclone is moving through TRZ and precipitation is observed, is only 20% to 36%, depending on the location, with an average of 26% or 97 days per year. The overall number of days with precipitation is 131 days per year (ranging from 91 to 171), in contrast to 180 days per year on which a cyclone moves through CE, so nearly 50% (83 days) of all track days are dry days. For the remaining part of a year (151 days) there is no track and no precipitation has been observed.

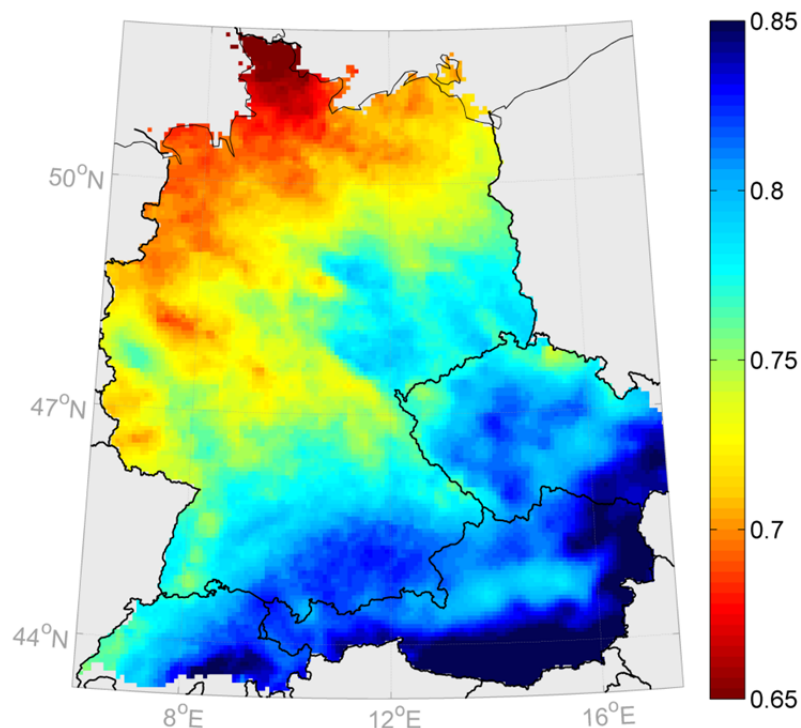


Figure 17: Fraction of precipitation attributed to the cyclones identified from 700hPa and from SLP (1961-2002).

The fraction of total precipitation associated with cyclones over Central Europe (62%) obtained here fits very well with other studies which attributed around 65% of the annual precipitation to stratiform type precipitation over the Czech Republic (Rulfová and Kysely, 2013) and the Spanish Mediterranean Coast (Ruiz-Leo et al., 2013). Over Central Europe the annual proportion of precipitation that occurs during cyclones ranges from 55% to 70% in summer and is about 75% in winter (Hawcroft et al., 2012) and between 60% and 70% were found to be associated with atmospheric fronts (Catto et al., 2012). The fraction of precipitation accounted for here depends on the location and is largest in the southeast of the focus region and smallest in the north. This spatial pattern cannot be explained by different proximities to the border of the TRZ, as the focus region is centered on the middle of TRZ at 47°N and 12°E. Rather, cyclones in the northern part of TRZ are able to trigger precipitation in the south, while the opposite is not the case. Cyclones that have not been recognized inside TRZ are able to cause precipitation in the north-western part of the focus

region, which is not counted in the analysis. This indicates that cyclones from the East Atlantic or North Sea have a larger spatial extent on average and are therefore able to reach into Central Europe over large distances. Precipitation also occurs in the absence of atmospheric cyclones or in weak gradient situations with ill-defined cyclone centers which may contribute to the pattern of Figure 17. Typically, however, such situations favor convective type precipitation and should therefore affect both the south and the north of the focus region.

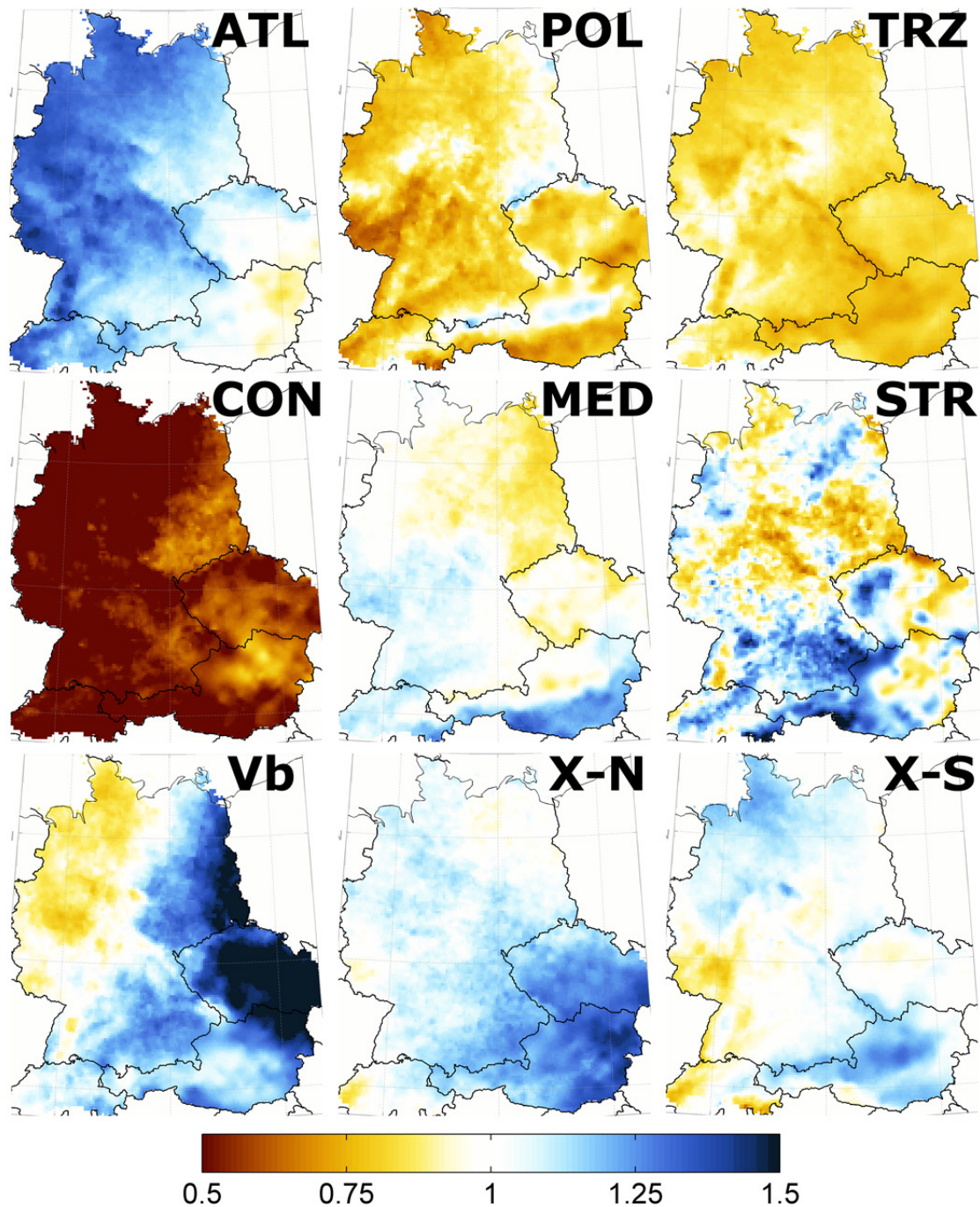


Figure 18: Ratio of mean precipitation of each track type and mean precipitation of all tracks. This ratio indicates track types and regions with high (blue) or low (brown) contributions to precipitation associated with cyclones over Central Europe.

One of the motivations of the classification has been the expectation that cyclone track types differ in their precipitation characteristics. Figure 18 shows mean precipitation for each track type, relative to the mean precipitation without stratification by type. The average precipitation over the focus region for days with cyclones traversing TRZ was found as 2.88 mm/d, which is between the estimates of 2mm/d (Hawcroft et al., 2012) and 4mm/d (Catto et al., 2012) for Central Europe. The number of 2.88 mm/d may appear small, but is an average over the whole focus region (545,000 km²) and all cyclone track dates, so includes numerous instances/locations without precipitation. The majority of cyclones are not associated with significant precipitation and only a small number of cyclones accounts for most of the annual total precipitation.

Track types ATL, Vb, X-N, X-S, STR and MED are associated with above average precipitation (3.66, 3.62, 3.50, 3.23, and 3.12mm/d, respectively) as an average over the whole domain. In contrast, track types POL, TRZ and CON are associated with below average precipitation of (2.60, 2.59 and 1.56mm/d, respectively). For some of the track types there are very clear spatial precipitation patterns that differ drastically between the track types, with even higher amounts in specific parts of the focus region. For example, ATL cyclones usually affect the western part of the focus region and cease in the eastern lee of the Central European mountain ranges. This pattern matches very well with climatology, where annual precipitation totals decrease from western to eastern Europe, in line with a weakened influence of Atlantic weather regimes.

POL cyclones have the strongest positive anomalies (a maximum of 3.89mm/d) in the northern stau regions of the Erzgebirge and Alps (light blue bands in Figure 18), implying a strong northerly flow against the orography and related lifting of moist air. MED cyclones show a stronger signal (max=4.51mm/d) in the regions south of the Alpine range (in the very south of the focus region). STR shows a noisy pattern, which can be related to the dominance of convective type precipitation leading to local minima and maxima over the domain (max=5.34mm/d). High precipitation totals are found for ATL cyclones in the western parts of Germany and Switzerland (max=4.30mm/d), for X-N cyclones (max=4.86mm/d) in the south-eastern parts of CE (Austria and Czech Republic). The clearest pattern appears for Vb cyclones with very high precipitation contributions over a large area in the Czech Republic (max=5.82mm/d). Vb cyclones develop around Genoa and move around the eastern Alps towards Poland. Moisture is advected towards the mountains in an anti-clockwise rotation and frontal lifting is intensified through orographic enhancement. As a result, very large precipitation depths are observed in the regions located along or west of the Vb cyclone track. Another reason for the large precipitation depths is the strong intensity of Vb cyclones (Figure 16).

3.4.2 Heavy precipitation events from 1961 to 2002

Major flood events in Central Europe are often attributed to particular cyclone types such as Vb. To demonstrate the practical applicability of the new cyclone track classification, the nine track types are attributed here to the most significant precipitation events in selected river basins in Central Europe. Müller et al. (2009) published a list of significant precipitation events for 25 river basins. The events were selected on the basis of runoff peaks compared to average flow conditions within the summer half years in the period 1951-2002. These events are listed in Table 7 for the period 1961-2002, along with the associated cyclone track type identified in the present study. The table shows that, in northwestern Germany

(Neckar, Main, Moselle, Ems, Aller, Weser rivers), eleven out of twelve events are associated with ATL or TRZ tracks and the remaining events are associated with tracks starting in the western Mediterranean (MED, Vb or X-N). In southern Germany and northern Austria (Upper-Danube, Inn, Enns rivers), some, but fewer, events can be attributed to TRZ, ATL or POL but a significant number to X-S, X-N or Vb. The latter are cyclones that mainly develop on the southern lee-side of the Alps.

Table 7: Significant precipitation events and track types^a.

Region →	NW-Germany		S-Germany, N-Austria		Czech Republic, W-Slovakia, SW-Poland	
Catchments →	Neckar, Main, Moselle, Ems, Aller, Weser		Upper-Danube, Inn, Enns		Vltava, Elbe, Oder, Morava, Váh	
Precipitation event	SLP	Z700	SLP	Z700	SLP	Z700
1965-06-11	TRZ	TRZ	TRZ	TRZ	TRZ	TRZ
1965-07-18	TRZ	TRZ				
1970-05-12	TRZ	TRZ				
1970-07-19					TRZ	Vb
1970-08-11			X-S	X-S		
1972-08-22					TRZ	Vb
1973-06-24			X-N	ATL		
1975-07-02			X-N	POL		
1977-08-01			Vb	Vb	Vb	Vb
1978-05-24	MED	X-N				
1980-10-10					Vb	Vb
1981-06-06	TRZ	TRZ				
1981-07-02	Vb	ATL				
1981-07-21			Vb	Vb	Vb	Vb
1981-08-13	TRZ	TRZ				
1983-05-26	TRZ	*				
1983-08-07					X-N	ATL
1984-06-02	TRZ	ATL				
1985-08-07			Vb	Vb	Vb	Vb
1986-10-24	ATL	ATL				
1993-10-06	TRZ	TRZ				
1997-07-08			TRZ	X-N	TRZ	X-N
1998-10-29	ATL	*				
1999-05-13			TRZ	TRZ		
1999-05-22			Vb	X-S		
2002-08-12			Vb	Vb	Vb	Vb

^aMost significant precipitation events over selected parts of Central Europe for the summer half years (May-October) between 1961 and 2002 (adapted from Müller et al., 2009) and attribution to cyclone track types. Empty fields indicate that the event is not among the top events in the respective catchment. Asterisk indicates that the event is not recognized as a cyclone which moves into TRZ.

In the Czech Republic, western Slovakia and southwestern Poland (Vltava, Elbe, Oder, Morava, Váh rivers) almost all of the significant precipitation events are connected to Vb cyclone tracks. Overall, this fits very well with the findings above, where the extreme intensity characteristics already pointed to Vb as a very special track type over Central Europe. For most of the events associated with TRZ tracks, either a cyclone was found

developing at the northern or southern lee-side of the Alps at SLP, or a stationary cut off low was found at higher atmospheric levels over CE. This comparison also indicates that the connection between track types and heavy precipitation is not uniform in space and may also depend on the season. With two exceptions at 700hPa (indicated by an asterisk in Table 7) all precipitation events can be associated with cyclones identified in this study, which adds credence to the consistency of the approach. For most of these events the same cyclone track type was found at SLP and 700hPa atmospheric levels, but there are a number of events where the track types are not consistent between the levels. Different cyclone paths can typically be observed when the vertical axis of a cyclone is tilted, for example, when the upper level trough amplifies and decelerates while the surface cyclone still moves ahead or circles around the upper level trough. In other cases, a major upper level trough approaches from the Atlantic and steers the formation of a new surface level cyclone with a different track type over Central Europe. Examples are the events on 1981-07-02, 1983-08-07 and 1984-06-02 in Table 7.

3.5 Discussion of classification results

3.5.1 Southern Alpine track types in comparison

A first assessment of the classification approach is performed by comparing the similar track types Vb, X-N and X-S. These types predominantly emerge from the western Mediterranean Sea – south of the Alpine ridge – with a general propagation to easterly directions in the course of their life time (Figure 14). The average number of cyclones per year is very different between these three types, with a total number of 3.1 (Vb), 7.7 (X-N) and 25.2 (X-S) cyclones per year for SLP. The number of Vb cyclones per year for the two levels are 3.1 and 4.1 at SLP and Z700, respectively, which is similar to results from the literature based on ERA-40 data with 3.0 at Z700 (Kummler, 2014), and 3.5 at Z700 (Hofstätter and Chimani 2012). A significantly lower count of Vb-type cyclones at SLP was found by Nissen et al. (2013) but they used a different recognition approach. As can be seen from Figure 14, type X-S shows a reasonable similarity to X-N, as a significant part of the former turn back to the north at some point, despite the restriction in the classification of a southward direction after recognition. This means that X-N and X-S do not necessarily have to be considered as different types in the early development phase as intensity (Figure 16), and intensity change (Figure 15) characteristics are not very different either. However, distinguishing these two types may be important if one is interested in a region further to the southeast, e.g. the Balkan region. Type X-N looks very similar to Vb, especially in terms of the propagation paths southeast of the Alpine ridge and the points of first detection, however, Vb tracks turn to the north approaching Central Europe more closely. This may be related to characteristic upper level cut-off lows located over CE (Grams et al., 2014) in case of Vb which, presumably, is not a dominant feature for X-N. A separation of the three track types therefore appears meaningful.

3.5.2 Sensitivity experiment for classifying Vb

As the number of Vb-type cyclones is low as compared to type X-N and X-S, and Vb tracks have similar, eastbound propagation paths as X-N (see Figure 14), a sensitivity experiment is carried out by varying the width of region “ $x_{(tn)}$ ” through the boundaries in the east and west (see Figure 10 for the original setup), and reapplying the classification procedure to SLP. The experiment shows that the number of Vb-type cyclones is somewhat sensitive to the eastward extent but almost not to the westward extent (Table 8).

Table 8: Sensitivity of classification to Vb tracks^a.

	Extended westward boundary		Original setup ^b	Extended eastward boundary				
	12°/-	13°/-		14°/20°	-/20.25°	-/20.5°	-/21°	-/22°
events per year	3.3	3.2	3.1	3.5	3.7	4.0	4.5	4.9

^aMean annual number of Vb type cyclone tracks for different longitudinal sizes of region “ $x_{(tn)}$ ”. ERA-40 data, 1961-2002, SLP. ^bOriginal size 14°E to 20°E as shown in Figure 10(b).

When changing the eastward boundary from 20°E (original setup) to 23°E, the number of Vb cyclones increases by about 20% per degree increment. Virtually all additional cyclones classified as Vb in this case are at the expense of X-N and X-S in equal shares. At the level of 700hPa the effect of altered boundaries is even smaller than at SLP (not shown). The sensitivity of the track number to the definition of the region suggests that preferred track streams do exist over CE but the spatial transition between different types is a smooth one.

3.6 Conclusions

In this paper, a procedure for tracking atmospheric cyclones has been adapted to ERA-40 data over Europe for the purpose of this study. A new classification approach is proposed for separating tracks into nine types, based on the geographical regions from where the cyclones propagate into Central Europe (CE). The regions were defined by large geographical domains with a consistent topography and similar surface characteristics, based on *a priori* knowledge from synoptic observations.

The resulting cyclone track types show distinct properties in terms of frequency and intensity. Atlantic cyclones and cyclones developing directly over CE (type TRZ) are the most frequent ones (about 25% relative frequency each), which is in good agreement with synoptic observations. Cyclones developing in the northern parts of the Mediterranean on the lee-side of the Alps (types Vb, X-N and X-S) have a combined frequency of 25%. The remaining cyclones are classified as CON, POL and MED types. Strong cyclones, both in terms of relative geostrophic vorticity and central pressure, are found among ATL, Vb, POL and CON tracks in the winter half year. More importantly, the frequency of strong Vb cyclones is particularly high during the summer half year, which can be explained by additional cyclogenetic processes acting on the lee-side of the Alps, as latent heat release at lower levels (Aebischer and Schär, 1998) or frontogenetic low-level wind convergence (Horvath et al., 2008), but not by dominant dynamic forcing between upper level winds and the Alps alone, as is usually the case in winter. The study also strongly suggests the existence of preferred cyclone propagation paths over CE. Although these are usually

affected by the underlying topography, specific dominant upper level circulation patterns may also play an important role for the within-type characteristics.

The new cyclone track catalog has the potential for interesting follow-up investigations on climatological characteristics, the temporal behavior and the relevance of track types for extreme precipitation in CE. As a proof of concept, long-term precipitation totals are analyzed stratified by track types here. Track types ATL, Vb, X-N and X-S are associated with above average precipitation while track types CON, STR, POL, and TRZ are associated with below average precipitation. The contributions of the track types to precipitation totals differ enormously in space. This suggests that the risk of heavy precipitation over Central Europe very much depends on the specific cyclone track type and location. A comparison of significant precipitation events (from Müller et al., 2009) with cyclone track types shows that almost all of the events have been identified by the proposed scheme. In south-western Poland, Czech Republic and western Slovakia seven of the top ten precipitation events can be attributed to Vb tracks.

Of course there are limitations to the approach and caveats in the applicability of the new track types which opens up room for new research. First, the approach has been applied independently to data from two atmospheric levels, SLP and Z700. Although tracking studies are usually based on one single level, the creation of a consistent and unique track catalog, combining information from different levels has potential and should be pursued in the future. The initial size of the tracking domain does not capture the eastern Atlantic region to its full extent. While Atlantic-type cyclones are correctly classified, some tracks may not be detected from the very beginning. This is not considered relevant to this study but could be to others. In this study, precipitation is always attributed to a cyclone moving through region TRZ, irrespective of the distance to the cyclone, its spatial extent and the location of the atmospheric front associated with the cyclone. By incorporating this kind of information even more detailed spatial patterns could be identified. Finally, it should be mentioned that the number of tracks identified is not fully independent between the different types, as certain geographical regions are given higher priority than others in the classification. If a track includes branches, the sub-track from high priority regions determines the type of the entire track-complex and the other sub-tracks (branches) are disregarded. This applies to 10 % of all tracks, with a higher proportion at SLP during the summer season and/or during weak gradient situations.

The cyclone track classification presented in this study is optimized for the Central European domain. However, the basic concept behind the classification can readily be transferred to other mid-latitude and possibly tropical regions of the world by adapting the setup according to local synoptic information, and their effect on precipitation (eg. Steinschneider and Lall, 2015; Huang Jr et al., 2012). Further research could also focus on the characteristics of continental scale processes controlling the formation, propagation and transformation of Central European cyclones by examining distinct track types. In subsequent studies, a climatology of European cyclone tracks, as classified with the current approach, will be presented and the track types will be related to extreme precipitation in Central Europe.



4 Large scale heavy precipitation over Central Europe and the role of atmospheric cyclone track types

Abstract

Precipitation patterns over Europe are largely controlled by atmospheric cyclones embedded in the general circulation of the mid-latitudes. This study evaluates the climatologic features of precipitation for selected regions in Central Europe with respect to cyclone track types for 1959-2015, focusing on large scale heavy precipitation.

The analysis suggests that each of the cyclone track types is connected to a specific pattern of the upper level atmospheric flow, usually characterized by a major trough located over Europe. A dominant upper level cut off low is found over Europe for strong CON and Vb cyclones which move from the East and Southeast into Central Europe. Strong Vb cyclones revealed the longest residence times, mainly due to circular propagation paths. The Central European cyclone precipitation climate can largely be explained by seasonal track type frequency and cyclone intensity, however, additional factors are needed to explain a secondary precipitation maximum in early autumn. The occurrence of large precipitation totals for track events is strongly related to the track type and the region, with the highest value of 45% of all Vb cyclones connected to heavy precipitation in summer over the Czech Republic and Eastern Austria. In Western Germany, Atlantic winter cyclones are most relevant for heavy precipitation. The analysis of the top-50 precipitation events revealed an outstanding heavy precipitation period from 2006 to 2011 in the Czech Republic, but no gradual long term change. The findings help better understand spatio-temporal variability of heavy precipitation in the context of floods, and may be used for evaluating climate models.

4.1 Introduction

Precipitation is a key element of the Earth's climate system through the vertical and horizontal transport of mass and energy (Trenberth and Stepaniak, 2004, Hantel, 2005, Tristan et al., 2015). The long-term characteristics of precipitation vary substantially between regions (Peel et al., 2004, Kottek et al., 2006, Rubel and Kottek, 2010) due to latitudinal difference and local geographical features such a proximity to large open water bodies and different land-surface properties, even within a rather small domain as Europe (Haylock et al., 2008). Beside regional differences in precipitation characteristics, seasonal patterns exist (Zveryaev, 2004 and 2006) which are typically caused by annual variations of air temperatures, solar insolation, dominant atmospheric weather patterns and vegetation dynamics. On top of that, internal climate variability induces large variations of dry or wet conditions at decadal and interannual time scales (Masson and Frei, 2016, Pauling et al., 2006, Schmidli et al., 2002, Rimbu et al., 2001, Haslinger and Blöschl, 2017, Casty et al., 2005). Hydro-meteorological extremes are of particular relevance. Extreme precipitation has caused several devastating floods in Central Europe over the last 20 years. Examples include the July 1997 flood in Poland (Kundzewicz et al., 1999), Germany, the Czech Republic and Austria, the May 1999 flood in Bavaria and Western Austria (BLFW, 2003), the August 2002 flood hitting several Central European countries (e.g. Grazzini and Van der Grijn, 2002), the

August 2005 flood in the German/Austrian Alpine Region (BLU, 2006), the June 2006 and May/June as well as August 2010 floods in the Czech Republic (Müller et al., 2015), the June/July 2009 flood in Central and Eastern Europe (Danhelka & Kubát, 2009), the June 2013 flood in Bavaria and Austria (Blöschl et al., 2013) and the May 2014 flood on the Balkans and in Southeast Europe (Stadtherr et al., 2016). A potential increase of the frequency or intensity of hydro-meteorological wet events is of great concern in the ongoing climate change debate (Westra et al., 2014, Trenberth et al., 2003). Such events tend to result from anomalous atmospheric circulation patterns over Europe (e.g. Dayan et al., 2015, Grams et al., 2014, Kaspar and Müller, 2014) in combination with specific hydrologic boundary conditions on the surface such as antecedent soil moisture and soil infiltration capacity (e.g. Hall et al., 2014, Nied et al., 2014). Additionally, seasonality is a very important factor both in terms of the atmospheric circulation as the driving mechanism (Scherrer et al., 2016, Fleig et al., 2015, Casanueva et al., 2014, Zveryaev and Allen, 2010) and for the resulting flood processes in terms of soil moisture, snow processes and frozen ground (Merz and Blöschl, 2003, Parajka et al., 2010, Müller et al., 2015; Blöschl et al., 2017). An increasing number of studies have focused on the specific characteristics of the atmospheric circulation during heavy precipitation events in recent years. For example, two circulation types have been isolated in for the heaviest Czech Republic rainfall events during 1958-2002 (Müller et al., 2009). The first circulation type consists of a major, quasi-stationary trough located over Europe, steering a number of fast moving, frontal short-waves over the Czech territory. In contrast, the second type is characterized by a cut off low (COL) over Central Europe, with a cyclone at lower atmospheric levels moving very slowly. This is a similar situation to those of the four historic flood events in Austria/Bavaria in Sept 1899, July 1954, Aug 2002 and May 2013, where a major upper level COL was observed over Central Europe, accompanied by cyclones located at the surface level around the eastern Alps (Blöschl et al., 2013). For Switzerland, stationarity of anomalous circulation patterns was a key issue for the top 24 floods between 1868 and 2005, leading to repeated periods of heavy precipitation over a few days (Stucki et al., 2012). For the Elbe river basin, a specific circulation anomaly (which the authors termed pattern 29) could be identified as producing long-duration rain episodes and hence floods, irrespective of the initial soil moisture (Nied et al., 2014). This circulation anomaly is characterized by an upper level COL over the Gulf of Genoa and was found to be more frequent in summer than in winter.

Selected outstanding events (May 2014, Jun 2013 and Aug 2002) have been investigated in very much detail by a number of authors (Stadtherr et al., 2016, Grams et al., 2014, Ulbrich et al., 2003b). For these cases, a quasi-persistent upper level COL induced a series of surface cyclones which propagated in anti-clockwise direction around the respective regions hit by heavy precipitation. Cyclones propagating from the region of Genoa into Central Europe are usually referred to as following a Vb-track after van Bebber (1891). This cyclone type has been investigated systematically in recent years. Nissen et al. (2013) found that 40% of all Vb cyclones are related to heavy precipitation (95th percentile) in the Elbe catchment, with about two thirds of these events occurring in April/May. Similarly, Messmer et al. (2015) revealed 30% of the summer Vb cyclones exceed the 95th precipitation percentile in the Alpine Region (2% in winter).

While all of these studies have highlighted the importance of specific cyclone tracks in producing heavy precipitation in Central Europe, the spatio-temporal characteristics of large scale precipitation have so far not been related to cyclone tracks in a systematic way.

The aim of this study therefore is

- to explore the climatologic characteristics of heavy and mean precipitation, observed in the vicinity of atmospheric cyclones, for selected regions in Central Europe and relate them to cyclone track types;
- to analyze the climatological characteristics of cyclone track types in this regard; and
- to identify dominant circulation patterns over Europe in the context of cyclone track types.

The findings are intended to foster the understanding of large scale heavy precipitation and related flood events from the perspective of the atmospheric drivers. They are also intended to provide a basis for evaluating climate models over Europe, e.g. by comparing modeled frequency, intensity, seasonality and temporal variability of each cyclone track type with observations.

4.2 Data and Analysis Procedure

4.2.1 Cyclone track types

The cyclone track types used in this study were identified by the classification scheme of Hofstätter et al. (2016) developed for the European domain. The tracking scheme has been developed by Murray and Simmonds (1991) and Simmonds et al. (1999). In addition it considers both open and closed systems (Pinto et al., 2005) and allows for splitting and merging of cyclone tracks. Closed systems are localized by finding local pressure minima whereas open systems are localized by identifying local vorticity maxima within open troughs. Cyclones are first identified at time t_n , then a first guess for the position at time t_{n+1} is calculated and finally tracks are identified by scoring the direction and distance between the first guess and all candidate cyclones at time t_{n+1} . For the tracking, geopotential height at the atmospheric level of 700hPa (Z700) and air pressure at sea surface level (SLP) are used separately. Cyclones are tracked within a domain ranging from 40°W to 50°E at 65°N and 20°W to 40°E at 30°N. In order to avoid entrance/exit problems, splitting and merging are refused near the margin. Weak cyclones and spurious tracks are excluded from the analysis (Hofstätter et al., 2016). In the current study, the cyclone track analysis is based on the Japanese 55-year reanalysis (JRA-55) of the Japanese Meteorological Agency (Kobayashi et al., 2015, Harada et al., 2016) retrieved from the Research Data Archive at the NCAR-National Center for Atmospheric Research (JMA, 2013) at 1.25 degree spatial resolution. JRA-55 is a regularly updated global atmospheric reanalysis at six hourly temporal resolution, extending back to 1958 and has been used instead of ERA-40 (Uppala et al., 2005) to cover the most recent years. In order to exclude small-scale or spurious cyclones, especially over mountain orography, the data are filtered by a discrete spatial low-pass filter (Freser and von Storch, 2005) that removes any structures smaller than 400 km, relaxes smoothly up to 1000 km, and lets all large scales pass through (see Hofstätter and Chimani,

2012). Cyclone track and precipitation characteristics only refer to those cyclones that are located within a “Track Recognition Zone” (TRZ, 0.5°E-23.9°E and 42.3°N-56.2°N) for at least 18 hours (Figure 19, left).

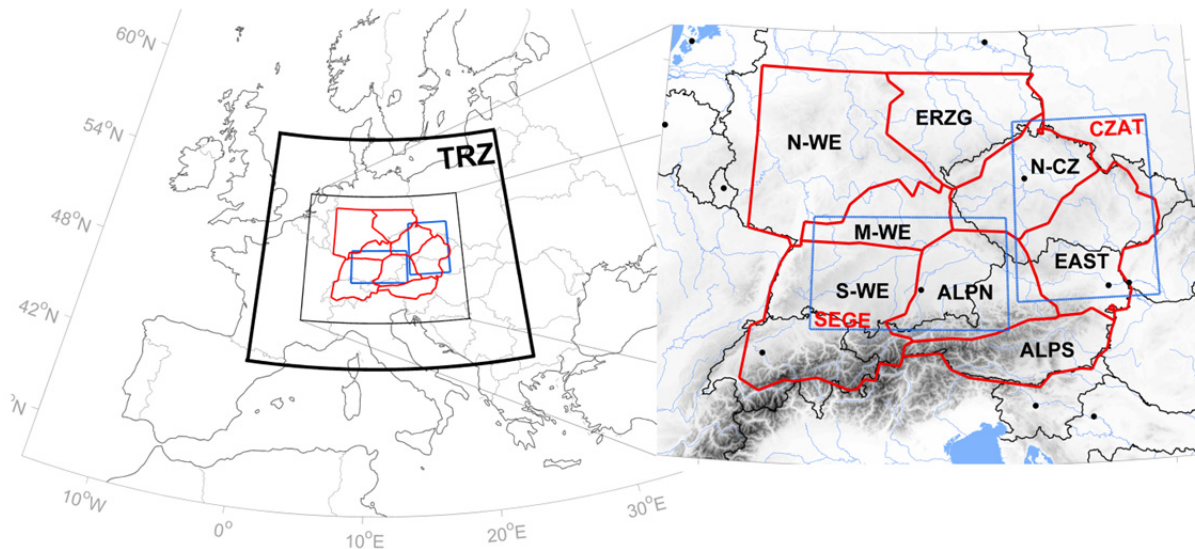


Figure 19: Study region located within the “track recognition zone” TRZ (black bold line) and subregions used for precipitation analysis shown in red for 1959-2006 (WETRAX data) and blue for 1959-2015 (E-OBS data).

For all other cyclones passing outside of TRZ, a track type cannot be assessed, hence such cyclones were not considered in this study. All cyclone tracks, either identified at Z700 or at SLP, were pooled into one sample denoted as “Z700/SLP”. In specific instances they were treated separately which is specifically indicated in this paper. The classification of Hofstätter et al. (2016) consists of nine different types, based on the geographic regions the cyclones traverse before entering Central Europe (Table 9). In this study an additional track type “Eastern Alpine track” (EA) was considered which represents cyclones propagating to the northeast over Eastern Europe, similar to type Vb (Van Bebber, 1891), but developing on the eastern leeside of the European or Dinaric Alps (Figure 20).

Table 9: Cyclone track types of Hofstätter *et al.* (2016) plus the additional type “Eastern Alpine track” (EA).

Number	Acronym	Type
1	Vb	van Bebbber’s type “five-b”
2	EA	Eastern Alpine track
3	X-N	Northward propagation, emerging from the northern Adriatic Sea or Mediterranean Sea
4	X-S	Southward propagation, emerging from the northern Adriatic Sea or Mediterranean Sea
5	MED	Mediterranean
6	STR	Subtropical
7	ATL	Atlantic
8	POL	Polar
9	CON	Continental
10	TRZ	All tracks emerging within TRZ (except Vb, X-N, X-S)

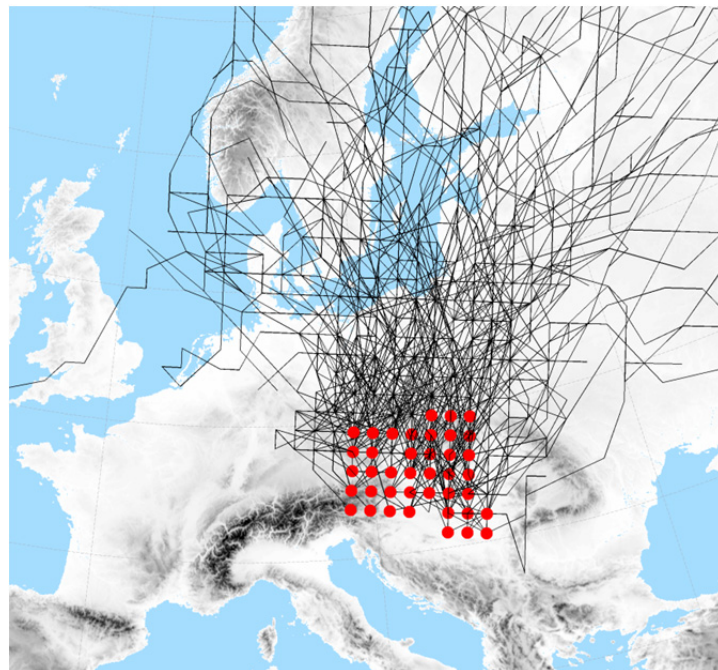


Figure 20: Members of the cyclone track type “Eastern Alpine – EA” (SLP and Z700, 1959-2015). Red dots indicate the location of first detection of individual tracks.

Cyclone tracks of type EA were previously a subset of type TRZ, but were classified separately here because of their peculiarity in terms of propagation and related precipitation characteristics, which have emerged in the course of this study. Cyclone tracks were determined for the years 1959-2015. As a measure for cyclone intensity, relative geostrophic vorticity ξ was used in this study. In order to make cyclones between different levels comparable, ξ was log-transformed by $\ln(\xi_{Z700})$ and $\ln(0.7*\xi_{SLP})$, and used as a score variable.

4.2.2 Precipitation data and study region

The study region for precipitation analysis is located over Central Europe within region TRZ, covering Austria as well as large parts of Germany, Switzerland and the Czech Republic (Figure 19, red and blue). Two gridded time series of daily precipitation were used in this study, the WETRAX data at 6km resolution covering the period 1959-2006 (Hofstätter et al., 2015), and the E-OBS data (v13.1) at 20km resolution, retrieved from the ECA&D data portal, covering the period 1959-2015 (Haylock et al., 2008). The WETRAX data are based on station data from the Austrian Weather Service (ZAMG) for the Austrian territory and for the remaining parts of the study region from the German Weather Service (DWD - the HYRAS data set, Rauthe et al., 2013). Since the motivation for this study was to understand the relationship between atmospheric cyclone tracks and large scale precipitation patterns over Central Europe, the WETRAX precipitation data were aggregated over regions deemed to exhibit similar spatio-temporal variability (red lines in Figure 19). These regions were delineated by S-mode (Richman, 1986), orthogonally varimax-rotated principal component analysis (PCA) on the gridded daily data. The Principal Components (PCs) are based on the correlation matrix of the input variables. The highest loadings of each PC were used to define regions of similar precipitation variability. The loadings are the correlation coefficients between the variables and the principle components. The number of PCs to be extracted was determined by the dominance criterion (Jacobeit, 1993) resulting in eight regions (Figure 19, red lines), which have an explained variance of $R^2=0.67$ on an annual basis.

The E-OBS data were used for a complementary analysis over two selected regions, SEGE and CZAT (Figure 19, blue lines), for the extended period 1959-2015. E-OBS is heavily affected by smoothing of large scale extremes (Hofstra *et al.*, 2010) as well as by a strong underestimation of smaller-scale events (Zolina et al., 2014) in regions with low station densities, particularly in the convective summer season. Station density is about 350km² in Germany and about 600km² in the Czech Republic, but much lower in the Austrian Alps. As the low density affects small parts of SEGE and CZAT regions, the extended analysis only considers highly ranked large scale precipitation events in these regions. The WETRAX data set, in contrast, provides a comparably high station density over Germany (~100 km²) and Austria (~140 km²) as well as a similar density as E-OBS over the Czech Republic (~550 km²). Precipitation events being smaller than about 50x50 km are therefore not well resolved in the N-CZ region and in the northern parts of the EAST region. Since this study focuses on large scale precipitation observed in the vicinity of cyclones, convective precipitation is much less relevant.

The cyclone track data are available four times a day at 00, 06, 12 and 18 UTC in contrast to the daily precipitation data, which are reported once a day at 06 UTC and refer to the subsequent 24 hours' time frame. In order to associate precipitation with cyclone tracks, regional averages of daily precipitation totals (dREF) were interpolated to six hourly values following the cyclone dates. A fourth of the daily precipitation was allocated to 18 UTC of the corresponding date and the missing values at 00, 06 and 12 UTC were estimated by applying a piecewise cubic spline. In order to evaluate the effect of interpolation, the six hourly data were re-aggregated into daily totals (dINT) and compared to dREF. Although the interpolation allows for considering information from adjacent time steps, it also leads to smoothing effects, with an overestimation of the total precipitation amount for $dREF < 5\text{mm/day}$ by about +17% and an underestimation for $dREF \geq 5\text{mm/day}$ by about -8%,

with some variations between regions. Therefore a quantile-mapping (QM) bias correction (Panofsky and Brier, 1968) was applied by estimating a transfer function based on the difference between the sorted values of dINT and dREF (Thiemeßl et al., 2011). The transfer function was approximated by first fitting a sinusoidal function (sin2), followed by fitting a Gaussian (gaus2) function to the residuals. The sum of both functions was applied as the transfer function to the six hourly precipitation according to the corresponding quantiles. As a result, the bias could be reduced to about +5% for small and to about -1% for high precipitation amounts. Although QM is able to adjust all statistical moments, it does not account for any changes in the temporal structure arising from interpolation. In the case of low precipitation amounts (dREF<1mm), the correlation between dREF and dINT drops to $R^2=0.45$ for the sqrt-transformed daily data. For larger precipitation amounts temporal correlation is preserved ($R^2=0.95$), particularly for heavy precipitation (dREF>95%) with $R^2\geq 0.96$ for all regions.

4.2.3 Analysis of mean and heavy precipitation

An overview of the analysis methods, as detailed below, is shown in Table 10. For the climatologic analysis of mean and heavy cyclone precipitation, six hourly precipitation (R^6) was assigned to a cyclone track if that cyclone was located within region TRZ at that time. The size of region TRZ is about 1600km x 1600km which was chosen in accordance with the mean radius of mid-latitude cyclones, which is between 350km and 800km, depending on the cyclones' life stage (Wernli and Schwierz, 2006). In case more than one cyclone was present at the same time, precipitation was assigned to every candidate cyclone, as a unique attribution would require a manual analysis of the specific synoptic situation. At SLP this is the case for 23% of the cyclones as compared to Z700 with just 15%.

Table 10: Precipitation measures used in this study.

(a) measure	R^6	R^{trc}	R^{24}
(b) description	regional average at time t	cyclone track precipitation	24-hour running total at time t
(c) calculation	interpolated values at $t=00, 06, 12$ and 18 UTC from daily rain gauge measurements	sum of R^6 for the duration T of a cyclone track in TRZ $\sum_{t=1}^{t=T} R^6_{(t)} \quad (13)$	$\frac{(R^6_{(t-12)} + R^6_{(t+12)})}{2} + \sum_{t=6}^{t+6} R^6_{(t)} \quad (14)$
(d) used for the analysis of	mean cyclone precipitation (ch. 3.2.a)	heavy cyclone precipitation (ch. 3.2.b)	top-50 precipitation events (ch. 3.2.c)
(e) data base	WETRAX (1959-2006)		WETRAX (1959-2006) E-OBS (1959-2015)
(f) drawback		depends on R^6 and on residence time rt	restricted to 24 hours, but longer and shorter intervals may also be relevant for floods

The total precipitation amount of a certain cyclone, denoted as R^{trc} , was determined by summing up precipitation (R^6) as long as a cyclone was within TRZ. R^{trc} is used for the heavy precipitation assessment and depends both on the magnitude of R^6 and the residence time

rt of an individual cyclone (Table 10, centre). In this study heavy precipitation is defined as precipitation exceeding 95th percentile of R^{trc} which is termed HP_{95} . In order to estimate HP_{95} robustly, the distribution of the largest values of R^{trc} was fitted by a generalized Pareto distribution $G(R^{trc})$

$$G(R^{trc}) = \begin{cases} 1 - (1 + R^{trc} * \sigma/\beta)^{-1/\sigma} & (\sigma \neq 0) \\ 1 - e^{-R^{trc}/\beta} & (\sigma = 0) \end{cases} \quad (15)$$

and

$$n = \text{round}(15 + N/10) \quad (16)$$

where β (scale parameter) and σ (shape parameter) were estimated by the maximum-likelihood method (Coles, 2001), n is the number of largest values from N values of R^{trc} . Equation 16 assures a sufficient sample size n , in case of track types with a low number of cyclones. The values in Equation 16 were chosen subjectively by examining the sample mean excess function in combination with a Hill plot for different track types on a seasonal basis. For example, in case of Vb summer (May-Oct) cyclones with $N=120$, the hill estimator stabilizes at $n=25$ and the mean excess function is nonlinear above a threshold of 33mm or $n < 24$. When using Equation 16 this leads to a computational threshold for fitting the generalized Pareto distribution of $n=27$. As a consequence, n always corresponds to at least 10% of the largest values of N and increases for low values of N .

4.2.4 Analysis of outstanding precipitation events

In order to further explore individual precipitation events, the 50 largest running 24 hr precipitation totals (R^{24}) in the period 1959-2006 as well as in the extended period 1959-2015 were identified. R^{24} was calculated by a centered moving average using weights of 0.5-1-1-1-0.5 on consecutive 6-hourly values (Table 10, right). There is an important difference between R^{trc} and R^{24} as the latter does not depend on cyclone residence time. Next a weighted cyclone intensity $rdv\sim$ is calculated (Equation 17 and Equation 18) for each cyclone, based on the relative geostrophic vorticity ξ and the distance dis between the cyclone center and the center of the respective study region.

$$rdv = \begin{cases} \xi * \left(1 - \left[\frac{dis}{d_{max}}\right]^2\right)^2 & (0 \leq dis \leq d_{max}) \\ 0 & (\text{otherwise}) \end{cases} \quad (17)$$

$$rdv\sim = \text{mean}(rdv_{(t-6)}; rdv_{(t)}) \quad (18)$$

By this approach cyclones are more likely attributed to a top-50 event at time t , if they are strong and/or if they pass by very close to the respective region. All cyclones located outside a distance of $d_{max}=1500$ km were disregarded since typical cyclone extents are far smaller than d_{max} (Schneider et al., 2010). Only the strongest/closest cyclone per track type τ were considered at each level, using

$$rdv_{Z7,SLP}^{\max(\tau)} = \max(rdv_{Vb}\sim; \dots; rdv_{TRZ}\sim)_{Z7,SLP} \quad (19)$$

Finally, the cyclone intensity for each track type was calculated by summing the cyclone intensities over both levels using $rdv^{\max(\tau)} = rdv_{SLP}^{\max(\tau)} + rdv_{Z7}^{\max(\tau)}$ which was used for the attribution, with higher values indicating a more conclusive attribution. This approach allows to reliably assign track types to the top-50 events, even in complex synoptic situations when several cyclones, and cyclones with different track types, are observed simultaneously.

4.3 Results

4.3.1 Cyclone track types

Characteristics of track types

Track type characteristics have been derived for the period 1959-2015 in the following. The mean annual frequency of cyclone track types is presented in Table 11. About 92 cyclones traverse region TRZ per year (108 at SLP; 76 at Z700), in correspondence with Messmer et al., (2015) who found 99 cyclones per year over a similar European domain at the level of Z850. The overall number of tracks is about 10% smaller than that of Hofstätter *et al.* (2016) which may be related to the different input data (ERA-40 in their case, and JRA-55 in this paper) as different reanalysis data usually result in different cyclone counts (e.g. Tilinina et al., 2013). Apart from resolution issues (Hodges et al., 2011), this effect tends to be strongest for weak, slow moving cyclones (Raible et al., 2008). The relative frequency of the track types, however, is almost identical with the largest contribution coming from type ATL (25%), TRZ (24%), X-S (17%) and MED (12%), which together accounting for nearly 80% of the cyclones. The other cyclones were allocated to types X-N, POL and Vb, as well as EA, STR and CON, with only 1 event per year found for the least frequent type STR. The ratio of cyclone tracks between SLP and Z700 is 1.42 as shown in Table 11. As splitting or merging of cyclones is only slightly more frequent at SLP (22%) than at Z700 (16%), the higher number of tracks at SLP arises from a higher number of individual cyclones found at this level. Neu et al. (2013) found a similar ratio of 1.22, however, their study covered the entire northern hemisphere. Types STR, EA, X-S and MED are relatively more frequent at SLP, while CON, Vb, POL and ATL are more frequent at Z700.

Table 11: Mean annual number of cyclone tracks in Central Europe 1959-2015 as well as the ratio of cyclone tracks between the level SLP and Z700.

	Vb	EA	X-N	X-S	MED	STR	ATL	POL	CON	TRZ	ALL
(y ⁻¹)	4.8	1.8	5.1	15.2	10.8	1.0	22.5	6.5	1.9	22.3	91.9
(%)	5.2	2.0	5.5	16.5	11.7	1.1	24.5	7.1	2.1	24.3	100
ratio SLP/Z700	0.84	2.12	1.70	2.00	1.96	2.93	1.15	0.90	0.51	1.53	1.42

The relative frequency of strong cyclones at SLP and Z700 is shown for the summer and winter seasons separately in Figure 21. Summer refers to the period May-October and winter to the period November-April. A value of unit relative frequency indicates that the

share of strong cyclones between summer and winter is identical for a given type at a given atmospheric level.

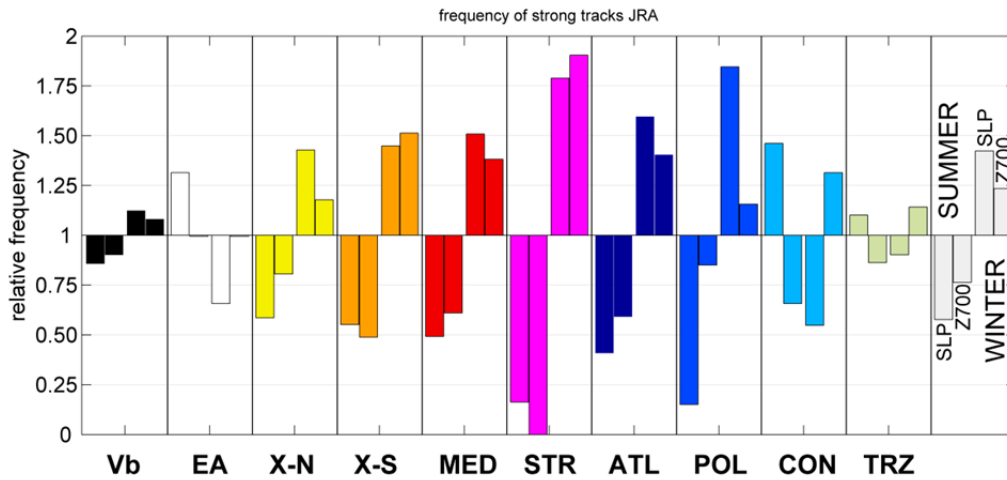


Figure 21: Share of strong cyclones between summer and winter at the level of SLP and Z700 (1959-2015) for each track type (colored bars) as well as for all tracks (grey bars). A value of one indicates an equal fraction of strong cyclones between winter and summer at a certain level.

Strong cyclones tend to be more frequent in winter than in summer (grey bars in Figure 21), with a larger difference at SLP (1.4 vs. 0.6) than at Z700 (1.2 vs. 0.8). This applies to most track types, but strong POL cyclones obviously do not occur at SLP in summer at all, indicating a special cyclone type “Kaltlufttropfen” (Llasat and Puigcerver, 1990) among this track type. Strong STR cyclones only occur in winter, at times when major upper level troughs propagate down to the Iberian Peninsula more frequently. In contrast to the overall characteristics, EA cyclones are twice as frequent at SLP than at Z700 (Table 11), as shown before, and strong EA cyclones mostly occur in summer at SLP. For these cases, a pronounced westerly flow is usually found over the Eastern Alps or the Dinaric Alps at upper atmospheric levels, promoting the development of a lower level vortex at the respective mountain’s lee side. This is plausible and consistent with synoptic observations. However, the reasons for a reversed seasonality for this type at SLP remain unclear. Almost all of the EA-systems emerge at the eastern lee-side of the Alps or the Dinaric Alps as a unique system and are not a consequence of an interrupted Vb track at SLP, or the successor of a Vb track at Z700, as confirmed by manual checks.

In order to analyze the seasonal characteristics more in depth, Figure 22 shows the seasonal distribution of the cyclone track frequency together with the frequency peak stated as the calendar month. Grey bars indicate the confidence intervals ($\alpha=0.05$) for the mean seasonal cycle which were calculated from 10^4 bootstrap samples with replacement. For this analysis, cyclone tracks were divided into strong and weak tracks based on the 85th percentile of cyclone intensity as a threshold. Cyclone intensity was quantified as the peak value of the relative geostrophic vorticity ξ observed within TRZ as an 18-hours running mean. The frequency of strong cyclones (Figure 22, bottom panel, right) exhibits a pronounced seasonal cycle, while this is not the case for the weak cyclones (top panel, right). Weak cyclones are most frequent at the beginning of April, whereas strong cyclones are most frequent during November to March with the frequency peak in mid-December. Strong TRZ, CON, EA and Vb cyclones may occur in any season. Summer cyclones of the Vb type are

particularly strong at SLP – similar to Atlantic winter cyclones – as shown by Hofstätter et al. (2016). A secondary maximum in frequency can be recognized for Vb in late autumn (Sept-Dec), at a time when sea surface temperatures are still high in the genesis region around Northern Italy. The secondary maximum has also been recognized by Hofstätter and Chimani for Vb (2012) as well as by Flocas (1988) for cyclones developing over the Western Mediterranean Sea, Northern Italy or the Northern Adriatic Sea between 40°N and 45°N, which corresponds very well with the Vb source region used in this study.

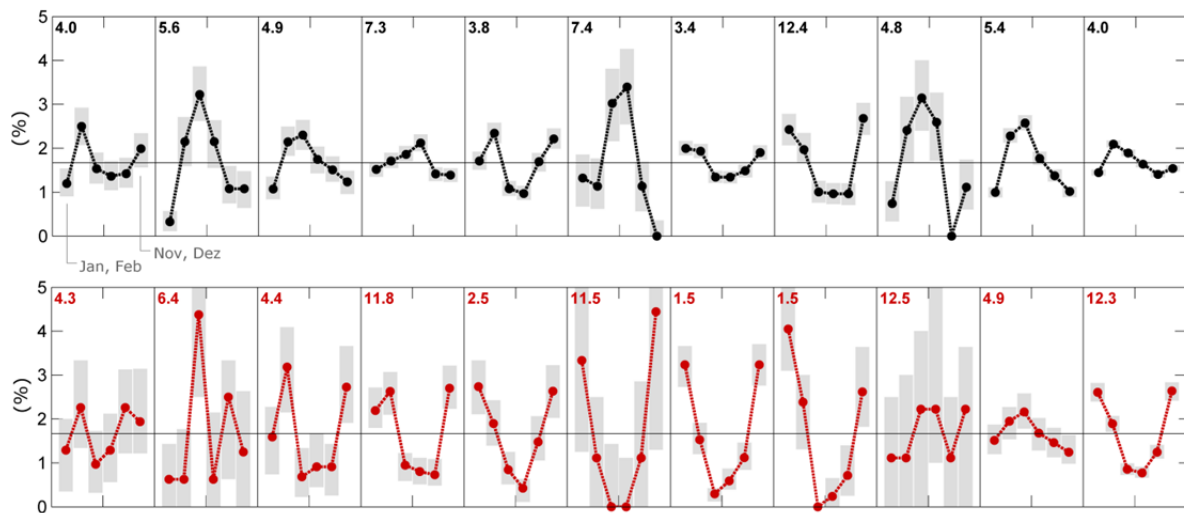


Figure 22: Mean annual cycle of the frequency of track types for bimonthly periods for weak (top, black) and strong (bottom, red) cyclones (1959-2015). Number in the top-left corner indicates the frequency peak (month, eg. 12.5 indicates mid December). Grey bars indicate the confidence intervals ($\alpha=0.05$).

Another characteristic that is relevant to precipitation is the time a cyclone remains close to the study region. The residence time within region TRZ has been therefore been calculated (Table 12). On average, cyclones remain about 35 hours or 1.45 days over Central Europe, except for type Vb with nearly 60 hours or 2.4 days. For strong cyclones (cyclone intensity > 85th percentile) the average is higher with 54 hours or 2.25 days, indicating a lower propagation speed for this group. In case of strong Vb cyclones, the residence times are even longer with more than 3 days or 80 hours. For all other types the residence time is close to the average. The residence time must either be related to the propagation speed or to the specific path of cyclones within region TRZ. On average, cyclones move at a speed of 8.7 ms⁻¹ and for 80% of all cyclones the propagation speed is between 6.5 and 11.8 ms⁻¹, with about 10% lower speeds in summer compared to the winter (not shown). The difference between Z700 and SLP is minor but strong cyclones are about 15% slower than all others. This means that strong summer cyclones move at considerably lower speeds over Central Europe which explains the difference in residence time. These velocities are very similar to the ones found in other studies, such as velocities in winter for the Northern Hemisphere (Neu *et al.*, 2013) or on an annual basis over the Western Mediterranean and parts of Central Europe (Lionello *et al.*, 2016). Stratified by the track type, the fastest and slowest cyclones are found among types ATL and X-S, respectively. There are also systematic differences between the other types, however these are not very pronounced and a broad range of speeds occurs.

Table 12: Mean duration cyclone centers remain within TRZ (days) 1959-2015.

residence time	Vb	EA	X-N	X-S	MED	STR	ATL	POL	CON	TRZ	ALL
all intensities	2.43	1.39	1.58	1.34	1.32	1.30	1.34	1.40	1.58	1.48	1.45
strong cyclones	3.50	2.00	2.25	2.00	2.00	2.00	2.00	2.00	2.25	2.25	2.25

As shown above (Table 12), the residence times of Vb are much longer than those of the other types, but this is not reflected by lower propagation speeds. This is because of the typical circular shape of propagation paths within TRZ, either steered by orographic features or by upper level atmospheric circulation patterns favoring quasi-stationary flow situations. The circular shape is important for flood generation, as this kind of cyclone may remain close to a particular river basin in the study region over an extended period and therefore have a high potential for triggering long-duration rainfall events.

Upper level circulation patterns

Precipitation patterns over Europe are largely controlled by atmospheric cyclones, which are embedded in the general circulation of mid latitudes. In the following, dominant patterns of the steering upper level atmospheric circulation over Europe are illustrated in the context of track types identified at SLP. In the left columns of Figure 23 and Figure 24, mean geopotential height anomalies at 500hPa are shown, 48 hours (t_{-48}) before the corresponding cyclone has reached its maximum intensity inside region TRZ, reflecting the antecedent state of the circulation. The black arrows indicate the typical propagation direction of cyclones at SLP. The center and left columns show the anomaly fields for weak and strong cyclones, 6 hours before the time the cyclones reach their maximum intensity over Central Europe (t_{-6}). The color shading indicates the mean vertical velocity at Z700 at time t_0 . From these figures it becomes clear that each cyclone track type is connected to a specific pattern of the upper level atmospheric flow.

In general the patterns are characterized by a major trough located over Europe (Figure 23 and Figure 6, left panel), however, the shape, amplitude and position of the trough differ substantially between the types. The axis of the major trough is located considerably eastward of Central Europe in case of types POL and CON, whereas it is located over Western Europe at time t_{-48} for all other types. As a consequence, the geostrophic wind vector at 500hPa has a strong northerly component towards the Alps for these two types, followed by X-S and ATL with a dominant northwesterly flow, X-N, MED, STR and TRZ with mostly westerly, and finally Vb and EA with prevailing southwesterly wind over the Alps during the initial phase. The amplitude of the dominant trough also differs between the types. For Vb, EA, POL, STR and CON cyclones the trough is well developed and has a large amplitude which leads to a strong meridional mass and energy exchange over Europe. In contrast, for X-S, X-N, MED, ATL and TRZ cyclones the major trough is more elongated with a strong zonal flow over Central Europe.

Later in the development (Figure 23 and 6, center and right panels), the major trough has propagated further and is located right over Central Europe. The exception is STR where the trough is found over the western European coastlines. At the same time the trough has amplified and large regions with enhanced vertical lifting can be seen (yellow colors). Specifically for strong cyclones, these regions are more widespread and contain a number of spots where vertical velocities are further enhanced (red colors). When comparing upper

level circulation patterns between weak and strong cyclones, the amplitude of the major trough is even larger for the latter, accompanied by stronger gradients and hence geostrophic winds over Europe. Another prominent feature of the strong Vb, EA and CON type cyclones is a major COL that emerges over Central Europe, the North Sea and Eastern Europe, respectively. Especially for types Vb and CON the COL is very pronounced and therefore prevails over a sizeable region together with circular upper level steering winds for a long time. In 15% of all cases, SLP cyclones of types Vb, EA or X-N are accompanied by TRZ cyclones at Z700, indicating the occasional presence of upper level cut off low situations also for the other types.

4.3.2 Precipitation stratified by track types

Both cyclone tracks identified from SLP and Z700 are used for the analysis of precipitation with respect to cyclone track types in the following .

Mean cyclone precipitation

Between 57% and 73% of the observed annual precipitation over Central Europe can be associated with the occurrence of atmospheric cyclones on average (Table 13), denoted as cyclone precipitation. These numbers are very similar to the findings from other studies for Central Europe (Rulfová and Kyselý, 2013, Hawcroft et al., 2012) and are about 5% higher than those of Hofstätter *et al.* (2016). The percentage in the current study is largest in areas located around the Eastern Alps close to the Adriatic Sea and decreases towards Western Germany. When higher precipitation amounts (>95pct of R^6) are considered, the fraction increases in all regions to values between 63% and 92%. The attribution of large scale precipitation to cyclones therefore appears to be more conclusive for higher precipitation amounts. Relatively low shares are found in region N-WE and M-WE, which are most affected by ATL cyclones (Hofstätter et al., 2016), but they are occasionally missed when passing by far outside of region TRZ.

Table 13: (a) Size of the eight study regions, (b) total annual precipitation and the percentage attributed to cyclones, and (c) mean precipitation in case a cyclone is located within region TRZ.

	region		N-WE	M-WE	S-WE	ALPN	ERZG	N-CZ	EAST	ALPS
(a)	size of region	(10^3 km^2)	83.5	26.0	77.8	49.2	48.7	39.6	50.3	34.8
(b)	annual precipitation based on R^6	(mm yr^{-1})	835	756	1140	1216	628	635	678	1098
	percentage attributed to cyclones	$R^6 > 0\text{mm}$	57%	62%	67%	65%	64%	66%	69%	73%
		$R^6 > 95\text{pct}$	63%	76%	83%	81%	86%	91%	90%	92%

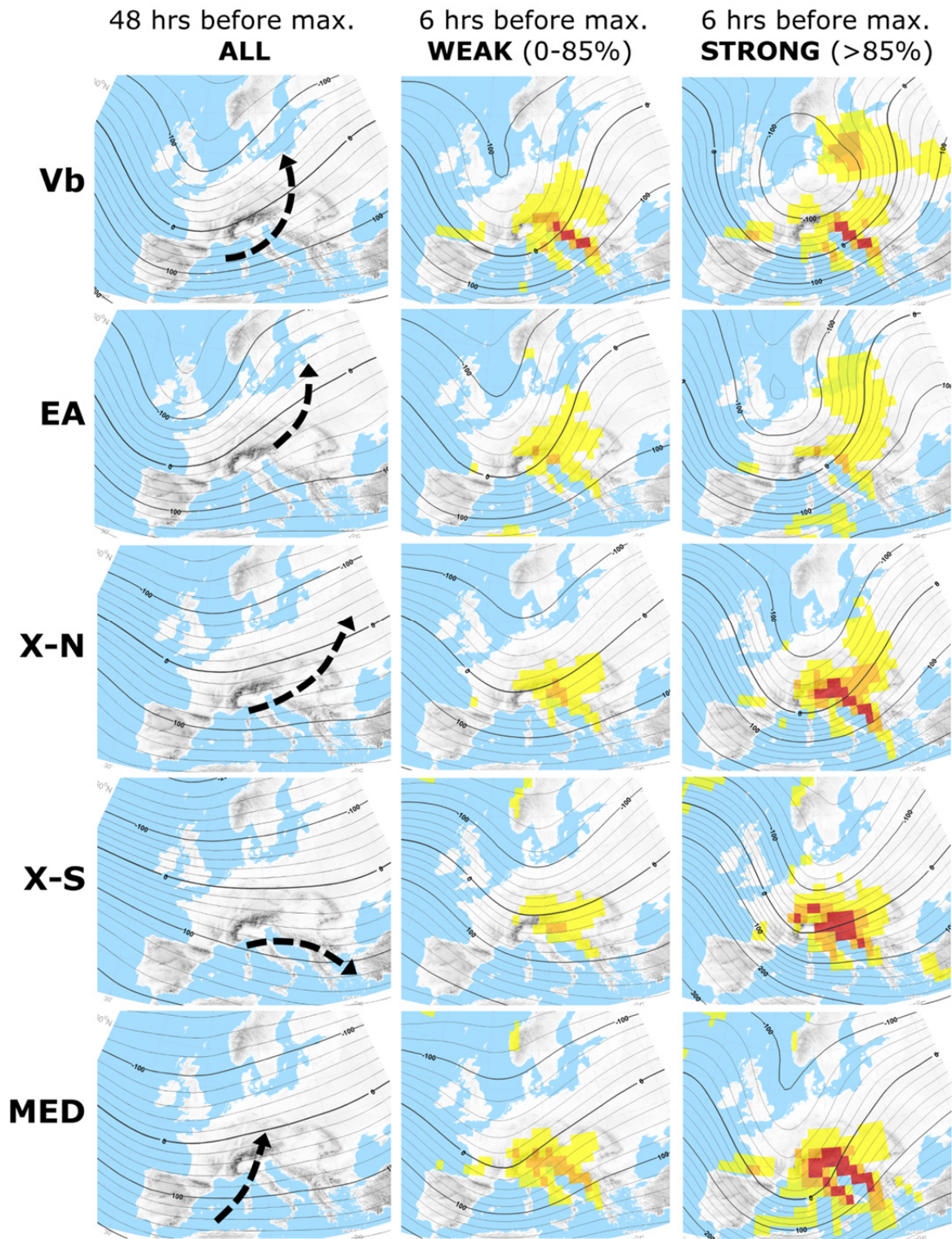


Figure 23: Mean upper level circulation patterns for the track types, 48 hours (left column) and six hours (center and right column) before the time t_{\max} the respective cyclone at SLP reaches its maximum intensity within Central Europe (500hPa geopotential height anomaly). Color shading indicates mean vertical velocity at time t_{\max} . -0.3 to -0.6 ms^{-1} shown in yellow, -0.6 to -0.9 ms^{-1} in orange and less than -0.9 ms^{-1} in red. Arrows indicate the typical propagation directions of cyclones at SLP. Type Vb, EA, X-N, X-S and MED.

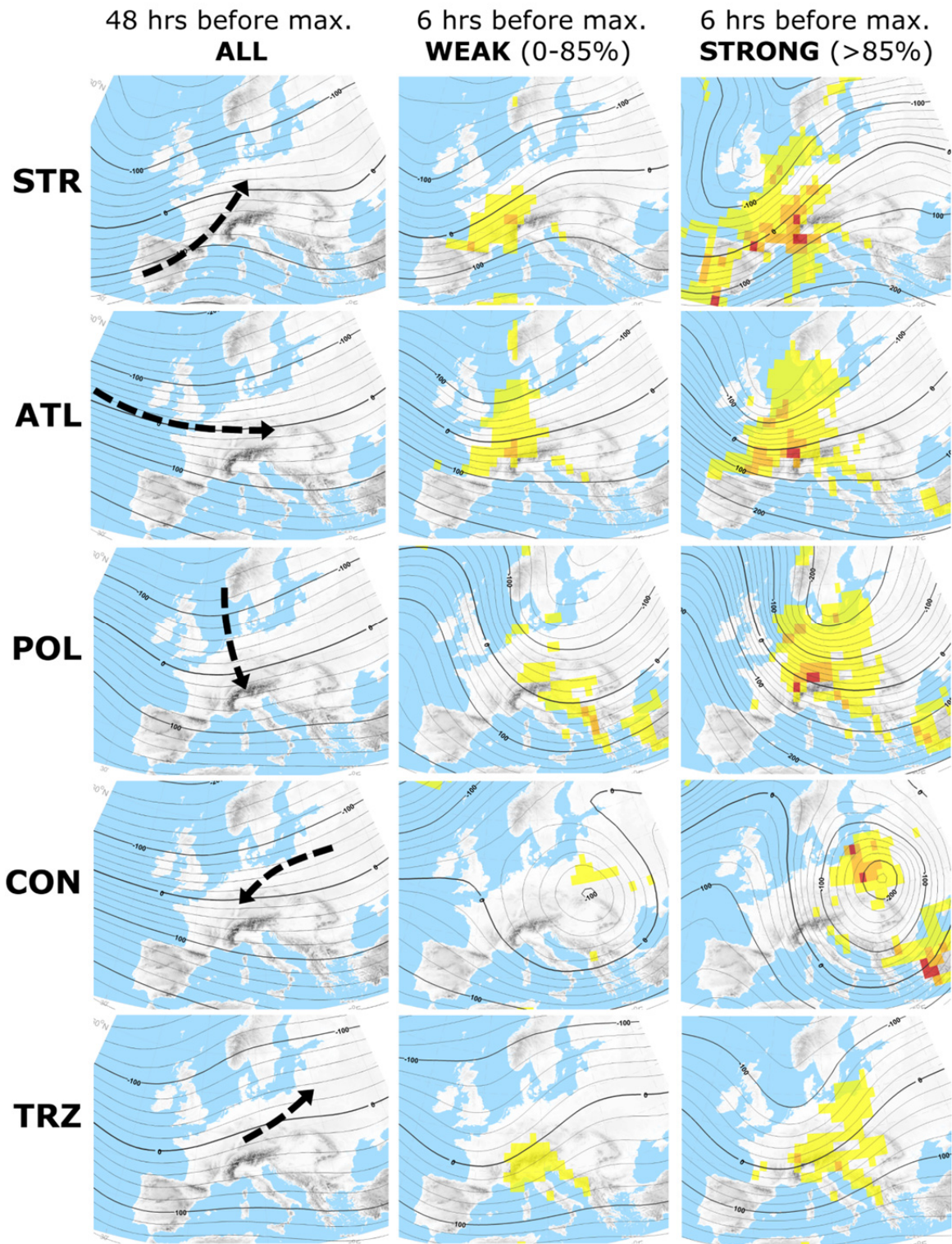


Figure 24: Same as Figure 23 but for types ATL, STR, POL, CON and TRZ.

In Figure 25a mean annual cyclone precipitation was partitioned into track types for all regions. On an annual basis about 60% is associated with the types TRZ, ATL and X-S in accordance with the relative frequency of 65% for the occurrence of these track types taken together. Nearly 11% is attributable to Vb cyclones, although their relative frequency is only 5%. In a similar vein, an above average contribution of 7.4% can be seen for type X-N, a congeneric track type to Vb, and 3% for type EA (consistent with 5.5% and 2% relative frequencies of occurrence). One fifth is attributable to Atlantic cyclones (ATL), another fourth to cyclones emerging straight over Central Europe (TRZ) and about one half is connected to cyclones moving from the Mediterranean into Central Europe (MED, X-S, X-N and Vb). These cyclone types appear as the main drivers of the Central European precipitation climate in terms of large scale precipitation.

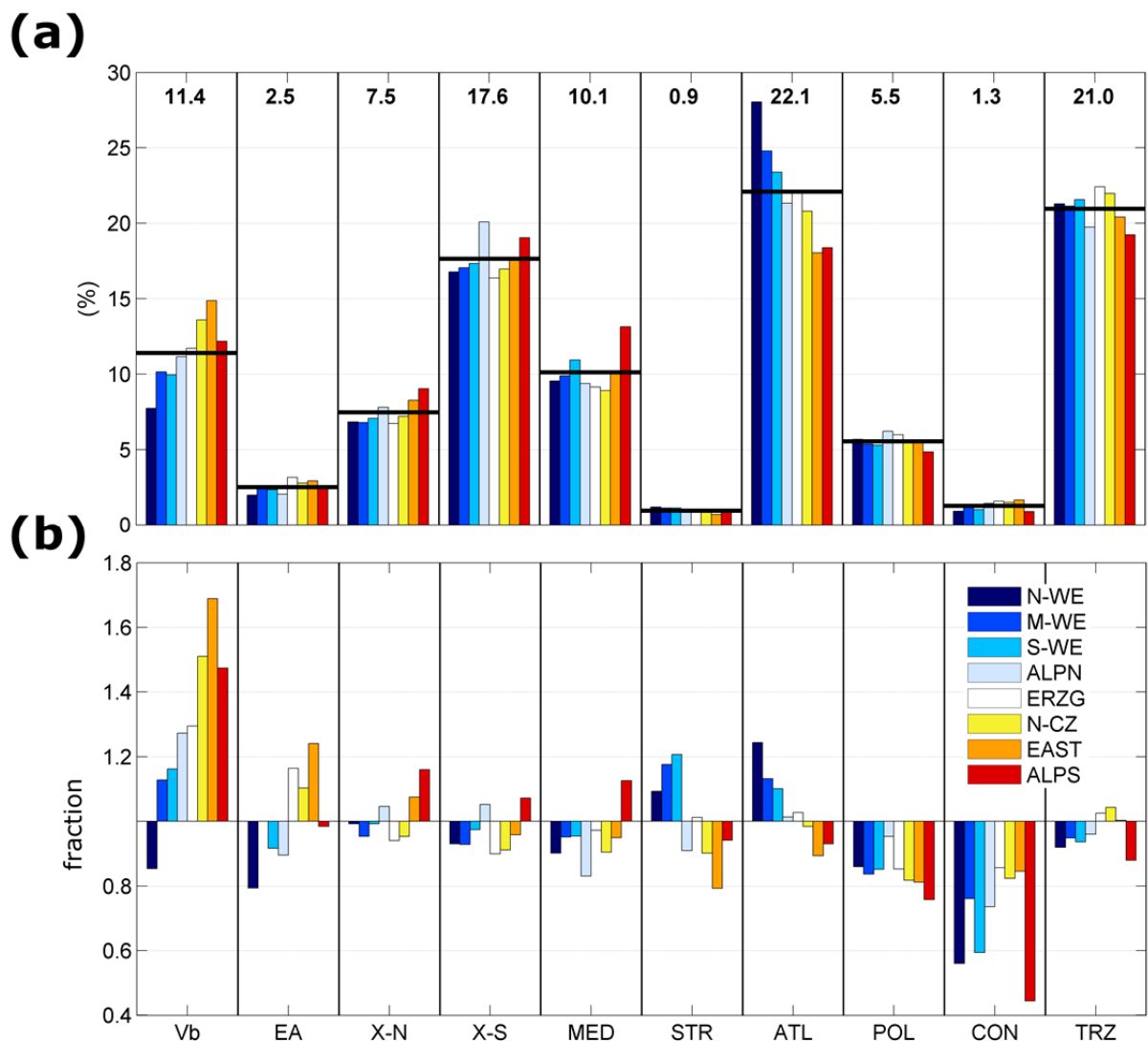


Figure 25: (a) Attribution of mean annual precipitation (based on R^6) associated with cyclones to track types (SLP and Z700 together) for the period 1959-2006 as percentages. Black horizontal lines and numbers on top indicate the average over all regions. (b) Regional mean precipitation intensity $\overline{R^6}_\tau$ for each track type τ relative to regional mean precipitation intensity for all track types $\overline{R^6}$.

The relative contribution from track types also depends on the region (Figure 25a). Type ATL, for example, contributes 28% of the annual cyclone precipitation over Western

Germany but only 18% in the regions east and south of the Eastern Alps (EAST, ALPS). The influence of the Atlantic clearly diminishes from the Northwest to the Southeast over Central Europe. At the same time, the influence of the Mediterranean increases from North West (41%) to South (53%) regarding type MED, Vb, X-S and X-N on an annual basis. Cyclones of types CON, EA, STR and POL only play a minor role in terms of mean annual cyclone precipitation over Central Europe. Total annual precipitation in Figure 25a is largely driven by cyclone frequency, as the relative share for each type (numbers at the top of Figure 25a) is very similar to the relative track frequency (Table 11). However, for some types, such as Vb or CON, the annual totals cannot be explained by frequency alone. Figure 25b shows the relative precipitation intensity for each track type, with values larger or smaller than unity indicating above or below average intensities over a certain region. Very high intensities occur for Vb cyclones, especially in regions ALPS, EAST and N-CZ, which are located close to the path of Vb cyclones. Below average intensities occur for POL and CON cyclones in all regions. STR and ATL cyclones show higher intensities in the western regions.

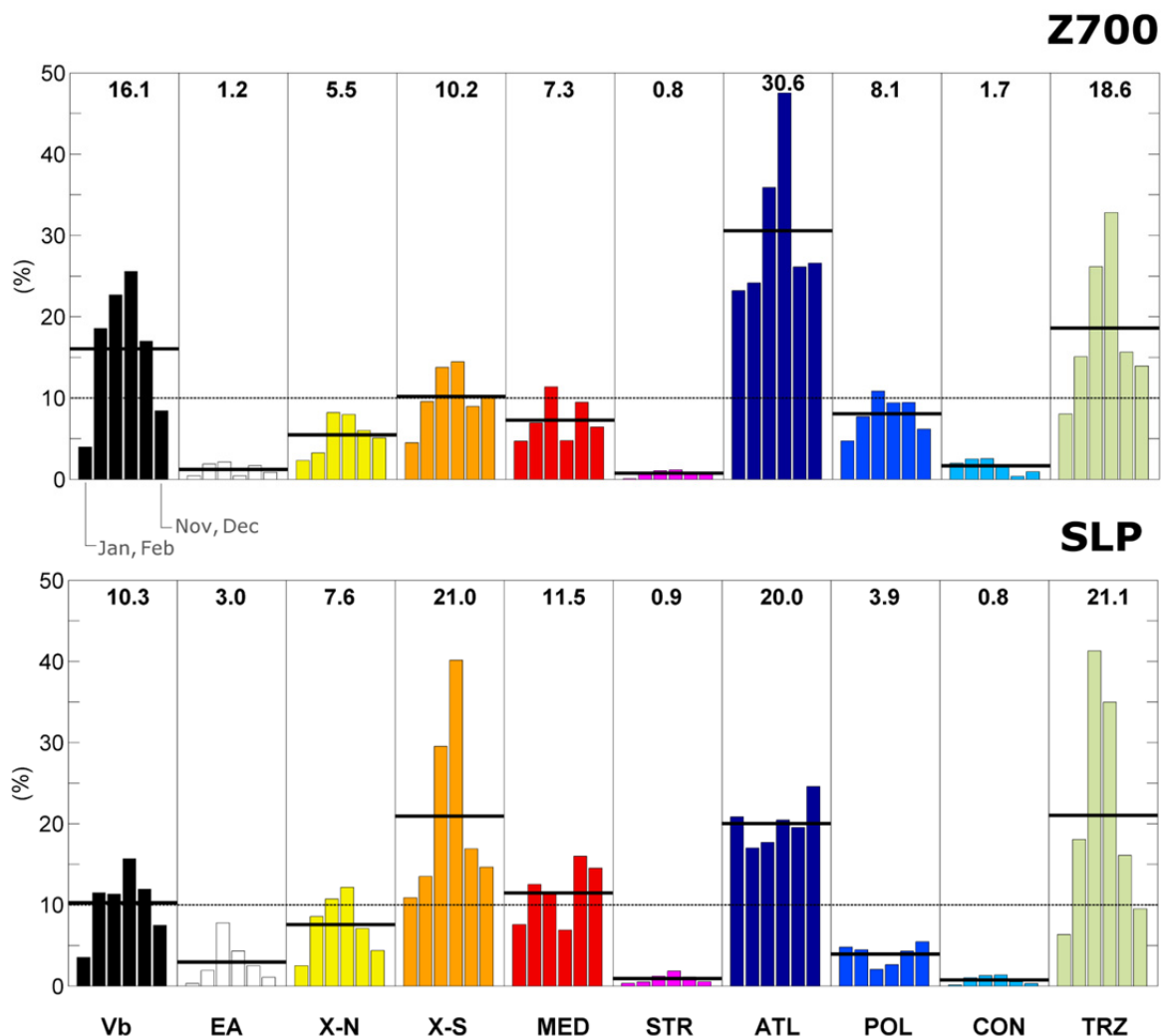


Figure 26: Mean annual cycle of precipitation (based on R^6) associated with cyclone tracks for two-month periods (bars) as an average contribution over all regions relative to all cyclone types. Black horizontal lines indicate the mean for each track type. Top: geopotential height at 700hPa. Bottom: surface level. Black horizontal lines and numbers on top indicate the average over all seasons.

While Figure 25 represents the mean annual contributions and fractions for each region, Figure 26 represents the seasonal cycle, averaged over all eight regions. The total relative contribution from all bimonthly periods sums up to 1 for each cyclone track type. Similar to Figure 25a, the relative contribution from the different levels for a certain track type (numbers at the top of Figure 26) corresponds with the ratio of cyclone frequency between SLP and Z700. A clear summer peak in frequency is found for most of the types at both levels. This peak is driven by high temperatures and associated high levels of atmospheric water content during the warm season. An inverse seasonal cycle with a winter maximum is found for ATL and POL at SLP which corresponds with the very high frequency of strong cyclones in winter for these types (Figure 22). Interestingly, there are two maxima of mean precipitation associated with MED cyclones. The first occurs in spring, the second in late autumn, two periods with very different Mediterranean Sea surface temperatures. The high frequency of Mediterranean cyclones in Mar-Apr and Nov-Dec found in this study (Figure 22) is consistent with findings from the literature (Lionello et al., 2016). However the second precipitation maximum already starts in Sept-Oct, indicating that additional factors are needed to fully understand the spatio-temporal characteristics of mean cyclone precipitation over Central Europe, apart from cyclone frequency and intensity.

Heavy cyclone precipitation

In this study, heavy precipitation is based on R^{trc} and has been defined as precipitation HP_{95} of a cyclone exceeded by 5% of the cyclones of the same type (Equation 13 and Equation 15). HP_{95} was calculated for each region and track type separately as well as for all tracks without differentiating between the types. The latter case is used as a reference value to estimate exceedance probabilities and will be denoted as HP_{95r} . The extreme value analysis was based on cyclone tracks identified at both atmospheric levels individually, because of important differences in the results. In general, winter heavy precipitation (HP_{95r}) is only about 60% of that observed in summer (Table 14), independently of the level. When differentiating between track types, summer HP_{95} is about 10% higher at SLP compared to Z700 for types Vb, EA, XN, XS, MED and CON, whereas it is about 20% higher at Z700 compared to SLP for types ATL, POL, TRZ and STR. In winter there are no major differences between track types from the two levels. Very high amounts of HP_{95} are observed in the specific case of Vb in both seasons at all levels, with heavy precipitation values between 140% and 190% of the reference. Above or close to average conditions are also found for track types X-N in both seasons, for EA, X-S and MED in summer as well as for ATL in winter.

Table 14: Heavy precipitation HP_{95} (mm) exceeded by 5% of the cyclone events of the same track type estimated from R^{trc} as well as reference value HP_{95r} , calculated from all tracks (regional means over all regions).
Summer: May-Oct. Winter: Nov-Apr.

season	level	Vb	EA	X-N	X-S	MED	STR	ATL	POL	CON	TRZ	HP_{95r}
summer	SLP	56.4	29.9	34.0	30.7	29.7	21.3	24.8	23.6	21.6	25.9	29.9
	700	53.9	21.2	33.6	25.4	28.2	/	30.6	28.5	17.0	28.8	32.4
winter	SLP	28.9	15.4	20.0	16.3	18.7	14.8	19.7	14.1	14.2	16.1	18.8
	700	25.7	13.3	15.7	14.6	15.2	/	19.8	14.1	12.2	16.2	18.1

In connection with the seasonal reference values shown in Table 14 (right), the probability $\Pr(R^{trc} > HP_{95r})$ of a precipitation event R^{trc} exceeding the threshold HP_{95r} depends on the track type (Figure 27). Probabilities different from 5% indicate a systematic connection between a certain track type and heavy precipitation. For track types ATL, POL and TRZ the probabilities are clearly higher at level Z700, whereas the opposite is the case for types EA and X-S. For all other types the differences are small. The obvious differences between the levels point towards the importance of considering more than a single atmospheric level in identifying cyclone tracks in the context of large scale heavy precipitation analysis.

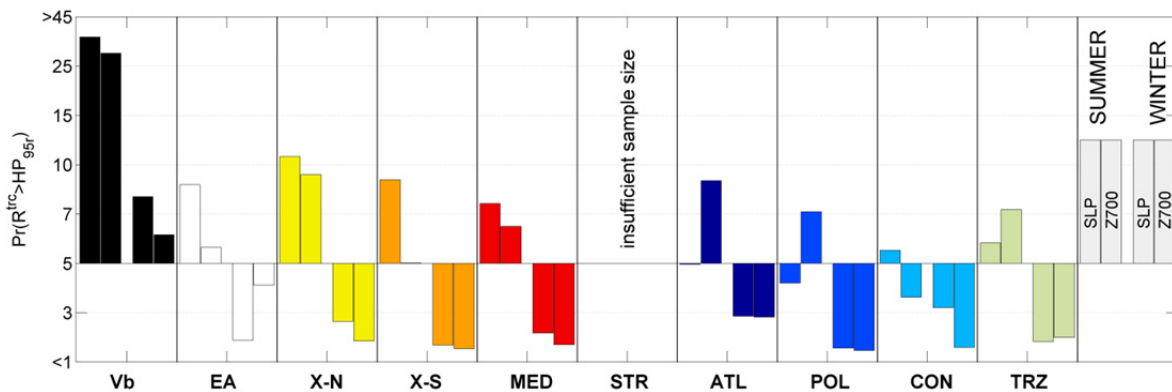


Figure 27: Exceedance Probability $\Pr(R^{trc} > HP_{95r})$ for a heavy precipitation event related to the occurrence of cyclones as an average over all regions.

In terms of differences between regions (not shown), EAST and N-CZ give the highest probabilities of Vb and EA precipitation, N-WE and M-WE the lowest. Type X-N and X-S are most relevant in regions located around the Eastern Alps. Some track types show high values ($x^{prb} > 5\%$) in specific regions, such as MED in region ALPS as well as ATL in region N-WE. Vb types are highly associated with heavy precipitation in all regions (except N-WE), or more specifically at least every fifth ($x^{prb} = 20\%$) to third ($x^{prb} = 30\%$) Vb cyclone is related to heavy precipitation in the summer season (Figure 27, leftmost). In regions EAST and N-CZ, HP_{95r} is exceeded during almost every second Vb summer cyclone ($x^{prb} = 45\%$).

Outstanding precipitation events

(a) *The period 1959-2006 for the eight regions using the WETRAX data:* From this analysis (Figure 28), Vb appears as the most frequent cyclone track type among the top-50 precipitation events in Central Europe (29 % of the events on average over all regions), followed by types TRZ (16 %) and ATL (16 %), accounting for two thirds of the top events in total. Another third can be attributed to types MED (13 %), X-S (10 %) and X-N (8 %). EA appears to be of minor relevance although this type has been related to high HP_{95} exceedance probabilities during summer in Figure 27. This is because this type occurs only rarely. In contrast, ATL and TRZ cyclones are more prominent among the top-50 events than would be expected from the exceedance probabilities. This is mainly because ATL and TRZ cyclones are very frequent, representing about 50% of the total annual frequency which raises the chance of a top event for these types. The attribution to track types strongly depends on the region, with a large number of ATL and TRZ cyclones dominating the top-50 precipitation events in N-WE (Figure 28). In the East of the study region between the German Erzgebirge and Eastern Austria, Vb cyclones are most important with nearly 40%.

Type X-S on the other hand is more relevant in regions located close to the Adriatic Sea around the Eastern Alps with 18% attribution rate in ALPS, for example. Interestingly, Mediterranean cyclones are also of relevance in this context, especially in regions located near the Western Alps. This finding clearly confirms that subtle spatial differences in the occurrence of heavy precipitation events, even within the limited domain of CE, are caused by different types of atmospheric cyclone tracks.

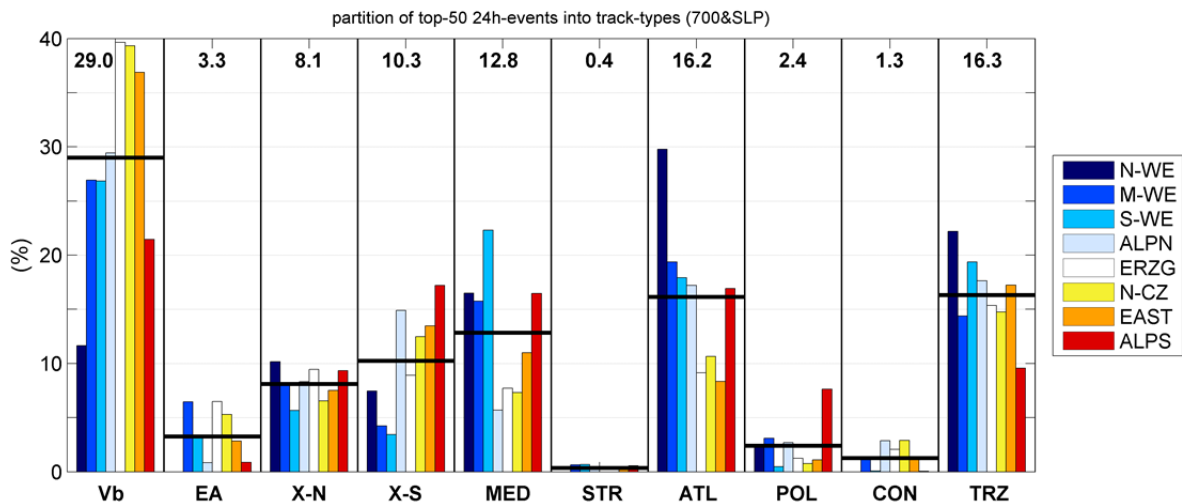


Figure 28: Attribution of the TOP-50 precipitation events (R^{24}) to track types for 1959-2006 as percentages. Black horizontal lines and numbers on top indicate the average over all regions.

(b) *The extended period 1959-2015 for SEGE and CZAT using the E-OBS data:* Table 15 presents a top-50 list of the largest 24 hrs precipitation events R^{24} of the period 1959-2015. Left shows the results for a domain in Southeastern Germany (SEGE), right the results for a domain located over Eastern Austria and the Czech Republic (CZAT). The table contains the rank, the date of the precipitation maximum and the corresponding precipitation amount (R^{24}) as well as the attribution to track types from both atmospheric levels using rdv^{max} as described above. The table covers many heavy precipitation events well known from flood history, such as the event 1981-07 (Rimbu *et al.*, 2016), 1977-07, 1978-8, 1979-06 and 1985-08 (Böhm and Wetzel, 2006), 1977-08, 1985-08 and 1997-07 (Müller *et al.*, 2015), 2002-08 (Ulbrich *et al.*, 2003a) and 2013-06 (Blöschl *et al.*, 2013, Schröter *et al.*, 2015). For some events, flooding was only minor, even though precipitation was massive, due to dry catchment conditions and/or due to incongruity between precipitation regions and river catchments. Some highly ranked events appear in both regions (e.g. 6th to 7th July, 1985) but also some of the low ranks appear in both lists (e.g. 6th to 7th Aug, 2010). About 25% of the events are among the top 50 in both regions, SEGE and CZAT, the rest is only in one of them. This indicates that spatio-temporal coherence, even between neighboring regions, is weak for large scale precipitation extremes.

Table 15: Top-50 of the largest 24 hr precipitation maxima (R^{24}) for 1959-2015, with the rank of the events, the corresponding date and the 24 hr precipitation amounts on the left. On the right the attribution to track types is given as $100 \cdot rdv^{max}$, with higher values indicating a more conclusive attribution. Shading indicates consecutive 5-year periods, beginning with 1961-1965 and ending with 2011-2015.

Region SEGE											Region CZAT														
rank	YYYYMMDD	mm	VB	EA	X-N	X-S	MED	STR	ATL	POL	CON	TRZ	rank	YYYYMMDD	mm	VB	EA	X-N	X-S	MED	STR	ATL	POL	CON	TRZ
6	20151120	35,0				23				8			29	20140911	22,6	12									
25	20140721	27,4					53					17	1	20130624	36,1	22	29		25						
3	20130601	36,3										23	21	20130602	22,4									25	24
43	20100806	25,0	29			13							22	20120912	24,0				49						
29	20100723	26,9		11	17								21	20110721	24,1							15			
48	20090718	24,9	61						11				23	20100926	23,9	45							50		
18	20070529	29,1				52						28	48	20100807	19,7	21									
32	20050822	25,9			21							29	10	20100717	27,9		11	17							
45	20040113	24,9							30				15	20100723	25,1										
4	20020811	35,5	59			21							37	20090718	21,5	67									
33	20020807	25,9			16				17	10		33	45	20090623	20,2	19									
12	20020320	33,6										17	18	20080815	24,7	60									18
27	20000921	27,1					64		7				7	20070906	31,1										55
13	19990521	33,1	31				39						9	20060807	28,0	25			12					20	
39	19981029	25,2										14	44	20060630	20,2				12	7					19
24	19970705	27,5	25			24							43	20031005	20,4	70									
26	19960708	27,3	44		38				45				5	20020812	31,6	74			27						
30	19950601	26,5		20		34							8	20010720	30,0	32						7			
10	19940413	33,7	99										30	19980912	22,6	54									
44	19931220	24,9											41	19980905	20,5				30		24				
42	19930711	25,0	13	32			28						2	19970707	34,8	33			14						
16	19910801	29,4				23	16						11	19970719	27,8	29			30						
8	19910617	34,1	14	20	22								13	19960708	27,0	38		38				44			
23	19910511	27,7	52				16						19	19960622	24,4	32	30			40					20
11	19900214	33,6	99						50				24	19950915	23,8	52									23
17	19881205	29,4							29				25	19950901	23,3			39						41	
49	19870926	24,8										10	26	19950513	23,2	82									
41	19870302	25,0								29	42	11	34	19910802	21,7				17				18	10	
5	19850806	35,0	57										38	19910627	21,1			12			46				
38	19840905	25,4							11			19	14	19880902	25,7	30				31					26
31	19830802	26,3				21						8	42	19860812	20,4			7							31
1	19810719	40,5	80										3	19850807	34,2	75									
19	19791106	28,7											40	19811022	21,0			40					43		19
22	19790921	28,3					25						6	19810719	31,5	68			30						
9	19790617	33,9				16			30				35	19801012	21,6	22						10			
36	19790311	25,5											17	19790924	24,9	34		25		37					
2	19780807	39,0	28				19		12				27	19790617	23,1				16			30			
47	19780320	24,9							15			11	49	19780808	19,4	48			25	50		7			
7	19770731	34,7	48			11					8	44	4	19770801	32,0	49			17				9		41
15	19731115	29,6										16	32	19770822	22,0	68			18						11
34	19710607	25,9			13			10				11	20	19750701	24,3						10				36
14	19700809	32,7				32							47	19741021	19,9	64						32	11		
46	19700222	24,9							50				46	19720519	20,0	24	24								
28	19680921	27,1							11				39	19701122	21,1	33							39		
50	19650609	24,8	24									18	33	19641009	21,8					47					37
21	19641117	28,3											16	19640810	24,9			9							21
40	19611212	25,1										27	28	19630615	22,7	20						25			11
35	19590715	25,6				23						23	36	19621101	21,5			29	31						24
20	19590613	28,4										17	50	19620514	19,3	26				29					
37	19590501	25,4	29	12					20				12	19600813	27,6	54							7		

Seasonality of the frequency of the top-50 events (Figure 29) shows another important feature. In region CZAT all events occur between May and November, with a distinct frequency peak in August (not shown) when air temperature and sea surface temperatures are highest. In contrast, in SEGE 30% of the top-50 events occur between October and April.

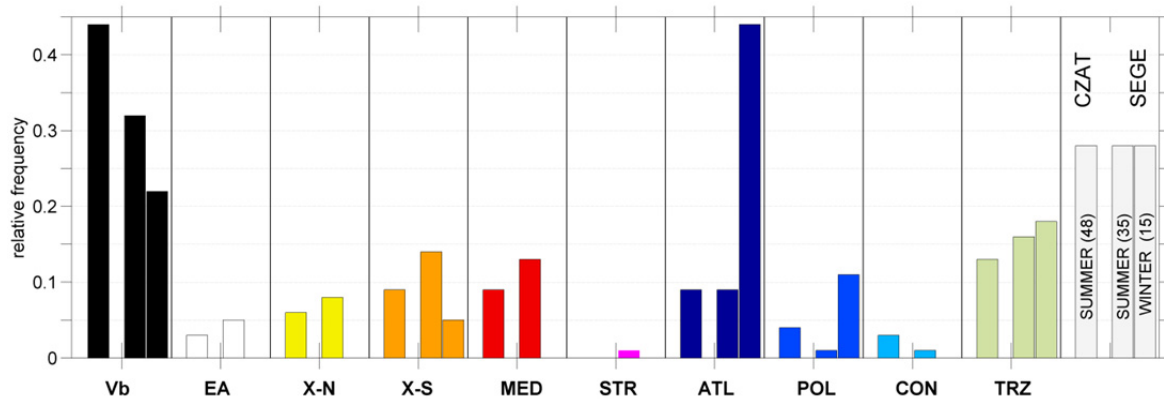


Figure 29: Seasonal relative frequencies of the top-50 precipitation events for the period 1959-2015 in regions CZAT and SEGE. No bars are shown for CZAT in winter with two events only.

In the cold season (Nov-Apr) 44% of the top events found in SEGE can be attributed to ATL cyclones in contrast to only 9% in the warm season (Figure 29). Another 51% can be attributed to Vb (22%), TRZ (18%) and POL (11%) in the cold season. There is also a striking difference between the two regions, although they are located just next to each other. In SEGE cyclone track types, such as ATL, come into play in the cold season, hence a seasonal differentiation is important for understanding Central Europe flood regimes from an atmospheric perspective. The most important track type for the extreme precipitation events, both in CZAT and SEGE, is Vb with relative frequencies of 43% (CZAT) and 30% (SEGE); other relevant tracks are TRZ, ATL, X-S and MED.

Finally, the top-50 events are evaluated in terms of temporal changes of event frequency, of 24 hr precipitation as well as of cyclone intensity. Linear trends are estimated from the averages of these variables for consecutive 5-year periods, beginning with 1961-1965 and ending with 2011-2015. Table 16 presents Mann-Kendall's tau, the according p-value, the observed trend magnitude estimated as the Sen-slope, the total trend relative to the overall mean as well as the probability *pct*. Probability *pct* indicates the likelihood to observe a trend larger than the observed one given 50 of the largest precipitation maxima from 1961-2015. This likelihood has been calculated from 10^4 bootstrap samples with replacement, by randomly selecting 50 years out of 1959-2015, assigning these to the given top-50 precipitation amounts and sorting the list by date. For each of these random samples, averages of 5-year consecutive periods were calculated as described above and trend analysis was applied repeatedly. The individual events were assumed to be independent from each other and the year of the events was assumed to be a result of a uniform random process. From this analysis a small and insignificant increase can be seen for region SEGE, both for the number of events (+4.1%) and the amount of precipitation (+6.9%). For CZAT the increase is stronger with 12.9% and 20.5%, and the change in R^{24} is significant ($p=0.06$). The increase in event number in CZAT is controlled by the exceptional period 2006 to 2014, comprising an unusually high number of heavy precipitation events, especially in the year 2010. One can therefore not assume that the increase over the last 50 years is monotonic.

The bootstrap analysis shows that the chance for getting a trend larger than the observed one is just 1.1% in region CZAT given the observed precipitation amounts. This clearly demonstrates that the period 2006 to 2014 was an extraordinary one, specifically in terms of heavy precipitation in the Czech Republic. However, it remains unclear whether this period is just a result of a clustering of events by chance (or natural variability) or related to an ongoing regime shift associated with global climate change. Although a comparable signal cannot be seen for the neighboring region SEGE, a series of heavy precipitation and related flood events hit other European countries as well in the last decade.

Table 16: Linear trend analysis of the top-50 precipitation events for consecutive 5-year periods (1961-2015), regarding 24hr precipitation (R^{24}), number of events and intensity of related cyclones for the CZAT and SEGE regions. Mann-Kendall's tau, the according p-value, the trend magnitude estimated as the Sen-slope, the total trend (difference 2015 - 1961) relative to the mean as well as the probability *pct* for getting a trend larger than the observed one given observed precipitation amounts.

		k-tau	p	Sens slope ($10y^{-1}$)	total trend (%)	pct (%)
CZAT	R^{24}	0.45	0.06	1.0 mm	20.5	1,1
	Number of events	0.29	0.23	0.67	12.9	3,6
	Intensity	-0.09	0.76	-	-	72,5
SEGE	R^{24}	0.24	0.35	0.4 mm	6.9	18,4
	Number of events	0.16	0.52	0.22	4.1	26,3
	Intensity	-0.09	0.76	-	-	74,9

4.4 Discussion and Conclusion

In this study, atmospheric open and closed cyclones over Central Europe have been analyzed at two atmospheric levels (SLP and Z700) and classified into track types using the scheme of Hofstätter *et al.* (2016). Atmospheric cyclone track types have been systematically linked to observed precipitation over Central Europe, to better understand spatial and seasonal characteristics of precipitation in general as well as of heavy precipitation in particular. Central European cyclone precipitation climate can largely be explained by seasonal track type frequency and cyclone intensity, however, additional factors are needed to explain the relatively high fraction of annual precipitation in September and November. The influence of Atlantic cyclones clearly diminishes from Northwest to Southeast, even within the limited domain of Central Europe. Conversely, MED cyclones mostly affect southern regions in autumn, when the Mediterranean Sea Surface temperatures are still high, as well as between December and April, when MED cyclone frequency is highest.

An upper level cut off low (COL) has been identified as a prominent circulation feature of strong Vb or CON cyclones in this study (Figure 23 and Figure 24). For Vb cyclones, the COL is typically located over Central Europe while for CON cyclones it is typically located over Eastern Europe. The formation of a COL is a consequence of an upper tropospheric Rossby wave breaking (e.g. Nieto *et al.*, 2008), inducing a persistent blocking regime and a series of consecutive cyclones at the surface level, as in June 2013 for example (Grams *et al.*, 2014). The occurrence of dominant COL's for selected heavy precipitation events has also been

recognized in other studies, however, the exact position of the COL differs in relation to the location of the respective study region. For example, for precipitation relevant to the Elbe basin, the COL is located over Northern Italy (Nied *et al.*, 2014); for the Balkan floods in 2014 it was located around the Dinaric Alps (Stadtherr *et al.*, 2016); and for flood events in the Czech Republic it is typically located over Central Europe (Müller *et al.*, 2009). For flood events in CE between 1948 and 2002 an upper level COL was identified, developing over Western Europe and propagating across the Northern Mediterranean into Eastern Europe afterwards (Jacobeit *et al.*, 2006). The development of an upper level COL ahead with the occurrence of strong Vb-cyclones was identified by Messmer *et al.* (2015), suggesting large-scale atmospheric dynamics as a main driver of heavy precipitation events. The COL patterns found in the current study for Vb and CON tracks induce an anti-clockwise circular propagation of the surface cyclone, leading to very long residence times (Table 12). Such a persistent cut off low might also favor a repetition of similar track types within a short time, which can result in soil moisture saturation at the beginning of a subsequent cyclone leading to enhanced flooding (Blöschl *et al.* 2013).

Vb has been identified as the most relevant track type for heavy cyclone precipitation in all seasons and affects large parts of Central Europe, regardless of the level at which the respective cyclone is observed. The reasons for this are: (i) strong Vb cyclones typically occur in all seasons (see also Hofstätter *et al.*, 2016), (ii) Vb cyclones remain close to Central Europe, much longer than other types, because of a circular cyclone track at the surface level and (iii) precipitation intensities, on average, are much higher than for all other types. In connection with the very high exceedance probability for a heavy precipitation event (Table 14 and Figure 28), these findings have serious implications for flood risk, as Vb cyclones can wet up soils within a short time, sometimes independently of the initial soil moisture state (Nied *et al.*, 2017, Schröter *et al.*, 2015). Another major type for heavy cyclone precipitation is ATL, especially in the western parts of Central Europe during the winter half year, when strong ATL cyclones are most frequent. This type explains nearly 50% of the top heavy precipitation events in the SEGE region in the cold season. It is typically connected with a strong northwesterly flow against the Alps, with an embedded warm front leading to northern Stau situations (Seibert *et al.*, 2007). Types X-N, X-S, EA and MED are mainly relevant for regions around the Eastern Alps in the vicinity of the Adriatic Sea and show highest precipitation amounts in late summer and early autumn.

For the analysis of heavy cyclone precipitation R^{trc} has been used, which depends on the residence time of cyclones over CE, so higher residence times may lead to exaggerated accumulation of precipitation. However, an extended analysis (not shown), based on the largest 24-hour running precipitation maxima for each cyclone track, gave very similar results as when using R^{trc} in most regions. This implies that cyclones with very high values of R^{trc} also show very high precipitation amounts on shorter time scales. However, the converse is not necessarily the case. Specifically, in regions N-WE and M-WE large scale precipitation frequently occurs on daily or sub-daily time scales because of fast propagating frontal systems connected to Atlantic cyclones. This also explains the lower share of precipitation found in the northwesterly regions such as N-WE or M-WE (Table 13b), those regions that are located closer to the Atlantic Ocean and far off from major orography as compared to the other regions.

The significance of track type Vb for heavy cyclone precipitation is rather high all over CE. It is especially high in Eastern Austria and the Czech Republic. This region is located directly along the path of the Vb cyclone center at SLP, typically an area with strongest pressure gradients and intense frontal lifting (Pfahl and Sprenger, 2016). At the same time, moist air masses are transported cyclonically around the Eastern Alps into CE (Messmer et al., 2015), ascending as a reversed warm conveyor belt over the cold sector of the cyclone (Grams et al., 2014). This study also revealed that that precipitation associated with Vb-cyclones is between 1.4 to 1.9 times larger than the 95% quantile of all tracks (Table 14); it is especially high in summer when seasonal air temperatures are highest. The sensitivity experiments of Messmer *et al.* (2017) using a numerical weather forecast model indicated an upper limit of the Vb cyclone intensities, but not for the related precipitation over Central Europe, when sea surface temperature in the Mediterranean is increased by several degrees. This supports the finding from our study of a significant increase of 24 hr precipitation for the top-50 events in region CZAT from 1961 to 2015, but the intensity of the related cyclones did not change (Table 16). During this time period a significant and rather monotonic increase of summer mean temperature of 1.5°C was observed in the Greater Alpine Region. Although a comparable precipitation signal cannot be seen for the neighboring region SEGE, a series of heavy precipitation and related flood events did hit other European countries in the last decade. Overall this indicates a potential increase of heavy precipitation in a warmer future climate for CE. Simulations using the ECHAM5 atmospheric global circulation model (Röckner et al., 2003) at 0.75° horizontal resolution show an increase in heavy precipitation of about 17% in the case of Vb-type cyclones over CE (Volosciuk et al., 2016). In line with Messmer et al., (2017), the increase was related to increased air moisture levels over the Mediterranean Basin, but no changes of cyclone intensity were found either.

A couple of caveats are in place regarding this analysis.

- (i) The cyclone track classification is based on a “Track Recognition Zone”, which has a well-defined geographical boundary. All cyclones moving into this zone are recognized, however very large and strong Atlantic systems occasionally move by north of region TRZ and a corresponding track type cannot be assigned, although precipitation was observed in parts of Central Europe.
- (ii) Another aspect concerns the exceedance probability for a heavy precipitation event based on R^{trc} . It is important to note that R^{trc} generally depends on the duration a cyclone remains within region TRZ. For cyclone types with a high residence time such as Vb, higher amounts of precipitation may be accumulated.
- (iii) Complex flow situations, with more than one cyclone found within region TRZ at the same time, either at SLP or Z700, account for 29% of the time steps with significant precipitation ($R^6 \geq 1\text{mm}$). When considering both levels independently, ambiguous cases are more frequent at SLP (27.4%) than at Z700 (15.1%) due to the underlying orography. This fact has also been pointed out by Wernli and Schwierz (2006) in connection with merging and splitting of cyclones. For a unique attribution of precipitation to one specific cyclone, additional information on the actual synoptic situation would be required.
- (iv) Attribution of precipitation to cyclones in this study only depends on the location of the cyclone centre, i.e. whether it is inside or outside region TRZ. This approach does not consider the actual extent or reach of a cyclone, and precipitation that is not causally related to a cyclone may be attributed incorrectly. Pfahl and Wernli (2012) used a different cyclone tracking scheme that considers the actual extent of cyclones (Wernli and Schwierz, 2006). They found a mean radius of cyclones of between 350km (genesis stage) and 800km (four

days later). In the current study 78.8% (77.6%) and 95.5% (94.1%) of precipitation ($\geq 1\text{mm}$) was attributed to a cyclone located within a distance less than 800km and 1000km at SLP (Z700), respectively, which is in line with Pfahl and Wernli (2012). However, when applying the approach of this study to other locations, we recommend a cyclone size assessment depending on the situation, which does not require comprehensive a-priori knowledge on the typical local synoptic conditions for the definition of region TRZ.

(v) The analysis of heavy precipitation (ch. 3.2.b) and of the top-50 events (ch. 3.2.c) is not affected by convective type and/or small scale precipitation, as regional averages have been used. Concerning the precipitation climatology (ch. 3.2.a), convective type precipitation is considered to the extent that station density of the WETRAX data set allows.

(vi) The size of the regions, over which precipitation has been averaged, may influence the results. Precipitation events with a spatial extent considerably smaller than the regions (Table 13) are systematically attenuated and therefore not fully considered. For these reasons, not every historic flood event observed in the Czech Republic for example (Müller et al., 2015) could be confirmed from this study (Table 15). However the occurrence of heavy precipitation alone does not necessarily induce a flood event. Other hydrologic factors can play a role such as antecedent soil moisture, snow melt, the presence of a snow cover and the position of the snowfall line (e.g. Merz and Blöschl, 2003), catchment characteristics (e.g. Gaál et al., 2012), river morphology and retention areas (e.g. Skublics et al., 2016), as well as flood hazard management.

From this study we conclude that cyclones identified at SLP are more strongly related to large scale heavy precipitation over Central Europe than those at Z700, in particular track types Vb, EA, X-N, X-S, MED and CON. This might be related to the presence of major mountain ranges promoting the genesis or intensification of surface cyclones through lee-cyclogenesis, as stronger large scale precipitation is generally observed in more intense cyclones and especially during the cyclone intensification phase (Pfahl and Sprenger, 2016). A higher precipitation amount is also expected for those cyclones that develop right down to the surface and show a strong signal there, as vertical lifting of moisture can be triggered from deeper atmospheric layers. Also, the association of observed precipitation at a certain location with cyclones appears more distinct at SLP. This is because of a marked horizontal displacement of cyclones between Z700 and SLP during the baroclinic development phase, at times when the vertical axis of a cyclone is tilted backward. At their major state, cyclones at SLP are usually located 300km ahead of the associated 500hPa trough (Lim and Simmonds, 2007). However, tracking cyclones at SLP has a number of challenges, both because of potentially deficient SLP patterns over major orography (e.g. Hoskins and Hodges, 2002) and a high number of spurious vorticity systems found at the lee side of mountain ranges under certain flow conditions. Also splitting and merging is more frequent at lower atmospheric levels as this study showed. On the other hand, higher heavy precipitation amounts were found in all seasons at Z700 for track types ATL, POL or TRZ. The geopotential height at 850hPa therefore appears as a good compromise for tracking cyclones or vorticity features in the context of heavy precipitation.

The findings of this study provide a new perspective on the Central European precipitation climate with a strong emphasis on heavy precipitation. The high frequency of strong cyclones was identified as the key factor in explaining seasonality of mean and heavy precipitation at a regional scale within CE. Strong cyclones not only show enhanced vertical lifting, but also move at considerably lower speeds across CE, resulting in longer residence times. These factors favor high moisture conversion rates as well as a prolonged duration of

precipitation. However, to fully explain above average contributions of certain track types in summer and late autumn, additional drivers are needed. Air temperature and Mediterranean Sea Surface temperature are likely candidates. Model simulations do indicate that Mediterranean Sea Surface warming amplifies Central European Precipitation extremes associated with Vb cyclones (Volosciuk et al., 2016). Future work could therefore focus on these potential drivers, not only in the context of air moisture supply, but as also on thermodynamic drivers of frontogenetic or cyclogenetic processes in the warm season (Aebischer and Schär, 1998). It remains unclear why Vb cyclones are strong in the warm season, and this appears crucial in understanding potential changes of heavy precipitation events under future climates.

Large scale heavy precipitation events have been the focus of this study. Future research could focus on different spatial and temporal scales, for example by considering high intensity short duration events. Serial clustering of cyclones appears to be another important issue, as soil moisture can build up during prolonged rain episodes, increasing the risk of flooding for moderate precipitation extremes. Likewise temporal changes of track type recurrence or cyclone frequency should be considered, as wet spell duration has changed in parts of Europe in recent decades (Zolina et al., 2013, Zolina, 2014).

The findings of this study are not only hoped to support the hydro-meteorological community in understanding the occurrence of large scale heavy precipitation and related floods from an atmospheric perspective, but could also provide a valuable basis for evaluating climate models over Europe. For example, frequency, intensity, seasonality and temporal variability of cyclone track types of the models could be compared with those of the observations.



5 Vb cyclones synchronized with the Arctic-/North Atlantic Oscillation

Abstract

Vb cyclones typically emerge in the Western Mediterranean and propagate to the Northeast into Central Europe. Some of the largest floods in Central Europe have been due to the heavy, large scale precipitation associated with Vb events. This paper explores the temporal characteristics of Vb cyclone occurrence based on cyclone tracks identified at the atmospheric levels of SLP and Z700, using JRA-55 reanalysis data for the period 1959-2015. The results suggest that the frequency of Vb cyclones was high in the 1960s and has remained at a lower level since then. Clusters of high Vb cyclone frequency exist and have occurred when both NAO and AO were negative. On the opposite Vb cyclone frequency is specifically low from 1988 to 1997 during a sustained positive phase of both NAO and AO. The coupling of the polar and the subtropical jet stream over the Western Mediterranean is identified as a main feature at the onset of Vb cyclones. Vb cyclone occurrence significantly lowers the NAO and AO indices, favouring successive Vb events, which suggests a $NAAO^- Vb^+$ feedback mechanism. By exploring the frequency and mechanisms of Vb cyclones we hope to advance our understanding of one of the most devastating weather/climate phenomena over Europe which will be of benefit for transnational flood management, climate modeling and impact research, and eventually for medium range forecasts of high impact weather events.

5.1 Introduction

Extreme weather events in Central Europe, such as large scale heavy precipitation and wind storms, are often related to the occurrence of mid latitude cyclones (Pfahl and Wernli, 2012; Hofstätter et al., 2018, H18 hereafter; Leckebusch et al., 2006; Donat et al, 2011). These types of events respectively account for about 53% and 15% of the economic losses due to natural hazards in Germany, for example (Munich Re, 1999), in addition to injuries and loss of life. Atmospheric research has traditionally prioritized wind storms, whereas large scale heavy precipitation events have gained increasing attention only after the 2002 summer floods in Central Europe (Ulbrich et al., 2003a & 2003b; Grazzini and van der Grijn, 2002) that were caused by Vb cyclones according to Van Bebber's (1891) classification. Historically, Vb cyclones have been vaguely described as low pressure systems propagating from the Western Mediterranean Sea to the Northeast, by crossing Northern Italy and leaving the Alpine ridge on the left. In recent years, it has become obvious that Vb cyclones are highly relevant for the occurrence of large scale (LS) precipitation extremes in Central Europe (CE) (Messmer et al., 2015), with up to 45% of these cyclones being associated with heavy precipitation in the Czech Republic and Eastern Austria (H18). At the same time, Vb cyclones are rather rare, as only 5% of all Central European cyclones can be attributed to this track type.

In the context of climate change it is expected that precipitation intensities will increase by $6.5\% K^{-1}$ with increasing mean air temperatures according to the Clausius Clapeyron relationship (Trenberth et al., 2003), with moisture availability, vertical atmospheric stability

and dynamical processes modulating this relationship (e.g. O’Gorman, 2015). Specifically for Vb cyclones, maximum daily precipitation increases of between 10 and 20 % have been simulated over the German Ore Mountains for 2071-2100 as compared to 1971-2000 (Nissen et al., 2013; Hofstätter et al., 2015). For assessing the risk of flooding due to Vb cyclones, the temporal evolution of their occurrence is another important factor which, however, has not been investigated so far. Observed trends of the total number of cyclones developing over the Western Mediterranean (WM) Sea may shed some light on the frequency of Vb cyclones. Lionello et al. (2016) examined WM cyclone tracks over the period 1979-2008 on an annual basis, but did not find any significant trends. Maheras et al. (2001) found a decrease in frequency of -4% per decade during 1958-1999, and a similar decrease was detected by Bartholy et al. (2009) which they attributed to the winter/spring season.

Another important, unresolved issue is whether Vb cyclones tend to occur in clusters, i.e. whether their arrival rate in some periods is significantly higher than the rate expected for a random Poisson point process (Cox and Isham, 1980). The occurrence of clusters would not only raise the question of their causal mechanism, but would also be of high practical relevance for flooding because of the accumulation of soil moisture by repetitive precipitation events (Grillakis et al., 2016). For example, a number of floods in the Isar catchment in southern Germany were exacerbated by a sequence of two Vb cyclones (Stahl and Hofstätter, 2018). Additionally, gearing flood risk management strategies towards flood rich periods is of enormous practical importance (Hall et al., 2014).

Serial clustering of cyclones is well known to occur over the Euro-Atlantic region (Mailier et al., 2006; Vitolo et al., 2009; Pinto et al., 2013) which is triggered by a persistent, zonally orientated and extended eddy-driven polar jet stream over the North Atlantic (Pinto et al., 2014). A persistent jet stream, which varies little in latitude, is typically associated with a strong jet (high wind speeds) located around 45°N (Woollings et al., 2010 and 2018). In contrast, if the jet stream is weak and shifted towards the South, i.e. the location of the WM, cyclogenesis and even clustering in the WM might be enhanced. The southern position of the jet stream is largely determined by a corresponding negative phase of the Northern Atlantic Oscillation (NAO) (Woollings and Blackburn, 2012; Wallace and Gutzler, 1981; Hurrell, 1995), which is usually associated with an increased frequency of high latitude blocking over Greenland or Northern Europe (Woollings et al., 2008). Indeed, during NAO⁻ conditions, the number of cyclone tracks in the WM is about +20% larger than during NAO⁺ (Nissen et al., 2014). Overall, these findings suggest that the occurrence of Vb cyclones could be connected to a specific state of the large scale atmospheric circulation. Conversely, Vb cyclones are one of the strongest European cyclone types (Hofstätter et al., 2016, H16 hereafter), so one would also expect a considerable effect of Vb events on the large scale circulation. If a favorable atmospheric flow state exists, this could also point towards a plausible, yet unexplored, mechanism explaining clusters of Vb cyclones. A link between cyclogenesis in the WM and the upper level dynamics interacting with major orography in a low-level baroclinic environment may contribute to these processes (e.g. Maheras et al., 2002; Trigo et al., 2002).

The aim of this paper is to understand the occurrence of Vb cyclones over time, and the atmospheric processes associated with them. Specifically, the paper addresses the following questions:

- Have Vb cyclones become more frequent in recent decades and does their rate of occurrence reveal characteristic variations over time;
- do Vb cyclones tend to occur in clusters or do they arrive fully randomly;
- do clusters, or hiatus periods, correspond with specific phases of the dominant modes of the large scale atmospheric circulation; and
- does such a relationship, if it exists, suggest a plausible mechanism for a possible self-exciting process of Vb occurrence?

By addressing these questions we hope to advance our understanding of one of the most devastating weather/climate phenomena over Europe which will be of benefit for transnational flood management, climate modeling and impact research, and eventually for medium range forecasts of high impact weather events. The paper is organized as follows: The data and methods used are explained in section 2, followed by an analysis of the temporal features of Vb cyclone occurrence and its relationship to the large scale atmospheric circulation in section 3. Section 4 provides the conclusions.

5.2 Data and Methods

The cyclone tracks used in this study are identified by the detection and tracking algorithm of Hofstätter et al. (2016, 2017) which is based on Murray and Simmonds (1991) and Simmonds et al. (1999). It considers both open and closed systems (Pinto et al., 2005) and allows for splitting and merging cyclones. The algorithm consists of four steps: (i) identification of cyclones at time t , (ii) prediction of a subsequent cyclone position at time $t+1$, (iii) association of cyclones between times t and $t+1$ by scoring the difference between the predicted and actual cyclone position(s), and (iv) removal of spurious tracks. The tracking procedure is applied within a domain ranging from 40°W to 50°E at 65°N and 20°W to 4 °E at 3°N for the years 1959-2015. The tracking analysis and all atmospheric fields are based on the JRA-55 reanalysis (Japanese Meteorological Agency, 2013; Kobayashi et al., 2015; Harada et al., 2016) retrieved from the Research Data Archive at the National Center for Atmospheric Research (NCAR) at 1.25° spatial and 6-hour temporal resolutions.

Recent studies (H18; Messmer et al., 2015; Nissen et al., 2013) have used different source and/or target regions for identifying Vb cyclone tracks which hampers a comparison of results. A less restrictive definition than the one of H16 and H18 is therefore used here. All cyclones that propagate northwards and cross a line at 47°N between 12°E and 22°E (“CL – Crossing Line” in Figure 30) are identified as Vb tracks (Vb-All). The arrival time d_0 is defined as the point in time when the cyclone crosses that line, which is estimated by linear interpolation between the track positions bracketing the line.

Tracks are first identified at two atmospheric levels (700 hPa geopotential height, Z700 and sea level pressure, SLP) independently and subsequently considered jointly. In order to avoid redundancies, Z700 tracks are removed from the data set if they are deemed to represent the same cyclone system as one of the SLP tracks. Two conditions are used to identify whether Z700 and SLP tracks refer to the same system: (i) the overlap lasts for at

least 18 hours; (ii) the median and the 20th percentile of the horizontal distances between the track positions at the same time are less than 1000km and 700km, respectively. This criterion is based on the observation that, at their peak, cyclones at SLP are typically 300km ahead of the associated Z500 trough (Lim and Simmonds, 2007); (iii) Only Z700 tracks separated by at least 24 hours when passing the CL line are considered, and the weaker cyclone in terms of relative geostrophic vorticity at d_0 is removed. By this screening, a total of 100 Vb events (30%) are disregarded at Z700. If one increases (decreases) the threshold distances by 30%, the detection rate remains very similar with 104 (97) events, so the rejection rate appears robust to the choice of the threshold distances. The remaining cyclones are classified into four Vb subtypes (Table 17), depending on the region the cyclone develops (Figure 30 left).

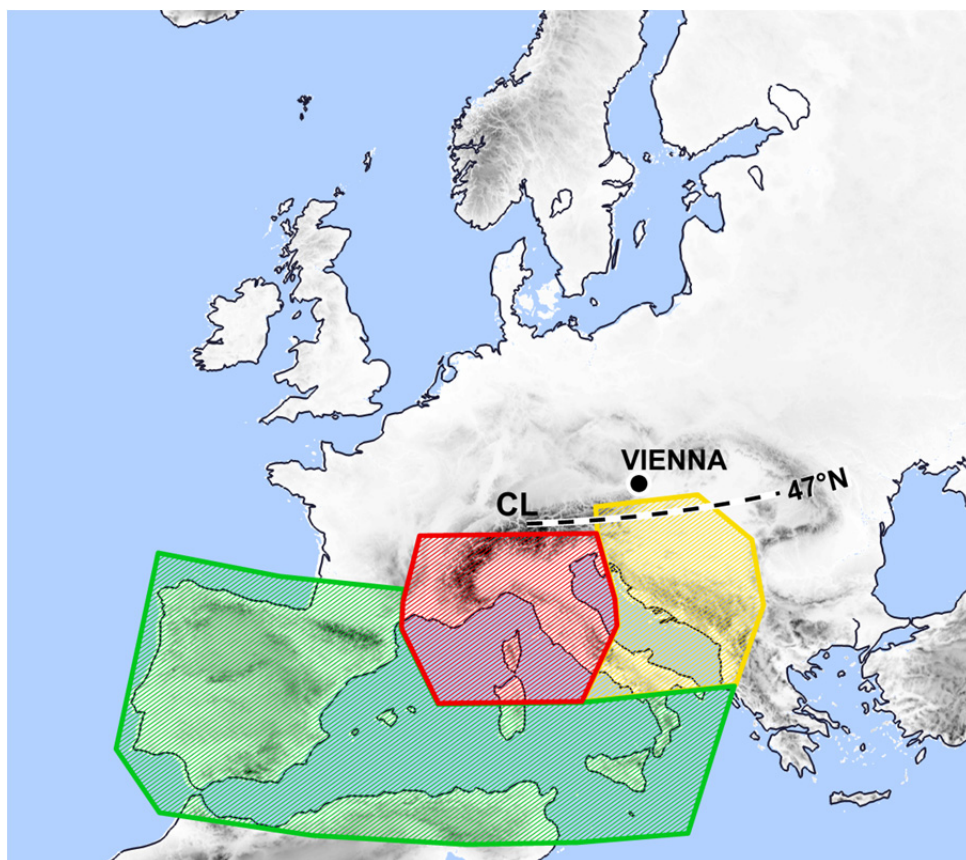


Figure 30: Study region with four source regions for defining Vb subtypes GoG (red), DiN (yellow), IbA (green), and OuT (all others) (Table 17). Cyclone tracks are identified as Vb if they cross the black dashed line (CL) from the South.

Table 17: Four subtypes of Vb cyclones, differentiated by their source region.

sub	Acronym	Colour	Description of source region
1	GoG	red	Gulf of Genoa/Ligurian Sea and Northern Italy
2	DiN	yellow	Adriatic Sea and Dinaric Alps
3	IbA	green	Iberian peninsula and North African Coast
4	OuT	blue	All other Vb cyclones that are not of subtype 1-3

Following the work of Mailier et al. (2006), Vitolo et al. (2009), Pinto et al. (2013 and 2016) and Walz et al. (2018), the arrival of a cyclone at a particular location is considered as a realization of a Poisson point process (Cox and Isham, 1980). The probability of n arrivals in time interval Δt is given by

$$P_{(N=n)} = \frac{\mu^n}{n!} * e^{-\mu} \quad (n = 0,1,2, \dots) \quad (20)$$

where N is the discrete random variable of the arrivals, μ is the expected number of arrivals in Δt with $\mu = \lambda \cdot \Delta t$, and λ the arrival rate. The ratio of the variance $\text{Var}(N)$ and the mean $E(N)$ is used to estimate the dispersion measure φ (Mailier et al., 2006) as

$$\varphi = \frac{\text{Var}(N)}{E(N)} - 1 \quad (21)$$

For a homogeneous Poisson point process (λ does not change over time) $\varphi = 0$, if $\varphi > 0$ (overdispersion) cyclones arrive more clustered, whereas if $\varphi < 0$ (underdispersion) they arrive more regularly than if the interarrival times were independent. The inter arrival times T are exponentially distributed with density

$$f_{(t)} = \lambda * e^{-\lambda t} \quad (\lambda > 0; t > 0) \quad (22)$$

and mean λ^{-1} . In order to test if the observed interarrival times are drawn from an exponential distribution, the Anderson Darling Test is applied (Stephens, 1974).

An alternative clustering measure is the firing regularity $\log(\kappa)$ (Mochizuki et al., 2016). The sum of κ independent, exponentially distributed arrival times is Gamma distributed with probability density function

$$f_{(T)} = \frac{(\lambda)^\kappa}{\Gamma(\kappa)} \cdot (T^{\kappa-1}) \cdot (e^{-\lambda T}) \quad (\kappa > 0; \lambda > 0; T > 0) \quad (23)$$

For a homogeneous Poisson point process, κ is unity. Deviations from unity can be used to identify clustering. The firing regularity $\log(\kappa)$ is calculated by maximum likelihood estimation. All Vb events are partitioned into consecutive and equal segments ($n=39$ events, $n=37$ for the last segment), a gamma distribution is fitted to each sample and the average value of $\log(\kappa)$ for all segments is estimated. Clustering is indicated if $\log(\kappa)$ is negative, regularity if $\log(\kappa)$ is positive.

Clusters are usually defined as distinct periods with a markedly higher arrival rate than the average rate λ_0 (Pinto et al., 2014). In this study a cluster is identified if the cyclone count C over a moving window of 180 days (6 months) exceeds twice the expected number for this period length, so if $C^{\pm 3m} > 2 \cdot \mu_{6m}$. Complementing clusters on a shorter time scale are identified over a window of 90 days (3 months), i.e. $C^{\pm 1.5m} > 2 \cdot \mu_{3m}$, and considered if continuing a precedent 6m-cluster. The selected thresholds correspond approximately to the 5% exceedance probability. Similarly, a hiatus is defined as a period with a much smaller number of Vb events, i.e. if the 6-month cyclone count drops below half the expected number, $C^{\pm 3m} < 0.5 \cdot \mu_{6m}$. This procedure results in a total of 16% of the days identified as clusters, and 35% of the days identified as hiatuses.

The Cox-Lewis U-statistic is used to test for a trend in the occurrence of Vb events in the period 1959-2015, using a parametric regression model (Cox and Lewis, 1966, p. 47) and the null hypothesis of a constant occurrence rate (H_0 : “no trend; $\lambda = \text{constant}$ ”). This test is superior to the Mann-Kendall test for extreme events (Mudelsee, 2014). Additionally, the time-depending arrival rate is estimated by a Gaussian kernel (width=5 years) with percentile-t confidence intervals $1-2\alpha=0.90\%$ calculated by ordinary bootstrapping ($K=8000$ resamples) with replacement (Cowling et al., 1996; Mudelsee et al., 2003 and 2004; Mudelsee, 2014). The seasonal change of Vb arrivals is analyzed by the Gasser-Müller (1984, 1979) kernel regression with a parabolic kernel function (width $h=10$ years, Mudelsee et al., 2012). The standard error bands are constructed by moving blockwise-bootstrapping using an adopted block length considering serial dependence (Mudelsee, 2014, his Equation 3.28) as estimated through persistence time τ (Mudelsee, 2002).

Most of the analysis in this study is based on daily time series but, at some instances, results are aggregated over seasons, either for winter (DJF), spring (MAM), summer (JJA) and autumn (SON) or for the winter and summer half years (November to April and May to October). If not stated otherwise, summer and winter refers to the half years.

To investigate the relationship between Vb cyclone occurrence and the large scale atmospheric circulation, time series (indices) of northern hemispheric teleconnection patterns are used in this study. These are the Northern Atlantic Oscillation (NAO) and the Arctic Oscillation (AO), the East Atlantic/Western Russia Pattern (EAWR), the Scandinavian Pattern (SCA), the Polar Eurasia Pattern (POL), the Eastern Atlantic Pattern (EA), the East Pacific/North Pacific Pattern (EPNP) and the Pacific/North American Pattern (PNA) (Barnston and Livezey, 1987; Feldstein and Franzke, 2017). As the most prominent pattern, the NAO (Hurrell et al., 2001) correlates with the European climate, and explains precipitation variability over Central and Western Europe (e.g., Hurrell et al., 2003). All indices are provided by the Climate Prediction Center (CPC) of the National Oceanic and Atmospheric Administration (NOAA). All CPC teleconnection patterns refer to 500hPa GPH anomalies with the exception of AO which refers to 1000hPa. For comparison with the CPC NAO index (denoted as NAO_c), an alternative index (denoted as NAO_n) from NCAR’s Climate Analysis Section based on the leading mode of SLP anomalies is used (Hurrell et al., 2003). For a number of analyses, confidence intervals are constructed by ordinary bootstrapping (with replacement) unless stated otherwise.

5.3 Results and Discussion

5.3.1 A brief climatology

For the period 1959-2015, a total of 557 Vb cyclones are identified, averaging about 10 cyclones per year (Table 18). The number of Vb cyclones at SLP (6.1 yr^{-1}) and at Z700 (3.7 yr^{-1}) is higher than that of Hofstätter et al. (2016) with 4.1 yr^{-1} and 3.1 yr^{-1} , and also higher than that of Messmer et al. (2015) with 2.5 yr^{-1} at Z850 and Nissen et al. (2013) with just 1.2 yr^{-1} at SLP. The latter two studies used a very stringent definition for Vb tracks (see their Figures 2), and they only used a single pressure level for track detection. In the current study the definition is less restrictive, classifying all cyclones propagating northwards at 47°N between 12°E and 22°E as Vb, either at SLP or at Z700.

Table 18: Vb cyclone climatology with the total number of cyclones for the period 1959-2015, the average number per year μ , the percentages for the summer and winter seasons, and the fraction of cyclones identified from sea level pressure relative to the total number of Vb cyclones (JRA-55: SLP and Z700)

Vb-cyclones	ALL	GoG	DiN	IbA	OuT
Total number	557	257	98	145	57
μ (year⁻¹)	9.77	4.51	1.72	2.54	1.00
May-Oct (%)	43.8	48.3	46.9	35.9	38.6
Sept-Apr (%)	56.2	51.7	53.1	64.1	61.4
Fraction of SLP cyclones	0.62	0.57	0.64	0.77	0.44

In terms of subtypes, Vb-GoG is most frequent (4.5 yr^{-1} or 46%), followed by Vb-IbA (2.5 yr^{-1} or 26%), Vb-DiN (1.7 yr^{-1} or 18%), and Vb-OuT (1.0 yr^{-1} or 10%). The Gulf of Genoa is not only the most active cyclogenesis region in the Western Mediterranean (Campins et al., 2010), but also appears to be the most relevant source region of Vb cyclones. IbA and OuT subtypes are more frequent in winter; the other subtypes are balanced between winter and summer. The individual cyclone tracks for each subtype are shown in Figure 31.

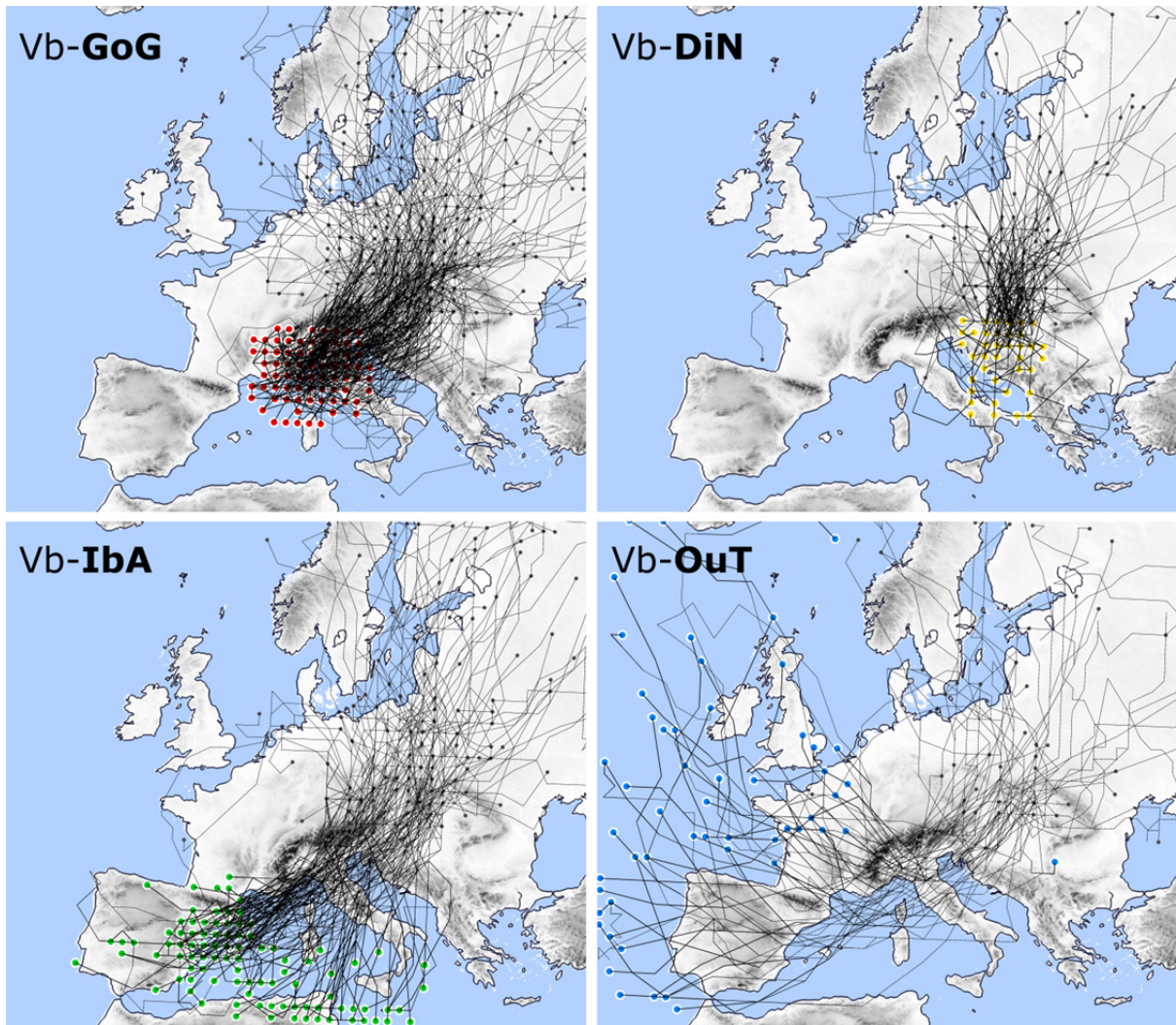


Figure 31: Individual Vb cyclone tracks, classified by their source region (point of first detection) into the four subtypes GoG, DiN, IbA and OuT (Table 17, Figure 30). (JRA-55, 1959-2015: composite of SLP and Z700). Points of first detection are colour coded according to Figure 30, the end points are indicated in black.

5.3.2 Occurrence rate and temporal changes

Vb cyclones are rather rare with only 5% of all Central European cyclones assigned to this track type (H18). Despite its rarity, 22 of the 50 largest precipitation events in the Czech Republic and eastern Austria (1959-2015) have been attributed to Vb cyclones (H18). This implies that the probability of heavy precipitation associated with Vb cyclones at a given location is high. The arrival of Vb cyclones is therefore regarded as an extreme event in the following.

As shown in Table 19a and 19b, the probability of occurrence of Vb (ALL) cyclones has decreased ($U < 0$) between 1959 and 2015 ($p = 0.05$) which can be mainly attributed to IbA winter cyclones. If one disregards IbA-Winter cyclones (second column in Table 19) the probability still decreases, however without significance ($p = 0.19$).

Table 19: (a-b): Cox-Lewis test for monotonic trends in the occurrence of Vb cyclones with $H_0 = \text{“constant probability”}$. (c): Lag-1 day correlation for the square root-transformed and linearly detrended interarrival times. (d-f): Mann Kendall trend test with Sen’s slopes of the interarrival time T. Relative trend (f) is calculated from the difference of the trend line between beginning and end of the period, divided by \bar{T} .

IbA_wi refers to winter cyclones from the Iberian peninsula and the North African Coast, for the other abbreviations see Table 17. Bold print indicates $p < 0.05$.

	Vb-cyclones	ALL	ALL except IbA_wi	GoG	DiN	IbA	OuT
(a)	U-test statistics	-1.67	-0.87	0.10	-1.67	-2.02	-0.01
(b)	p-value (one-sided)	0.05	0.19	0.46	0.05	0.02	0.50
(c)	R_1 : lag-1 correlation of T	0.05	/	0.02	0.13	-0.09	-0.18
(d)	Mann Kendall τ_b	0.06	/	-0.01	0.16	0.11	-0.02
(e)	p-value (two-tailed)	0.03	/	0.82	0.02	0.05	0.81
(f)	Relative trend (%) (Sen’s slope)	+2.6	/	-0.4	+8.2	+5.2	-1.6

For comparison, a non-parametric linear trend for the interarrival times (T) is estimated by the Sen’s slope method (Burkey, 2006) and tested for significance with the Mann Kendall test (Table 19, d-f). First the square root-transformed and linearly detrended interarrival times are checked for serial dependence which gives lag-1 correlation coefficients between $R_1 = -0.18$ (OuT) and $+0.13$ (DiN), and $R_1 = +0.05$ for ALL (Table 19c), indicating weak autocorrelation. The Mann-Kendall trend-test (Table 19d and 3f) shows increases of the interarrival times for DiN and IbA cyclones, but almost no change for the other cyclones. Overall this means that the probability of Vb cyclones to occur has decreased over the last six decades ($p = 0.05$), which is mainly caused by a significant decrease of Vb cyclones developing in winter over the Iberian Peninsula or North Africa.

Figure 32 shows the occurrence rate of Vb cyclones for the period 1959–2015 estimated by a Gaussian kernel using a bandwidth of $h = 5$ yrs. (Mudelsee et al., 2004; Mudelsee, 2014). The black horizontal line indicates the average rate $\bar{\mu}$ with the numbers given in each panel. Clearly, Vb occurrence is time dependent with distinct decadal variations.

For all cyclones (Vb-All, Figure 32a) the rate is highest in the 1960s but does not change much between 1975 and 2015, despite near surface air temperatures having increased by 0.9° over the Northern Hemisphere (Osborn & Jones, 2014; Jones et al., 2012; Morice et al., 2012). The stationary behaviour in the last decades is in agreement with Lionello et al. (2016), who found the frequency of Mediterranean cyclones including Vb not to have significantly changed between 1979 and 2008. When considering the entire period 1959–2015 the rate does decrease by -4% per decade which is identical with the changes of Western Mediterranean cyclones for 1958–1999 identified by Maheras et al. (2001).

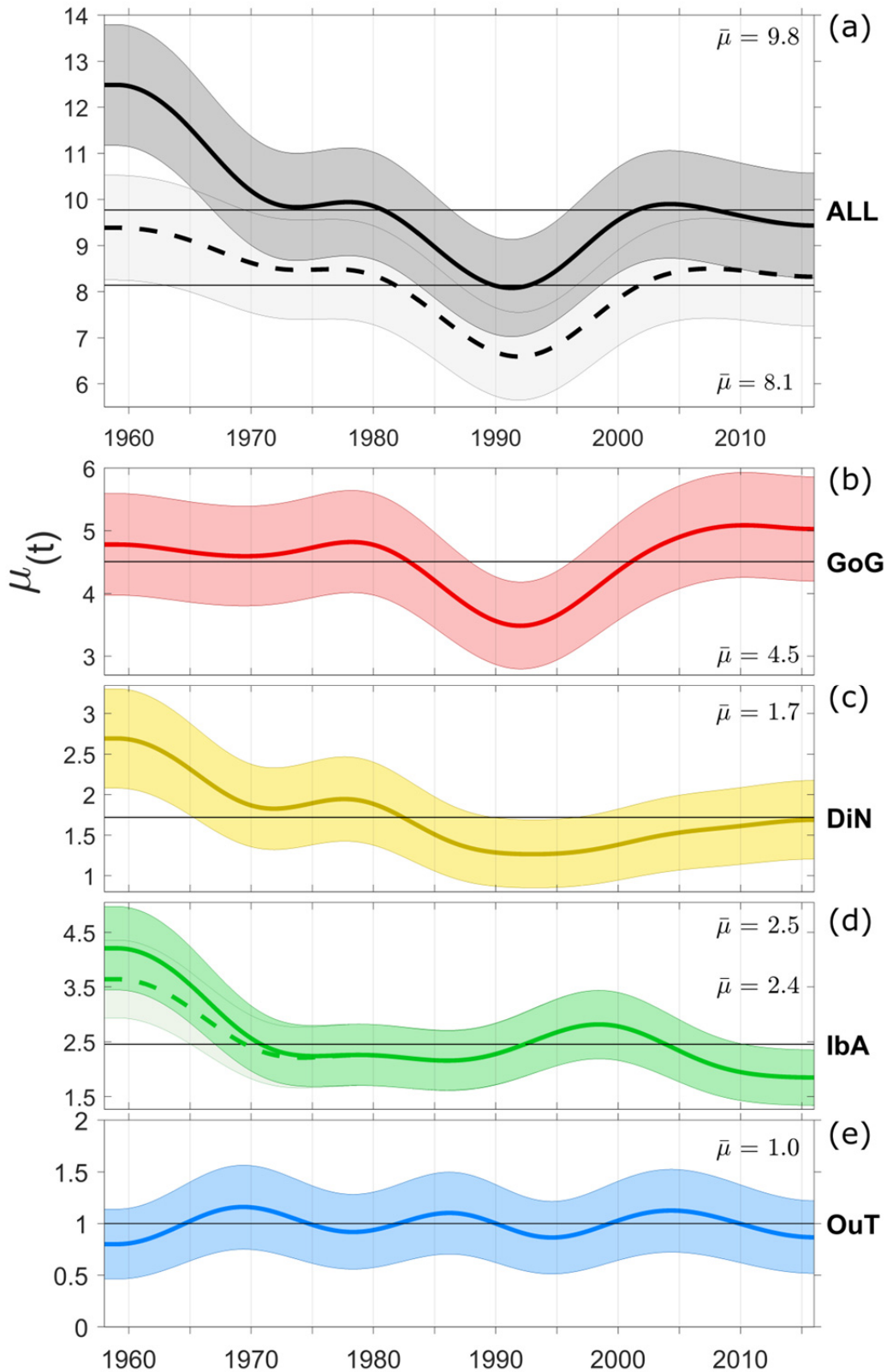


Figure 32: Vb cyclone frequency. All Vb cyclones (top), and subtypes (lower panels). Occurrence rate (yr^{-1}) estimated by a Gaussian kernel of bandwidth $h=5\text{yrs}$ with percentile-t confidence intervals (CI) $1-2\alpha=0.90\%$ indicated as shaded areas. The top panel gives the occurrence rate for all Vb-cyclones (solid line, dark grey CI) and for all cyclones excluding IbA-winter (broken line, light grey CI). The dashed green line for IbA indicates the occurrence rate if 5 out of 9 cyclones in winter 1962/63 are disregarded. The stationary occurrence rate $\bar{\mu}$ (yr^{-1}) is indicated on the right.

The frequency of Vb-ALL is at a very low level of 8.2yr^{-1} during the early 1990s. This hiatus phase is denoted as H7 and investigated in more detail later in this paper. In the early 1960s the occurrence rate is larger than 12yr^{-1} , which can be attributed to the high number of IbA winter cyclones, as illustrated by the dashed black line in Figure 32a for which IbA-winter cyclones have been excluded. During this phase, IbA (Figure 32d) exhibits a substantially higher rate of $>3.5\text{yr}^{-1}$ than after 1965. However, when removing every other IbA cyclone (5 out of 9) in winter 1962/1963 as a sensitivity experiment, the rate drops remarkably (Figure 32d, dashed line). During this specific winter, a total of 9 Vb-IbA cyclones have occurred compared to the long term average of 1.6 per winter. The winter 1962/1963 was a severely cold one in Northern and Central Europe and was associated with a sustained negative NAO regime (Greatbatch et al., 2015). DiN exhibits a similarly high rate before 1970, followed by a rather stable occurrence rate afterwards.

Vb winter cyclones were significantly more frequent before 1967 than later and are now at their lowest rate since 1959 (Figure 33). The rate in winter has decreased significantly by about 40% from $8.03\text{ yr}^{-1} (\pm 1.40)$ in 1959 to $4.68\text{ yr}^{-1} (\pm 1.44)$ in 2015, in line with Figure 32d. A similar decrease of WM cyclones in winter/spring was detected by Bartholy et al. (2009). The summer occurrence rate in this study is generally close to its long term average and is at $4.3\text{ yr}^{-1} (\pm 1.0)$ in 2015. The significantly lower rate during the early 1990s (H7) not only emerges from Vb-GoG (Figure 32a and 32b) but it is also more prominent in the summer (Figure 33).

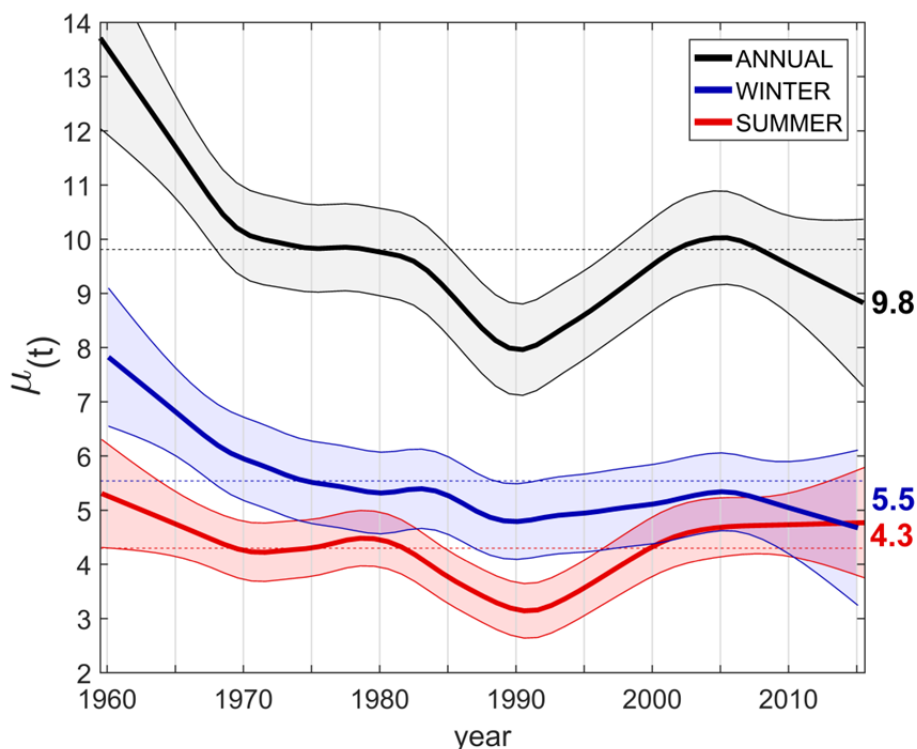


Figure 33: Seasonal and annual occurrence rate (yr^{-1}) of Vb cyclones. Gasser-Müller kernel regression estimation with a parabolic kernel function and 1- σ error bands from K moving block bootstrap experiments (K=8000) using a pre-defined persistence time $\tau=0.3$ (winter), $\tau=0.1$ (summer) and $\tau=0.15$ (annual).

5.3.3 Dispersion of Vb cyclones

So far we have shown that Vb cyclones occur at a time-varying rate with largely independent interarrival times. For a Poisson point process, interarrival times T should be exponentially distributed which is examined in Figure 34. Additionally, the Anderson-Darling test is used to test whether the sample comes from an exponential distribution (H_0 : “interrarrival times are iid exponentials”). The test statistics ($AnDa$) at the 5% significance level are given at the upper left corners of the panels. The associated p-value is the probability of observing $AnDa \geq cv$ under H_0 . For ALL (not shown), GoG and IbA (Figure 34) H_0 is rejected as $AnDa$ is much larger than the critical value of $cv=1.31$, whereas this is not the case for DiN and OuT. Figure 34 and the tests therefore suggest that the interarrival times of GoG and IbA cyclones are not exponentially distributed which may be related to the time-varying rates $\lambda_{(t)}$ (Figures 3 and 4) and the enhanced frequency of short interarrival times (Figure 34, GoG, IbA). This is a clear indication of overdispersion, implying clustering of the arrivals. This finding raises the question of the driving mechanisms of clustering, and the relevance for flooding due to the accumulation of soil moisture in the same catchments (Grillakis et al., 2016; Komma et al., 2008).

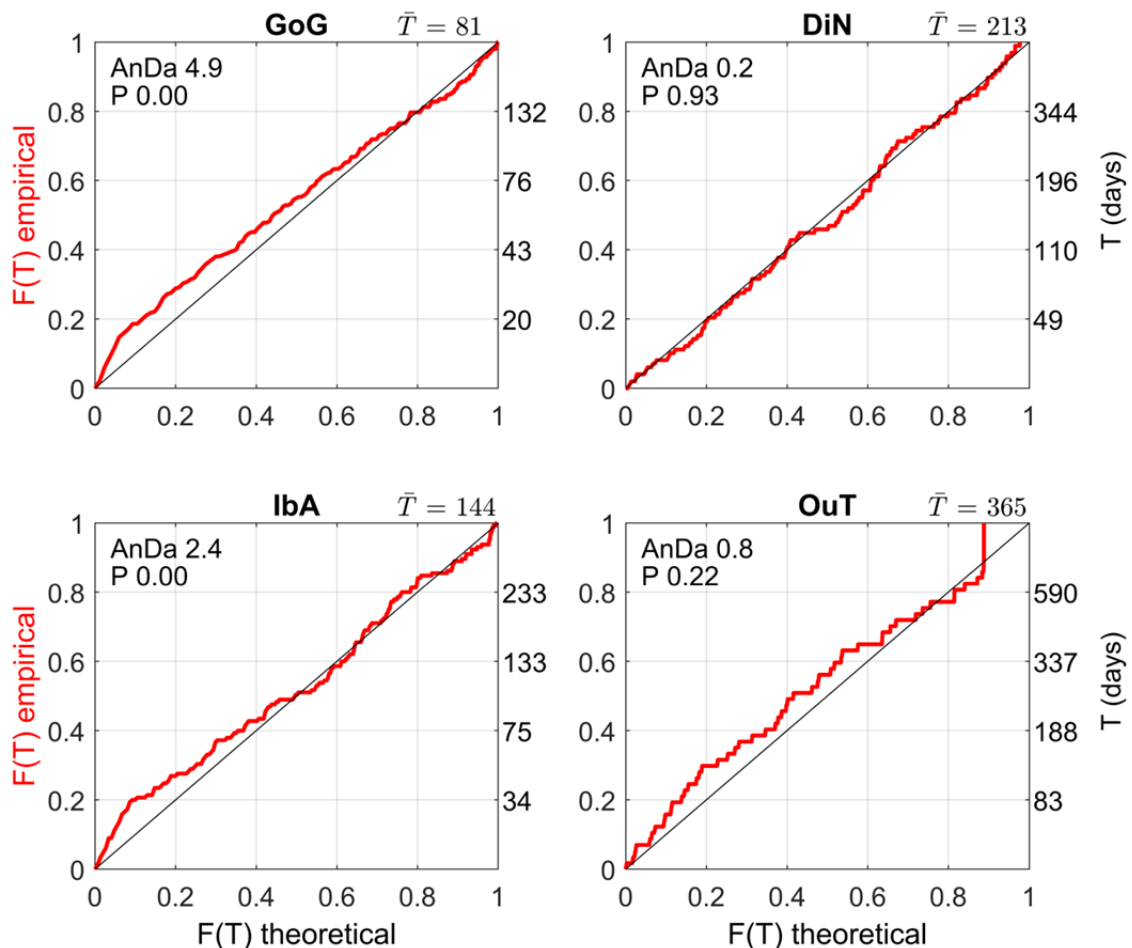


Figure 34: Cumulative distribution functions (cdfs) of observed interarrival times T (red) plotted against exponential cdfs (black). AnDA (Anderson Darling) test statistics and associated p-values ($\alpha=0.05$) are given, as well as the mean interarrival times $\bar{T} = \lambda^{-1}$ (days).

In order to more explicitly test for clustering of the cyclone arrivals, the dispersion measure ϕ (Mailier et al., 2006) is estimated for the annually and seasonally aggregated number of cyclones, and the firing regularity $\log(\kappa)$ (Mochizuki et al., 2016) is used for assessing the non-aggregated time series for comparison.

As shown in Table 20, Vb cyclones indeed occur in clusters, which can be mainly attributed to the GoG and IbA subtypes in accordance with Figure 34. Subtype DiN cyclones occur more regularly than a random Poisson process. On an annual basis, both $\log(\kappa)$ and ϕ indicate clustering for all types. Seasonally (Table 20e), clustering is much more pronounced in winter ($\phi=0.78$) which is mainly due to IbA ($\phi=0.61$). In contrast, clustering of GoG cyclones which develop on the southern Alpine lee side is particularly strong in summer ($\phi=0.71$). This finding points towards differences in the formation processes of clusters in different seasons. The mean interarrival times \bar{T} (Table 20, a, b), as derived from the inverse of the rate parameter of the exponential (Equation 22) and the Gamma (Equation 23) distributions, are about 37.4 days for all Vb cyclones in correspondence to the rate of 9.77 events per year of Table 18.

Table 20: Dispersion statistics of the Vb cyclone arrivals. $\log(\kappa) < 0$ and $\phi > 0$ indicate clustering of cyclone arrivals, $\log(\kappa) > 0$ and $\phi < 0$ indicate regularity.

	Clustering indicator	ALL	GoG	DiN	IbA	OuT
(a)	\bar{T} -Poisson (days)	37.43	81.0	212.5	143.6	365.3
(b)	\bar{T} -Gamma (days)	36.00	79.4	204.2	131.8	348.3
(c)	Firing regularity $\log(\kappa)$	-0.16	-0.25	+0.08	-0.24	0.00
(d)	Dispersion measure ϕ (annual)	+0.69	+0.33	-0.09	+0.56	+0.11
	(summer)	+0.25	+0.71	-0.10	-0.09	+0.00
(e)	(winter)	+0.78	+0.05	-0.13	+0.61	+0.21

The higher arrival rates of Vb cyclones during clustering periods could be caused (i) by a sustained large scale atmospheric state which forces a repetitive development of Vb cyclones in the Western Mediterranean, and/or (ii) by a self-exciting process in which the Vb event itself reinforces the large scale atmospheric circulation into a state that favors the development of a successive Vb cyclone (positive feedback).

Figure 35 identifies cluster and hiatus periods for Vb-ALL by plotting the sample cumulative arrivals minus their average over the period ($\bar{\mu}=9.77 \text{ yr}^{-1}$). The breakpoints separating the major episodes E1 to E5 are detected by a break regression model (Mudelsee, 2009). The highest arrival rate of 13.4 yr^{-1} occurs between 01/1959-12/1966 (episode E1), the lowest arrival rate of 6.9 yr^{-1} between 4/1988-12/1996 (hiatus H7). During other periods, the rate is close to the long term average. In total there are eleven cluster and eleven hiatus periods between 1959 and 2016 (Table 21).

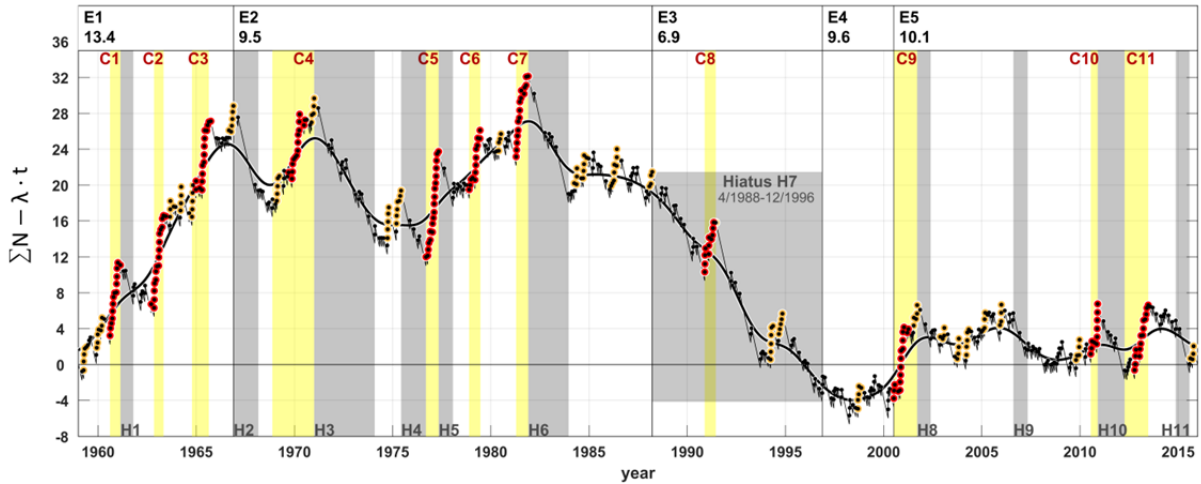


Figure 35: Arrivals of Vb-All cyclones: Observed cumulative number of cyclones (N) relative to the number expected on average over the period ($\lambda_0=9.77 \text{ yr}^{-1}$). Individual Vb events ($n=557$) are shown as black dots. Clustered events are indicated by red dots. Cluster periods (C) and hiatus periods (H) are indicated by yellow and grey shading, respectively. The observation period has been partitioned into five main episodes E1 to E5 with average arrival rates (per year) given at the top.

Figure 35 clearly shows the existence of well separated and distinct clusters (C1-C11) with a relatively high arrival rate of $\bar{\mu}=21.5 \text{ yr}^{-1}$, and a low average interarrival time of $\bar{T}=17.0$ days on average, compared to $\bar{\mu}=7.5 \text{ yr}^{-1}$ and $\bar{T}=48.5$ days outside the clusters. During the hiatus periods the mean interarrival time is particularly long with $\bar{T}=70.4$ days and the rate is only $\bar{\mu}=5.2 \text{ yr}^{-1}$, suggesting that the cyclone clusters exhibit an average rate about four times that of the hiatuses. It is interesting to note that cyclone clusters over the Northern Atlantic Ocean occur at a much higher rate of about 1 day^{-1} and with much shorter cluster duration of just 6 days on average for the main winter (Pinto et al., 2014). Obviously, the formation processes of cyclone clusters over the Northern Atlantic are different from those in the Western Mediterranean. Nevertheless, the ratio of the number of clustering days to all days over the Northern Atlantic of 13% is very similar to the one found here for the WM (16%).

Table 21: Vb clustering (C) and hiatus (H) periods 1959 - 2016, with beginning and end dates, duration, mean interarrival times T, number of arrivals, and the ratio (fR) of arrival rates and the mean rate of 9.77yr^{-1} .

C/H	beginning	end	duration (months)	T (days)	number of arrivals	fR (%)
C1	1960 08 11	1961 02 20	6.33	14.9	14	271
C2	1962 11 08	1963 05 04	5.80	11.8	16	338
C3	1964 10 13	1965 08 24	10.33	16.6	20	237
C4	1968 11 17	1971 01 03	25.48	23.5	34	164
C5	1976 09 13	1977 05 07	7.74	13.1	19	301
C6	1978 11 26	1979 06 23	6.85	17.4	13	233
C7	1981 04 16	1981 11 28	7.41	15.1	16	265
C8	1990 11 22	1991 06 17	6.79	18.8	12	217
C9	2000 07 09	2001 09 17	14.26	19.8	23	198
C10	2010 07 22	2010 11 29	4.26	14.4	10	288
C11	2012 04 11	2013 06 25	14.43	23.2	20	170
H1	1961 02 20	1961 10 18	7.87	60.0	4	62
H2	1966 11 24	1968 03 02	15.21	154.7	3	24
H3	1971 01 03	1974 02 03	36.95	75.1	15	50
H4	1975 06 09	1976 09 13	15.15	92.4	5	40
H5	1977 05 07	1978 01 28	8.72	133.0	2	28
H6	1981 11 28	1983 12 19	24.62	93.9	8	40
H7	1988 03 21	1996 11 17	103.71	52.7	60	71
H8	2001 09 17	2002 05 26	8.23	83.7	3	45
H9	2006 08 13	2007 05 05	8.69	88.3	3	42
H10	2010 11 29	2012 04 11	16.36	99.8	5	37
H11	2014 11 19	2015 08 01	8.36	127.5	2	29

5.3.4 Large scale atmospheric circulation

In order to better understand the drivers of Vb cyclone arrival rates, the relationship between the large scale atmospheric circulation (LAC) and arrival rates is investigated by selected teleconnection indices (TCI). The main questions are: (i) which circulation modes favour the development of clusters or hiatus periods and can therefore explain long term changes in arrival rates, (ii) does the LAC affect Vb cyclones at the event scale, and (iii) does the evolution of the LAC during Vb events support the hypothesis of a positive feedback during different seasons? The last question is particularly intriguing as cyclogenesis strongly depends on a sufficient upper level forcing which is usually much stronger in the winter than in summer while Vb cyclones are just as frequent in the winter as in summer (Table 17) and Vb summer cyclones, on average, are equally strong as the winter ones (H16). In the Western Mediterranean, upper level troughs are usually affected by major mountain orography inducing lee-cyclogenesis in a low-level baroclinic environment (Egger et al., 1988; Pichler et al., 1990; Aebischer and Schaer, 1998; Trigo et al., 2002), suggesting that either low level baroclinic forcing compensates a weakened upper level dynamics during summer or Vb occurrence rates are modulated by different states of the LAC in different seasons.

Greatbatch et al. (2015) found an exceptionally high number of nine Vb-IbA events during the winter 1962/1963 when a sustained negative phase of the winter NAO was observed, and Nissen et al. (2010) found Mediterranean cyclones to occur about 20% more frequently during negative NAO phases. Negative NAO conditions are typically related to a weakened and southwards shifted, eddy-driven jet stream (e.g. Woollings et al., 2008 and 2010), hence steering cyclogenesis and cyclone tracks towards more southern latitudes than usual. The

mean monthly state of selected teleconnection indices ($\overline{T\overline{CI}}_k$) is shown in Figure 36, stratified by the monthly count k of Vb cyclones into five groups ($k=1,2,3,4$, and 5 or more). The mean of the respective TCI for all months without Vb cyclones ($\overline{T\overline{CI}}_0$ at the top of Figure 36) is used as a reference and subtracted from $\overline{T\overline{CI}}_k$. Very clearly the AO, NAO and EAWR patterns are in a negative state during months when Vb cyclones occurred ($\overline{T\overline{CI}}_k < 0$) but are in a more positive state otherwise ($\overline{T\overline{CI}}_0 > 0$). The straight black lines, estimated by linear least absolute deviations regression, indicates that the TCI are more strongly negative with an increasing number of Vb events per month. A similar, however reverse relationship can be seen for the SCA pattern. For the other modes such a clear tendency cannot be seen. Although this relationship does neither confirm nor falsify the feedback hypothesis, it does demonstrate a systematic and close association of Vb events in Central/Southern Europe with the Northern hemispheric LAC.

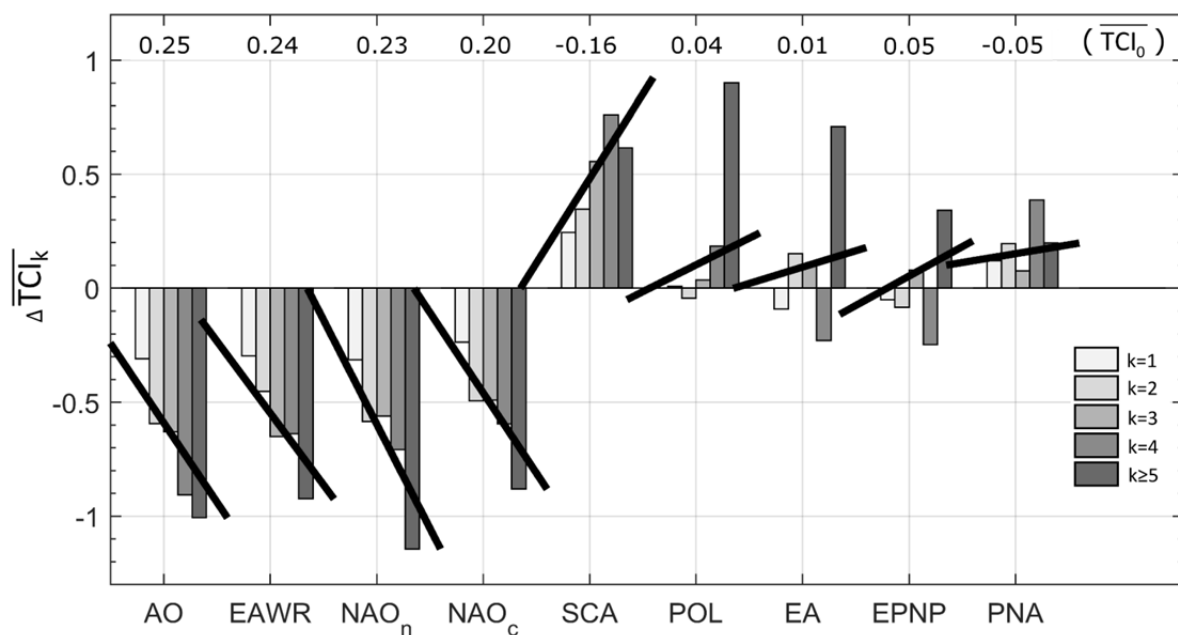


Figure 36: Mean monthly teleconnection index $\Delta\overline{T\overline{CI}}_k$ as an average over those months with $k=1,2,\dots,5$ or more Vb events per month $\overline{T\overline{CI}}_k$ minus the reference state $\overline{T\overline{CI}}_0$ for months without Vb events ($k=0$) for the AO, EAWR, NAO_n, NAO_c, SCA, POL, EA, EPNP and PNA patterns. $\Delta\overline{T\overline{CI}}_k = \overline{T\overline{CI}}_k - \overline{T\overline{CI}}_0$.

Numbers on top indicate reference state. $\overline{T\overline{CI}}_0$ Classes $k= 1, 2, \dots, 5$ consist of 230, 78, 33, 10, 4 months, class $k=0$ of 329 months. The AO, NAO and EAWR patterns are in a negative state during months when Vb cyclones occurred ($\overline{T\overline{CI}}_k < 0$) but are in a positive state otherwise ($\overline{T\overline{CI}}_0 > 0$).

Figure 37 shows the standardized and de-seasonalized composite time series of the averaged NAO/AO index (denoted at NAAO in the following) together with the clustering (yellow) and hiatus (grey) phases. The combined NAAO index is averaged (running mean) over 3 years (dark red and blue) and 6 months (pale red and blue). The most prominent hiatus phase H7 between April 1988 and Dec 1996, which has been attributed to the summers (Figure 33) occurs during a sustained and strongly positive phase of the NAAO (also see, e.g., Delworth et al., 2016). The high annual arrival rate of Vb cyclones found before 1970 (Figures 3 and 4), which has been attributed to the winters (Table 20 and Figure 32), goes hand in hand with a predominantly negative phase of the NAAO. This suggests that the rate of Vb cyclones may be elevated under negative NAAO conditions in the winter and suppressed under positive NAAO conditions in the summer.

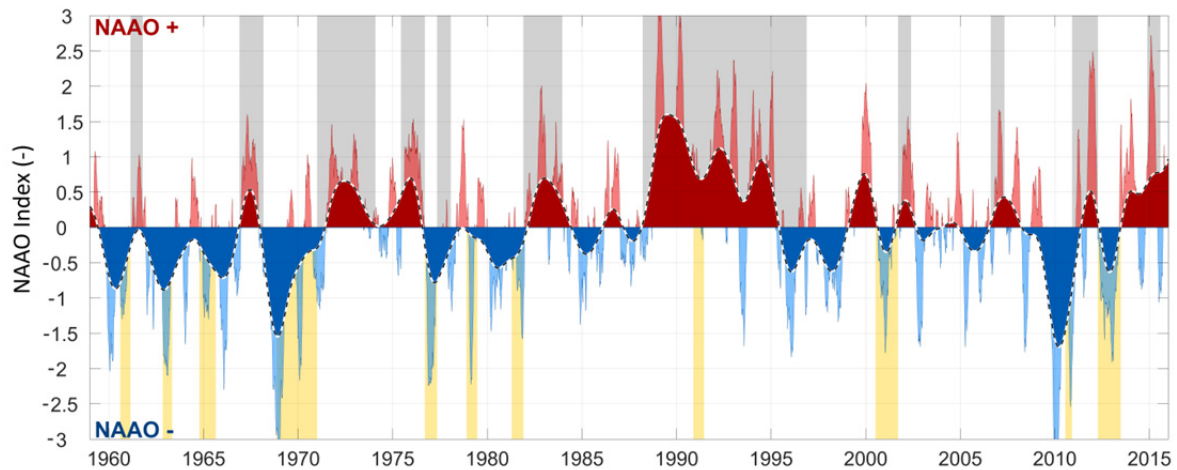


Figure 37: Time series of the combined standardized daily NAO/AO index for 1959-2015. Dark blue/red: 3-year Gaussian-Low Pass filtered; Light blue/red: 6-month Gaussian-Low Pass filtered index. Yellow shaded areas indicate cyclone clusters, grey shaded areas hiatuses as in Figure 35.

Almost all the hiatus phases (grey) and most cyclone clusters (yellow) in Figure 37 coincide with positive and negative phases of the NAO, respectively. For a more quantitative assessment, the mean states of the NAO index during clusters and hiatuses are evaluated in Figure 38, top. At the bottom of Figure 38 the probability of observing an even stronger negative (positive) phase of the NAO is shown, given the duration d (unit days) of the particular cluster (hiatus) under consideration. The probabilities are calculated by drawing 10^6 ordinary bootstrap samples with replacement, whereas the period under consideration is always omitted. Significance is indicated by a probability of 0.10, shown as dashed lines in Figure 38, bottom.

For all clusters, except C8, the average NAO is clearly negative with a rather low probability (less than 0.20) of observing an even more negative phase of the NAO for the given period length. For six clusters the state of the NAO is significantly ($p < 0.10$) more negative as compared to random occurrence. A similar conclusion can be drawn for nine of the ten hiatus periods with six of them being significantly more positive than random occurrence. Only hiatus H5 occurs during a slightly negative phase of the NAO. This finding confirms that, on the medium term (6 months), hiatuses almost always occur during positive phases of the NAO and cyclone clusters during negative phases. This is in line with the observation of Nissen et al. (2010) that the number of cyclones in the WM is about 20% lower during NAO^- phases than during NAO^+ phases. Similarly, strong WM cyclones were found to be correlated ($R=0.50$) with a NAO^- type pattern in winter (DJF), whereas this relationship was lost in summer (JJA) (Raible, 2007).

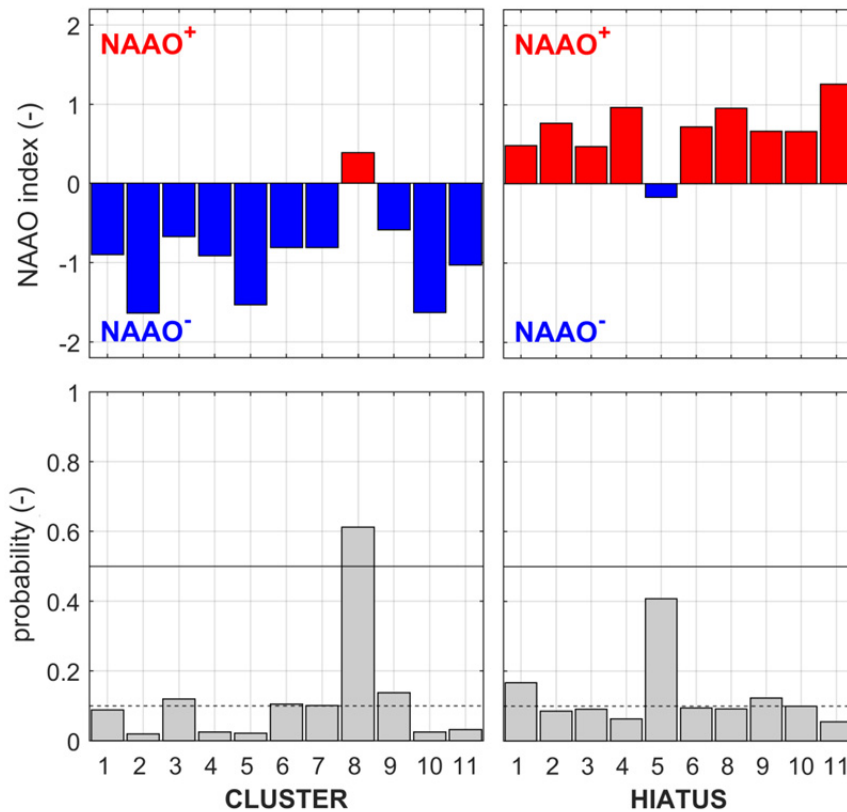


Figure 38: Mean state of the NAOO for the cluster and hiatus periods as an average over their duration (top) as well as the probability (bottom) of observing an even stronger negative (positive) phase of the NAOO, given the duration d of a particular cluster (hiatus). Dashed lines indicate significance ($p=0.10$). Hiatus H7 has been omitted because of its exceptionally long duration.

This general relationship between Vb occurrence and the NAOO, however, does not strictly apply to each cluster or hiatus. From inspecting individual Vb events of C8 (not shown), we find that some Vb cyclones occur during a positive NAOO phase. In other instances, the AO or NAO drops as expected, but remains positive most of the remaining time, so is not captured well by the 6-month running average of the NAOO. To better understand the large scale processes during Vb events, the mean temporal evolution of the NAO and AO indices is shown in Figure 39 as an average over all 557 Vb events. The timeline starts from 60 days before and ends at 70 days after d_0 , the point in time when the cyclone is closest to Vienna ($48^\circ\text{N}/16^\circ\text{E}$, see Figure 30). This location was chosen to also include cyclones that emerge just before crossing CL at 47°N .

From 40 to 10 days before the cyclone crosses the CL line, the AO and the NAO are generally in a negative phase, although not significantly low. A few days before Vienna is reached, AO and NAO drop dramatically, even when averaging over the 557 events. The drops last for about 23 and 19 days, respectively. The drop is more pronounced for the AO and starts as early as 10 days before the minimum. Obviously, a strong imprint on the large scale atmospheric circulation appears during Vb events, realized as a positive pressure anomaly at different atmospheric levels (Z500 and Z1000) at higher latitudes, even far upstream of the WM and Central Europe over the North Atlantic Ocean.

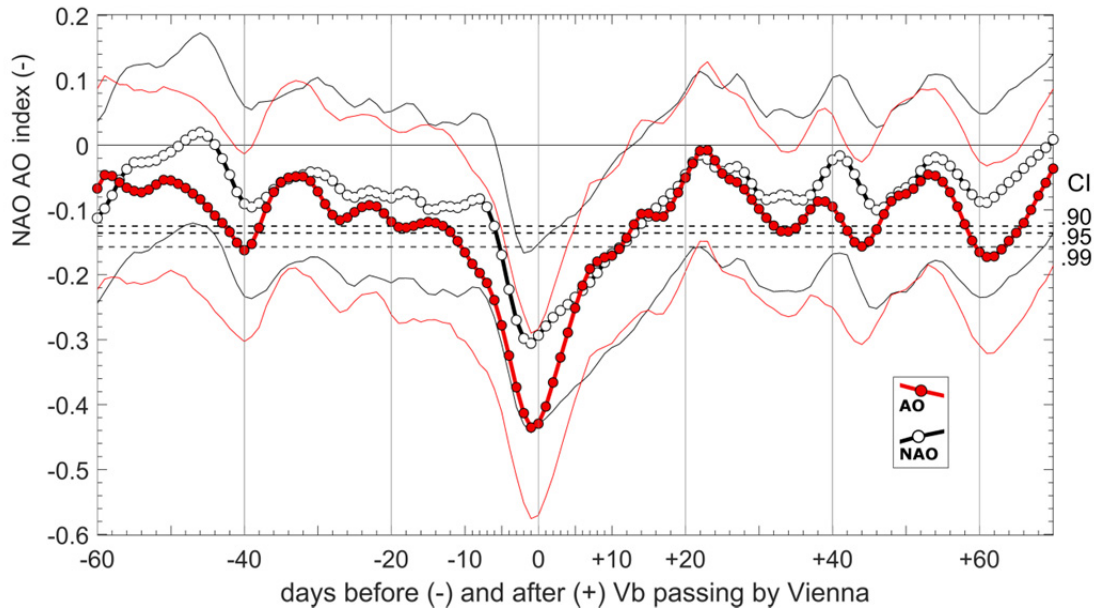


Figure 39: Evolution of the NAO and AO indices over four months as an average over 557 Vb events. The central point is defined as the day d_0 when the cyclones reach the crossing line (CL in Figure 30). The dashed lines show the 0.90, 0.95 and 0.99 percentile confidence Intervals (CI), calculated from 10^6 Monte Carlo experiments. For each experiment 557 time-intervals (length=130d) from the period 1959-2015 are chosen randomly, the mean evolution of the NAO/AO is calculated and the lowest value out of the 130-day period is determined. The thin solid lines indicate 0.90 and 0.10 percentiles from 10^6 ordinary bootstrap experiments using 80 out of the 557 Vb events.

After the minimum, the AO and NAO rise steadily, but remain at a low level for two weeks and reach a similar level to the one observed before the drop after about 17 days. This time span corresponds very well with the average interarrival time of $T=17.0$ days of the 11 cyclone cluster periods found above. This similarity points to a potential feedback mechanism, as the negative pre-state of the NAO is further lowered by the occurrence of a Vb cyclone, increasing the likelihood for another Vb event within a short time. Although the mean drop of the NAO shown in Figure 39 is significant, it is just half the standard deviation and therefore not very strong. When analyzing individual Vb events, it turns out that the NAO has occasional strong positive peaks. These may explain why the mean NAO is not negative for C8 as expected (Figure 38). To shed more light on this issue, the temporal evolution of the AO and NAO is further stratified into four groups, as a function of the sign of the NAO and AO at the time d_0 the Vb event crossed the CL line (Table 22). The largest number of cyclones (266 events or 47.8%) occurs when both NAO and AO are negative (Vb-mode 1). If only mode 1 events are considered, the drop of both the NAO and AO is considerably stronger than for all events and reaches one times the standard deviation (Figure 40a, top left).

Table 22: Partitioning of the 557 Vb events into four modes by the sign of the NAO and AO indices at the time the cyclones crossed the CL line.

Vb mode	NAO index	AO index	Number of events (n)	Relative number (%)
1	-	-	266	47.8
2	+	+	123	22.1
3	-	+	76	13.6
4	+	-	92	16.5

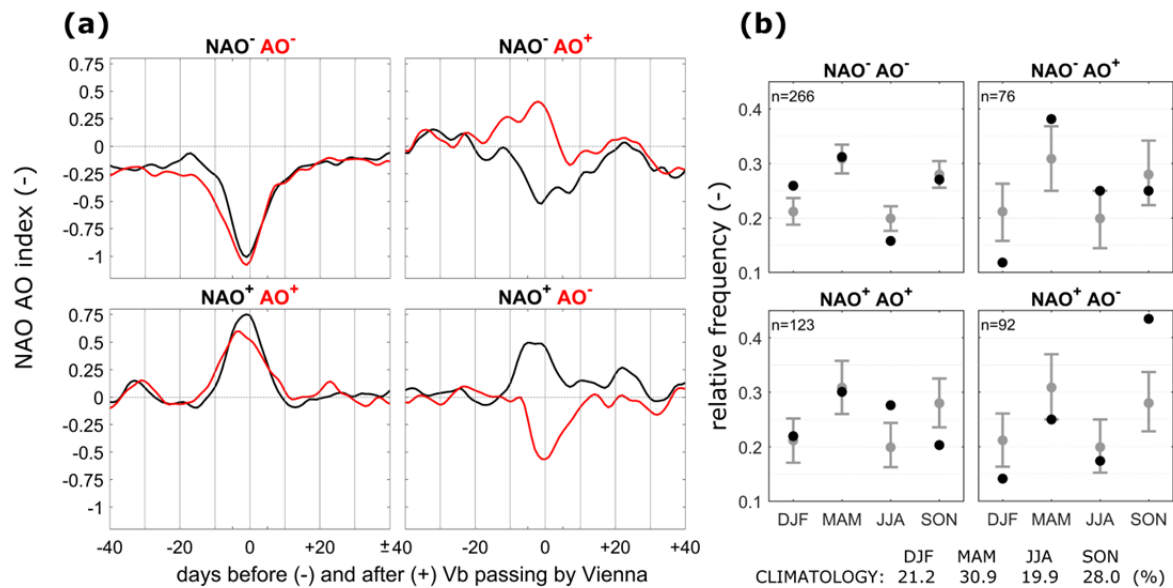


Figure 40: (a) Mean evolution of the NAO and AO indices for three months similar to Figure 39 but for the four NAO/AO modes of Table 22. (b) Seasonal relative frequency of Vb cyclones (black dots) compared to their climatology without stratification (grey dots and numbers at bottom). Grey whiskers indicate 10th and 90th percentile confidence intervals calculated from 10⁶ ordinary bootstrapping resamples of size=n without replacement by randomly shuffling the underlying dates. The number of events for each group is given in the top left corners.

Above it has been speculated that the high number of Vb winter cyclones before 1970 may be connected to a dominant negative phase of the NAAO observed during the 1960ies which is in line with, e.g., Delworth et al. (2016). This notion is further supported by the seasonal number of Vb cyclones for each of the four NAAO Vb-modes as compared to its climatology without stratification (Figure 40b). Vb cyclones inducing NAO⁻AO⁻ conditions (mode 1), show a significantly higher number of cyclones during winter (DJF) and a lower number during summer (JJA) so mode 1 appears to be a feature of the winter half year. As a consequence, the hypothesised positive feedback between NAAO⁻ and a high frequency of Vb events should also be interpreted as a main feature of the winter. This is in agreement with an equatorwards shifted eddy-driven jetstream and storm tracks over the Northern Atlantic observed under NAO⁻ in winter (Athanasiadis et al. ,2010; Wettstein and Wallace, 2010; Woollings et al., 2010).

For the 123 cyclones of the Vb-mode 2 (NAO⁺ AO⁺) conditions, both NAO and AO exhibit a clear positive peak at d_0 (Figure 40a, bottom left). These cyclones are relatively more frequent during the summer (JJA) as compared to climatology. In absolute numbers, Vb-mode 2 is more clearly a phenomenon of spring/summer and less so of autumn/winter. This mode could therefore drive the prime April/May frequency peak of Vb events, apart from the secondary peak found in late autumn (Hofstätter et al., 2012; H18). The temporal evolution of mode 2 is opposite that of mode 1 and therefore seems to counteract or dampen the proposed Vb feedback. This reasoning is supported by the neutral NAO conditions found 30 days before and after d_0 . During summer an extensive and strong high pressure system is usually found over the Azores Islands, which may be further intensified by the downstream development of a major Vb cyclone in the Western Mediterranean. This would be a plausible mechanism explaining a strengthened NAO at the northern flank of the high pressure system for mode 2.

The other two modes (Figure 40a, right) account for 13.6% (NAO⁻ AO⁺) and 16.5% (NAO⁺ AO⁻) of all Vb events (Table 22). These types show a peak of the NAO and a drop of the AO at the same time, which are weaker than modes 1 and 2. Most importantly, 40 out of the 92 Vb events associated with mode 4 (NAO⁺ AO⁻) occur in autumn, the season when upper level dynamics are regaining strength in the Northern Hemisphere and when the Mediterranean sea surface temperatures are still high.

If one assumes that a LAC/Vb-feedback does not exist for any of the modes, one would expect that the 197 Vb events found during a clustering period (Table 21) divide into the four modes following the share of all 557 Vb cyclones (Table 22). However, this is not the case as the relative number is 55.3% compared to 47.8 % for mode 1 (i.e. by a factor 1.16 larger) and 16.2% compared to 22.1% for mode 2 (by a factor 0.74 smaller), in line with a presumed mode 1 feedback between NAO⁻ and above average Vb frequency. The shares of modes 3 and 4 slightly decrease by a factor of 0.93 and 0.95, respectively.

As a further interesting result, the average date for mode 1 and mode 4 Vb events differs significantly from the overall mean (1986-04-16) as shown in Table 23, with mode 1 events occurring earlier in time (the mean is 1984-10-12), in contrast to mode 4 events occurring later in time (the mean is 1988-10-03) than expected by random cyclone occurrence. Significance (0.10 and 0.90 percentiles) has been tested by a Monte Carlo experiment, drawing 5×10^7 random samples of size n (Table 23) for each mode from the given 557 Vb dates (at time d_0). 60% of the winter (DJF)-mode 1 events are found during the first 20 of the 57 years. The winter (DJF)-mode 1 events might be related to the predominantly negative phase of the winter NAO observed during the years 1955-1971 (Iles and Hegerl, 2017), as this mode is associated with the cold season (Figure 40b). Mode 4 events are not only most frequent in Autumn (about 42%) but also 53% of the (SON)-mode 4 events occurred during the last 17 of the 57 years. This may be due to the strong increase of Western Mediterranean sea surface temperatures of about +1°C after 1990 (Ionita et al., 2017; their Figure 40d), apart from possible decadal background variations of the LAC, leading to a higher frequency of Vb-mode 4 cyclones during autumn in recent years.

Table 23: Mean date for mode 1-4 Vb events and confidence intervals from drawing 5×10^7 random samples of size=n (shown in Table 22) with replacement. Mean dates outside the 0.10 or 0.90 percentile values are printed in bold.

Vb mode	mean date	0.10 percentile	0.50 percentile	0.90 percentile
1	1984-10-12	1984-12-13	1986-04-15	1987-08-17
2	1988-05-23	1984-04-27	1986-04-15	1988-04-04
3	1985-07-24	1983-10-15	1986-04-15	1988-10-18
4	1988-10-03	1984-01-05	1986-04-15	1988-07-26

Finally we present the temporal evolution of the 500hPa geopotential height anomaly, averaged over 263, 127, 75 and 92 days for the respective modes 1-4, as a sequence from 10 days before to 10 days after the cyclones crossing the CL line (Figure 41). For this analysis, the time series of GPH500 are first detrended and the annual cycle is removed at each grid point (Barriopedro et al., 2010). In addition, wind velocity is shown at the level of 300hPa in colour shading, indicating the mean strength and position of the jet stream. The partitioning of the Vb events into four groups is based on the sign of the NAO and AO at time d_0 (3rd row in Figure 41).

For mode 1 slightly negative NAO conditions are present 10 days before d_0 (d-10), with a negative pressure anomaly found as precursor of the subsequent Vb event located over Western Europe. This anomaly subsequently develops into a major baroclinic trough, leading to a strengthening and southward shift of the eddy-driven jet stream into the Western Mediterranean at d-3. Next, a superposition of the eddy-driven polar jet stream and the subtropical jet stream can be seen over the Western Mediterranean Sea at d_0 . In fact, this superposition occurs in all of the four modes and already starts (not shown) at d-4 over the Balearic Islands (mode 1), at d-3 over the Gulf of Genoa (mode 2), at d-2 over Sardinia (mode 3) and at d-1 over the Gulf of Lyon (mode 4). However, for mode 1 the coupling appears to be strongest, continues even until d+10 (d+5 for modes 2-4) and regains the same strength as at d-10. This further supports the $[NAO^- \leftrightarrow Vb^+]$ feedback hypothesis, as the superposition imposes a zone of increased baroclinity and wind speed, favouring the development of cyclones through an enhanced ageostrophic circulation (Christenson et al., 2017) for another 10 days or more in the Western Mediterranean for mode 1.

Apart from the superposition of jets, a pronounced high pressure anomaly develops over Scandinavia in modes 2-4, inducing a blocked flow situation over Europe and a split and/or tilt of the polar jet stream. The positive anomaly remains until d+10 in all these modes, so lasts for at least one week after the Vb event. A strong link between European/Scandinavian blocking and a discontinued or branching jet stream over the North Atlantic (NA) has been found by Madonna et al. (2017) and classified as the fourth main North Atlantic eddy jet regime (mixed type M_4 , see Figure 6g therein) beside the mean zonal framework (Woollings et al., 2010) in accordance with the flow situation shown in Figure 41. The current study suggests Vb cyclones to be precursors of the development of Scandinavian high pressure anomalies in modes 2-4. Apart from wave breaking and isentropic advection of air comprising low potential vorticity, adiabatic heating through latent heat release from ascending air has been identified as another important mechanism for blocking occurrence (Pfahl et al., 2015).

The poleward advection of warm and moist air through the warm conveyor belt (Madonna et al, 2014) from Southern/Eastern Europe during Vb events (Grams et al., 2014) could therefore be a crucial ingredient fuelling Scandinavian blocking apart from anti-cyclonic wave breaking (Masato et al., 2012). Another high pressure anomaly can also be seen over Greenland at d_0 (mode 1) and at $d+5$ (mode 3), but how this relates to the Vb cyclone developing downstream appears to be less clear.

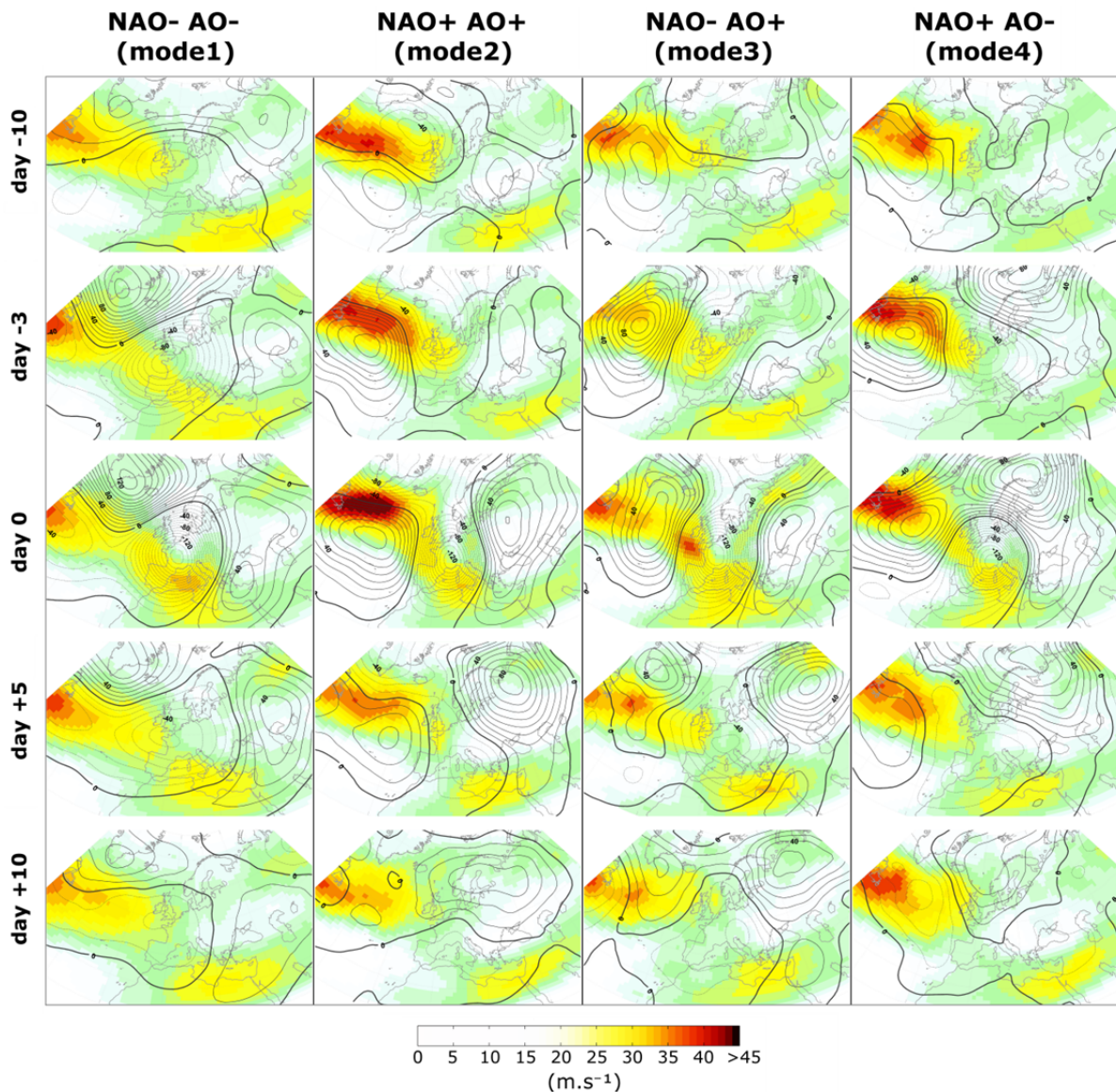


Figure 41: Temporal evolution of the large scale atmospheric circulation during Vb events from 10 days before to 10 days after crossing line CL at 47°N. Anomalies of 500hPa geopotential height are shown as black contours (gpm), upper level (300hPa) wind speeds are shown as colour shading. At day 0, a coupling of the eddy-driven polar jet stream and the subtropical jet stream can be seen over the Western Mediterranean. In all modes, a strong impact of the Vb events on the large scale atmospheric circulation can be seen, with large positive pressure anomalies developing over Greenland (mode 1) or around Scandinavia (modes 2-4).

5.4 Conclusions and Outlook

This paper explores the temporal characteristics of Vb cyclone occurrence based on cyclone tracks identified at the atmospheric levels of Z700 and SLP, using JRA-55 reanalysis data for the period 1959-2015. Vb cyclones typically emerge in the Western Mediterranean (WM) and propagate to the Northeast into Central Europe. The cyclones are classified into four Vb-subtypes, denoted as GoG, DiN, IbA and OuT (Table 17), based on the region they are first detected. The temporal characteristics are assessed by analysing changes of the cyclone occurrence rate as well as by identifying individual cluster and hiatus periods as compared to a random Poisson point process. The relationship between the large scale atmospheric circulation (LAC) and Vb occurrence rate is investigated by examining selected teleconnection indices (TCI), in particular the Northern Atlantic Oscillation (NAO) index at Z500 and the Arctic Oscillation (AO) index at Z1000. Finally the temporal evolution of the geopotential height and upper level wind speeds over Europe and the Atlantic is analysed to identify linkages between Vb cyclones and the LAC at the event scale. From the analyses, five major findings have been obtained.

(i) The risk of Vb occurrence has decreased significantly between 1959 and 2015 from 12.4 to 9.4 events per year, which is mainly due to the very high number of Vb cyclones developing over the Iberian Peninsula or North Africa during the winters before 1970. Between 1970 and 2015 the risk has remained rather constant for all Vb subtypes, apart from decadal variations, which is in line with trends of other Western Mediterranean cyclones (Lionello, 2016; Nissen et al., 2014; Maheras et al., 2011). The current rate of subtype Vb-GoG cyclones developing on the southern Alpine lee side is close to its long term average. This is a counterintuitive result as mid latitude storm tracks are expected to shift polewards due to climate change (Seneviratne et al., 2012; Woollings and Blackburn, 2012) and near surface air temperatures have already increased by 0.9 °C since 1950 over the Northern Hemisphere (Osborn & Jones, 2014; Jones et al., 2012; Morice et al., 2012). This suggests that, either internal variability is considerably large and masks any externally driven changes in recent decades, or other processes are compensating for climate change effects. Vb cyclogenesis is strongly linked to the upper level atmospheric dynamics interacting with major orography in a low-level baroclinic environment in the WM (e.g. Maheras et al., 2002; Trigo et al., 2002). The increase of WM sea surface temperatures of about +1°C after 1990 (Ionita et al., 2017; their Figure 11d) appears as a plausible explanation for a sustained Vb cyclone occurrence rate.

(ii) Vb cyclones do not occur fully randomly according to a Poisson point process, i.e. they arrive either clustered or more regularly at times. Clustering is very prominent in the case of Vb-GoG cyclones and is particularly strong in summer for this type. On the other hand, clustering also occurs in winter, but primarily for Vb-IbA cyclones that develop over the Iberian Peninsula or the North African Coast. This major difference could be related to differences in the formation processes of clusters in different seasons between the Iberian Peninsula and the Genoa region, but further research is needed on this matter. Eleven well separated and distinct clusters as well as eleven hiatus periods are identified, with average occurrence rates of 21.5 yr⁻¹ and 5.2yr⁻¹, respectively. As Vb cyclones are strongly related to large scale heavy precipitation over Central Europe (H18; Messmer et al., 2015; Nissen et al., 2013) these phases are expected to correspond to flood-rich and flood-poor periods in catchments mainly affected by Vb cyclones (Hall et al., 2014). The duration of the Vb clustering periods are typically between 0.5 to 1.5 years (Table 21), in consistency with

clustering found in German flood time series on an intra-annual to inter-annual time scale (Merz et al., 2016).

(iii) Large scale atmospheric patterns, specifically the NAO, AO, EAWR and SCA, appear to be synchronized with the occurrence of Vb cyclones. During months of Vb cyclone occurrence, NAO, AO and EAWR are much more negative than in months without Vb cyclones. SCA is more positive. Ten of the eleven clusters of Vb events occur during a negative phase of the NAO (Figure 37) which is significantly more negative than random occurrence (Figure 38). The latitudinal position of the polar jet stream appears to be a responsible mechanism explaining this relationship, as its location is shifted to more southern latitudes under negative NAO conditions (Woollings et al., 2010), in correspondence with high latitude blocking at the same time (Woollings et al., 2008), thus pushing cyclogenesis towards the WM (Nissen et al., 2014a). We find this mechanism to be most relevant for Vb occurrence during the winter half year. Cyclone clusters over NW-Europe, in contrast, are associated with a persistent and intensified eddy driven jet stream located at 50°N over the NE-Atlantic (Pinto et al., 2014 & 2016) in coherence with a positive phase of the NAO (Mailier et al., 2006). One should also note that the interarrival times between subsequent Euro-Atlantic cyclones are 5 times shorter than those of Vb cyclones.

(iv) Superposition of the eddy-driven polar jet stream and the subtropical jet stream over the Western Mediterranean is identified as a prominent feature at the onset of Vb events (Figure 41). Superposition events (e.g. Christenson et al., 2017) are usually marked by a vanishing latitudinal separation and vertical merging of the jet axes, leading to increased horizontal wind speeds (e.g. Reiter and Whitney, 1969). At the same time, stratospheric and tropospheric baroclinity is combined within a narrow zone resulting in high available potential energy and a further intensified ageostrophic circulation steering cyclogenesis (Handlos and Martin, 2016). Apart from major synoptic eddies developing over Western Europe and amplifying in the WM, the superposition of the jet streams over the WM seems to invigorate Vb cyclogenesis. Superposition is more likely if the latitudinal separation of the jets is small, which tends to occur during negative NAO phases.

(v) The NAO (at Z500) and AO (at Z1000) show a remarkable response to Vb events, which manifests itself as a statistically significant drop of the respective indices, lasting for about three weeks (from 9 days before until 14 days after the peak near Vienna), even when averaging over a total of 557 events. As the negative phase of the NAO goes hand in hand with a higher number of Vb cyclones, this drop leads to a re-enforcement of the large scale atmospheric circulation into a state favoring the genesis of another Vb event for a sustained period and is therefore proposed as a positive feedback mechanism between NAO^- and above average frequency of Vb events ($\text{NAO}^- \Leftrightarrow \text{Vb}^+$). This interpretation is supported by the mean interarrival time of 17 days found during clustering periods in correspondence with the mean duration of the drop in NAO. During Vb events an extensive and strong positive pressure anomaly develops over the southern tip of Greenland (Figure 41) in 63% of all events (mode 1 and mode 3 events, Table 22), nudging the NAO further into negative values (Figure 40). The superposition of the jet streams therefore seems to be the important physical link explaining the proposed feedback [$\text{NAO}^- \Leftrightarrow \text{Vb}^+$] at the process scale. Superposition of the jet streams was also found to occur over the WM/East Atlantic at 40°N during a negative phase of the NAO (Woollings et al., 2010) and to be associated with Greenland blocking events (Woollings et al., 2008). Another strong, positive pressure anomaly develops over a larger region around Scandinavia in 52% of the events (modes 2, 3

and 4). Poleward advection of warm and moist air (e.g. Madonna et al., 2014; Grams et al., 2014) appears as a plausible mechanism for fuelling Scandinavian blocking through latent heat release from ascending air leading to adiabatic heating during Vb events, apart from wave breaking and isentropic advection of air comprising low potential vorticity (Pfahl et al., 2015). Further research is needed on this issue as well.

Finally, some specific limitations of the study are mentioned. The NAAO/Vb-rate relationship applies on average, but not every single cluster or hiatus period follows this relationship. This may be due to (i) an opposed state of the NAO or AO occurring from time to time, leading to blurring in the combined and temporarily averaged NAO/AO index, (ii) in some instances the Vb cyclones are weak and limited in extent, so have no strong feedback with the LAC, and (iii) Vb events are rare so cannot fully account for all the NAO or AO variability. Also, cluster or hiatus periods were not observed in a number of instances although the state of the NAAO suggested their occurrence. Local factors may also be important for cyclogenesis in the WM apart from the large scale forcing (e.g. Aebischer and Schaer, 1998; Trigo et al., 2002), and 22% of the Vb events involve a positive peak of the NAO and NAO (mode 2 events) so Vb occurrence is not strictly tied to a negative phase of the NAAO, especially in the summer. It should also be noted that the identification of Vb cyclones is restricted to all systems moving northwards into Central Europe between 12°E and 22°E at 47°N, so some cyclones might have been missed if they passed outside the line or had already dissipated in the WM.

6 Overall conclusions

The overall goal of this thesis was to improve our understanding of the nature of atmospheric cyclones triggering large scale heavy precipitation in Central Europe (CE). The relationship between European cyclone track types and the characteristics of mean and heavy precipitation in different parts of CE was investigated. Cyclones moving from the Western Mediterranean across Italy into CE (track type Vb) were identified as the most relevant ones concerning heavy precipitation and floods in CE and were thus given particular attention in this study.

The main objectives of this study have been phrased as seven questions which were addressed in Chapters 2-5, leading to the following answers and conclusions:

1. *Are characteristic circulation type classifications or cyclone tracking analyses preferable in capturing Vb events?*

Characteristic circulation type classifications (CTC) are able to capture Vb cyclones, but to a rather limited extent. For a few CTC-variants, days with a Vb cyclone are largely concentrated in a small number of circulation types (CTs). Subjective schemes generally outperform objective ones as the former typically invoke a priori knowledge of related high impact weather events such as Vb. The subjective classifications ZMGo43 and GWLo30 are commendable in this respect. Despite the high probability of Vb to occur coherently during a few CTs, the chance of observing Vb during other CTs is rather large. This implies a strong blurring and a low discrimination rate, depending on the respective CTC, suggesting that CTCs really cannot replace tracking analyses.

2. *How are different cyclone track types related to mean and heavy precipitation in different parts of CE?*

There exist very clear spatial precipitation patterns within CE that differ drastically between the track types. For example, Atlantic cyclones mostly affect the western parts of CE and cease in the eastern lee of the Central European mountain ranges. MED cyclones mostly affect southern regions in autumn, when the Mediterranean Sea Surface temperatures are still high, as well as between December and April, when MED cyclone frequency is highest.

In terms of large scale heavy precipitation, very high totals are observed in the specific case of Vb in both seasons, with values between 140% (winter, 700hPa tracks) and 190% (summer, sea level pressure tracks) of the reference. The outstanding relevance for heavy precipitation applies both to the 24-hour maximum and the total precipitation aggregated over the whole duration of a track within CE.

Overall, the high frequency of strong cyclones was identified as the key factor in explaining seasonality of mean and heavy precipitation at a regional scale within CE. However, to fully explain above average contributions of certain track types in summer and autumn, additional drivers such as air temperature and Mediterranean sea surface temperature may be needed.

3. *Is track type Vb indeed the most relevant one for CE, large scale heavy precipitation events as suggested by observations?*

Vb has been identified as the most relevant track type for heavy cyclone precipitation in all seasons, regardless of the atmospheric level at which the respective cyclone is observed. The reasons for this are: (i) strong Vb cyclones typically occur in all seasons, (ii) Vb cyclones remain much longer in or close to Central Europe than other types, because of the circular shape of the cyclone track at the surface level, and (iii) precipitation intensities, on average, are much higher than for all other types. These findings have important implications for flood risk, as Vb cyclones can wet up soils within a short time which, along with persistent rainfall, will enhance floods. While Vb cyclones affect large parts of Central Europe, their highest precipitation amounts occur in a region covering parts of Austria, Slovakia, Poland and the Czech Republic.

Vb cyclones account for 30% of the 50 largest events in CE, whereas Atlantic and Mediterranean cyclones only account for 15%. Other track types are also important when assessing the overall risk of heavy precipitation, as most of the other types are much more frequent than Vb. In total, between 60 % (Czech Republic) and 88% (W-Germany) of the 50 largest precipitation events (1961-2006) were triggered by track types other than Vb. However, out of the 10 most extreme events in the Czech/Austrian region 8 were due to Vb tracks.

4. *What are the climatological characteristics of Vb cyclones? How do these relate to other track types?*

Only 5% of cyclones moving into CE are classified as track type Vb. When considering both cyclone tracks at sea level pressure and 700hPa, nearly 10 Vb cyclones per year have occurred in the period 1959-2015, corresponding to a mean interarrival time of 37 days. 50% of the Vb cyclones have developed in the lee of the Alps in the vicinity of Genoa (GoG). Vb cyclones are most frequent in early April and in late November. In summer, Vb cyclones are less frequent, however, this does not apply to subtype GoG that occurs evenly throughout the year. The reasons for this peculiarity as well as for the bimodal occurrence remain unknown and require additional research. It is also unclear why Vb cyclones are so strong in all seasons, unlike other the types which are usually strongest in the main winter. Vb cyclones remain in or close to Central Europe much longer than other types (2.5 instead of 1.5 days), because of their circular track at the surface level but not due to difference in the propagation speed. Vb cyclones therefore have a high potential for triggering long-duration rainfall events. Irrespective of the rainfall intensity, this is an additional factor increasing the flood risk.

-
5. *Has the frequency of Vb cyclones changed in recent decades given that global temperatures have increased by almost one degree Celsius?*

The frequency of Vb cyclones was significantly higher in the 1960s and has remained close to the average rate of 9.8 yr^{-1} since then. In winter, the rate has decreased by about 40%, whereas in summer it has remained close to its long term average. The high rate during the 1960s occurred during a repeatedly negative phase of the Arctic-/North Atlantic Oscillation (NAAO). In contrast, the significantly lower rate of 6.9 yr^{-1} between April 1988 and December 1996 occurred during a sustained positive phase of the NAAO. Overall, Vb cyclone frequency has varied strongly on a decadal scale which appears to be related to internal climate variability. There is little indication of a change in the annual risk of Vb associated with increasing global mean temperatures considering the period 1959-2015.

6. *How are Vb cyclones related to the large scale atmospheric circulation? Is there a prominent atmospheric mode explaining variations in the Vb occurrence rate on a monthly to decadal scale?*

There is indeed a close association between large scale atmospheric circulation characteristics and the occurrence of Vb events, with the NAAO index dropping significantly into negative for about three weeks. As the negative phase of the NAAO goes hand in hand with a higher number of Vb cyclones, this sustained drop leads to a re-enforcement of the large scale atmospheric circulation into a state favoring the genesis of another Vb event. A positive feedback mechanism is therefore proposed to exist between NAAO^- and above average frequency of Vb events ($\text{NAAO}^- \Leftrightarrow \text{Vb}^+$). The latitudinal position of the polar jet stream appears to be a responsible mechanism explaining this relationship, as its location is more variable and also shifted to more southern latitudes under negative NAO conditions pushing cyclogenesis over the Eastern Atlantic towards the Western Mediterranean. Superposition of the eddy-driven polar jet stream and the subtropical jet stream over the Western Mediterranean was identified as a prominent feature at the onset of Vb events, which is more likely to occur if the latitudinal separation of the jets is small. This tends to be the case during negative NAO phases.

7. *Do Vb cyclones occur in clusters, i.e. more frequently than by chance in certain periods, and what are the consequences for flood risk?*

Vb cyclones do arrive in clusters, and also are more regular than chance at times. During clusters the inter arrival time is about 17 days whereas it is nearly 70 days during hiatuses. Clustering is very prominent in winter for cyclones developing over Spain and the North African Coast as well as in summer for Vb-Genoan cyclones. Serial clustering of Vb cyclones appears as a critical issue, as soil moisture and groundwater storage can build up during prolonged rain episodes, increasing the risk of flooding. In winter clustering is strongly associated with a weakened and southerly shifted polar stream favoring the genesis of cyclones in the Western Mediterranean. In summer this relationship is weaker.

An upper level cut off low over CE has been identified as a prominent circulation feature during strong Vb cyclones. Major cut off lows are usually very persistent and favor the occurrence of consecutive cyclones with similar tracks at the surface level. How the formation of a persistent cut off lows over CE relates to Vb clustering remains an open question for future work.

This thesis has advanced our knowledge of the nature of atmospheric cyclones triggering large scale heavy precipitation in Central Europe in general and of the cyclone track type Vb in particular. A new classification of Central European cyclone tracks was proposed and the requirements for a reliable cyclone tracking were stated. For example, we conclude that cyclones identified at sea level pressure are more strongly related to large scale heavy precipitation over Central Europe than those at 700hPa, in particular track types Vb, EA, X-N, X-S, MED and CON. Given the difficulties of tracking at sea level pressure, especially in the vicinity of major mountain ranges, the geopotential height at 850hPa appears as a sound height compromise for future tracking studies.

Vb cyclones were found as the most relevant cyclones regarding CE heavy precipitation at the large scale. The outstanding relevance mainly applies to the eastern parts of CE (Czech Republic, E-Austria, W-Slovakia). For example, in southern Bavaria the importance of Vb is still considerable, but Atlantic cyclones are also important there, especially in the main winter and for less than extreme events. Apart from large scale summer floods resulting from excessive rain episodes, other flood types are also of importance in certain CE regions such as flash floods (in small catchments), snow-melt floods, rain on snow floods and short rain floods (Merz and Blöschl, 2003). In this study the focus was on large scale heavy precipitation, so the findings do not relate to other flood types. Future research could therefore focus on different spatial and temporal scales, for example by considering high intensity - short duration events. Beside high precipitation totals other hydrological factors also determine the risk of flooding, so a combined study considering both hydrological and meteorological factors on different spatio-temporal scales appears necessary for comprehensively assessing the risk of flooding under climate change.

Future work should also explore the processes relevant for Vb cyclogenesis in the Western Mediterranean. A number of questions have arisen in this study pointing regarding the genesis of Vb as a key factor in understanding the peculiar characteristics of Vb cyclones. This appears crucial in assessing potential changes of heavy precipitation under future climate conditions in a more comprehensive way. For example, a strong positive pressure anomaly has developed over a large region around Scandinavia in about 50% of the Vb events. Poleward advection of warm and moist air appears as a plausible mechanism for fuelling Scandinavian blocking through latent heat release from ascending air leading to adiabatic heating during Vb events, apart from wave breaking and isentropic advection of air comprising low potential vorticity. Scandinavian Blocking is a very persistent phenomenon and has strong implications up and downstream with relevance for high impact weather events. Vb cyclogenesis possibly initiates or reinforces Scandinavian Blocking.

References

- Aebischer, U., & Schär, C. (1998). Low-Level Potential Vorticity and Cyclogenesis to the Lee of the Alps. *Journal of the Atmospheric Sciences*, 55(2), 186–207. doi.org/10.1175/1520-0469(1998)055<0186:LLPVAC>2.0.CO;2
- Akima, H. (1978). A Method of Bivariate Interpolation and Smooth Surface Fitting for Irregularly Distributed Data Points. *ACM Transactions on Mathematical Software*, 4, 148–164. doi:10.1145/355780.355786.
- Akima, H. (1996). Algorithm 761: scattered-data surface fitting that has the accuracy of a cubic polynomial. *ACM Transactions on Mathematical Software*, 22, 362–371. doi:10.1145/232826.232856.
- Akperov, M.G., & Mokhov, I.I. (2010): A comparative analysis of the method of extratropical cyclone identification. *Izvestiya Atmospheric and Oceanic Physics*, 46(5), 574-590.
- Apostol, L. (2008). The Mediterranean cyclones – the role in ensuring water resources and their potential of climatic risk in the east of Romania, *Present Environment and Sustainable Development*, 2, 143–163.
- Athanasiadis, P. J., Wallace, J. M., & Wettstein, J. J. (2010). Patterns of Wintertime Jet Stream Variability and Their Relation to the Storm Tracks*. *Journal of the Atmospheric Sciences*, 67(5), 1361–1381. doi.org/10.1175/2009JAS3270.1
- Barnston, A. G., & Livezey, R. E. (1987). Classification, Seasonality and Persistence of Low-Frequency Atmospheric Circulation Patterns. *Monthly Weather Review*, 115(6), 1083–1126. doi.org/10.1175/1520-0493(1987)115<1083:CSAPOL>2.0.CO;2
- Barriopedro, D., García-Herrera, R., & Trigo, R. M. (2010). Application of blocking diagnosis methods to General Circulation Models. Part I: a novel detection scheme. *Climate Dynamics*, 35(7–8), 1373–1391. doi.org/10.1007/s00382-010-0767-5
- Bartholy, J., Pongrácz, R., & Pattantyús-Ábrahám, M. (2009). Analyzing the genesis, intensity, and tracks of western Mediterranean cyclones. *Theoretical and Applied Climatology*, 96(133). doi.org/10.1007/s00704-008-0082-9
- Bebber van, W.J., & Köppen, W. (1895). Die Isobarentypen des Nordatlantischen Ozeans und Westeuropas, ihre Beziehung zur Lage und Bewegung der barometrischen Maxima und Minima. *Archiv der Deutschen Seewarte*, 18, 27 Seiten, 23 Tafeln.
- Bebber van, W.J. (1891). Die Zugstrassen der barometrischen Minima nach den Bahnenkarten der Deutschen Seewarte für den Zeitraum 1875-1890. *Meteorologische Zeitschrift*, 8, Seite 361-366; mit 12 Monatskarten.
- Bebber van, W.J. (1882). Typische Witterungserscheinungen. *Archiv der Deutschen Seewarte*, 5(3), 45 pp.
- Beck, C. (2000). *Zirkulationsdynamische Variabilität im Bereich Nordatlantik-Europa seit 1780 (Variability of circulation dynamics in the North-Atlantic-European region)*. Würzburger Geographische Arbeiten, 95 (in German).
- Beck C., & Philipp, A. (2010). Evaluation and comparison of circulation type classifications for the European domain. *Physics and Chemistry of the Earth*, 35, 374–387.
- Bengtsson, L., Hodges, K.I., & Röckner, E. (2006). Storm Tracks and Climate Change. *Journal of Climate*, 19, 3518–3543. doi.org/10.1175/JCLI3815.1.
- Blender, R., Fraedrich, K., & Lunkeit, F. (1997). Identification of cyclone track regimes in the North Atlantic. *Quarterly Journal of the Royal Meteorological Society*, 123(539), 727–741. doi:10.1002/qj.49712353910.
- BLfW - Bayerisches Landesamt für Wasserwirtschaft (Hrsg.), (2003). *Hochwasser Mai 1999, Gewässerkundliche Beschreibung*. Bayerisches Landesamt für Wasserwirtschaft, München, 2003. (URL http://www.lfu.bayern.de/wasser/hw_ereignisse/aktuell/doc/bericht_pfungsten99.pdf, 03-2017-18).
- Blöschl, G., J., et al. (2017). Changing climate shifts timing of European floods. *Science*, 357(6351), 588-590. doi: 10.1126/science.aan2506.
- Blöschl, G., Nester, T., Komma, J., Parajka, J., & Perdigão, R.A.P. (2013). The June 2013 flood in the Upper Danube basin, and comparisons with the 2002, 1954 and 1899 floods. *Hydrology and Earth System Sciences*, 17, 5197-5212. doi:10.5194/hess-17-5197-2013.

-
- BLU (Bayerisches Landesamt für Umwelt). 2006. *August – Hochwasser 2005 in Südbayern (August 2005 flood in Southern Bavaria): Endbericht vom 12. April 2006*. Bayerisches Landesamt für Umwelt, München, 49 pp., 2006.
- Böhm, O., Wetzol, K.F. (2006). Flood history of the Danube tributaries Lech and Isar in the Alpine foreland of Germany. *Hydrological Sciences Journal*, 51(5), 784-798. doi:10.1623/hysj.51.5.784
- Burkey, J. (2006). *A non-parametric monotonic trend test computing Mann-Kendall Tau, Tau-b, and Sen's Slope written in Mathworks-MATLAB implemented using matrix rotations*. King County, Department of Natural Resources and Parks, Science and Technical Services section. Seattle, Washington. USA. <http://www.mathworks.com/matlabcentral/fileexchange/authors/23983>
- Buzzi, A., & Tibaldi, S. (1978). Cyclogenesis in the lee of the Alps: A case study. *Quarterly Journal of the Royal Meteorological Society*, 104, 271–287. doi:10.1002/qj.49710444004.
- Campins, J., Genovés, A., Picornell, M. A., & Jansà, A. (2010). Climatology of Mediterranean cyclones using the ERA-40 dataset. *International Journal of Climatology*, 31, 1596–1614. doi:10.1002/joc.2183.
- Campins, J., Jansà, A., & Genovés, A. (2006). Three-dimensional structure of western Mediterranean cyclones. *International Journal of Climatology*, 26(3), 323–343. doi:10.1002/joc.1275. doi:10.1002/joc.1275.
- Casanueva, A., Rodríguez-Puebla, C., Frías, M.D., & González-Reviriego, N. (2014). Variability of extreme precipitation over Europe and its relationships with teleconnection patterns. *Hydrology and Earth System Sciences*, 18, 709-725. doi:10.5194/hess-18-709-2014.
- Casty, C., Wanner, H., Luterbacher, J., Esper, J., & Böhm, R. (2005). Temperature and precipitation variability in the European Alps since 1500. *International Journal of Climatology*, 25(14), pp. 1855-1880. doi: 10.1002/joc.1216.
- Catto, J. L., Jakob, C., Berry, G., & Nicholls, N. (2012). Relating global precipitation to atmospheric fronts. *Geophysical Research Letter*, 39. doi:10.1029/2012GL051736.
- Christenson, C. E., Martin, J. E., & Handlos, Z. J. (2017). A Synoptic Climatology of Northern Hemisphere, Cold Season Polar and Subtropical Jet Superposition Events. *Journal of Climate*, 30(18), 7231–7246. doi.org/10.1175/JCLI-D-16-0565.1
- Coles S. (2001). *An Introduction to Statistical Modeling of Extreme Values*. Springer Series in Statistics. Springer Verlag London. 208p.
- Cowling, A., Hall, P., & Phillips, M. J. (1996). Bootstrap confidence regions for the intensity of a Poisson point process. *Journal of the American Statistical Association*, 91, 1516– 1524.
- Cox, D. R., & Isham, V. (1980). *Point processes*. London ; New York: Chapman and Hall.
- Cox, D. R., & Lewis, P. A. W. (1966). *The Statistical Analysis of Series of Events*. Dordrecht: Springer Netherlands. doi.org/10.1007/978-94-011-7801-3
- Dacre, H.F., & Gray, S.L. (2009). The Spatial Distribution and Evolution Characteristics of North Atlantic Cyclones. *Monthly Weather Review*, 137, 99–115. doi.org/10.1175/2008MWR2491.1.
- Danhelka, J., & Kubát, J., (eds). (2009). *Flash Floods on the Territory of the Czech Republic in June and July 2009*, (in Czech). Praha, Ministry of the Environment of the Czech Republic. Czech Hydrometeorological Institute.
- Davis, R.E., Demme, G., & Dolan, R. (1993). Synoptic climatology of atlantic coast North-Easterns, *International Journal of Climatology*, 13(2), 171–189. doi:10.1002/joc.3370130204.
- Dayan, U., Nissen, K., Ulbrich, U. (2015). Review Article: Atmospheric conditions inducing extreme precipitation over the eastern and western Mediterranean. *Natural Hazards and Earth Systems Sciences*, 15, 2525-2544. doi:10.5194/nhess-15-2525-2015.
- Dee, D.P., et al. (2011). The ERA-Interim reanalysis: configuration and performance of the data assimilation system, *Quarterly Journal of the Royal Meteorological Society*, 137, 553–597. doi:10.1002/qj.828.
- Delworth, T. L., Zeng, F., Vecchi, G. A., Yang, X., Zhang, L., & Zhang, R. (2016). The North Atlantic Oscillation as a driver of rapid climate change in the Northern Hemisphere. *Nature Geoscience*, 9(7), 509–512. doi.org/10.1038/ngeo2738.

-
- Dittmann E., Barth, S., Lang, J., Müller-Westermeier, G. (1995): Objektive Wetterlagenklassifikation (Objective weather type classification). *Bericht des Deutschen Wetterdienstes*, 197, Offenbach a. M., Germany (in German).
- Donaldson R.J., Dyer R.M., & Krauss, M.J. (1975). *An objective evaluator of techniques for predicting severe weather events*. Preprints: 9th Conf. Severe Local Storms, Norman, Oklahoma, American Meteorological Society, 321-326.
- Donat, M. G., Pardowitz, T., Leckebusch, G. C., Ulbrich, U., & Burghoff, O. (2011). High-resolution refinement of a storm loss model and estimation of return periods of loss-intensive storms over Germany. *Natural Hazards and Earth System Science*, 11(10), 2821–2833. doi.org/10.5194/nhess-11-2821-2011.
- Donat, M.G., Leckebusch, G.C., Pinto, J.G., & Ulbrich, U. (2010). Examination of wind storms over Central Europe with respect to circulation weather types and NAO phases. *International Journal of Climatology*, 30, 1289–1300. doi:10.1002/joc.1982.
- Egger, J. (1988). Alpine Lee Cyclogenesis: Verification of Theories. *Journal of the Atmospheric Sciences*, 45(15), 2187–2203. doi.org/10.1175/1520-0469(1988)045<2187:ALCVOT>2.0.CO;2.
- Egger, J., & Hoinka, K.P. (2008). Mountain torques and synoptic systems in the Mediterranean, *Quarterly Journal of the Royal Meteorological Society*, 134, 1067–1081. doi:10.1002/qj.248.
- Feldstein, S. B., & Franzke, C. L. E. (2017). Atmospheric Teleconnection Patterns. In C. L. E. Franzke & T. J. O’Kane (Hrsg.), *Nonlinear and Stochastic Climate Dynamics* (S. 54–104). Cambridge: Cambridge University Press. doi.org/10.1017/9781316339251.004.
- Fleig, A.K., Tallaksen, L.M., James, P., Hisdal, H., & Stahl, K. (2015). Attribution of European precipitation and temperature trends to changes in synoptic circulation. *Hydrology Earth System Science*, 19, 3093-3107. doi:10.5194/hess-19-3093-2015.
- Flocas, A.A. (1988). Frontal depressions over the Mediterranean Sea and central southern Europe. *Méditerranée, Troisième série*, Tome 66, 4-1988. Recherches climatiques en régions méditerranéennes II., 43-52.
- Freser, F., & von Storch, H. (2005). A Spatial Two-Dimensional Discrete Filter for Limited-Area-Model Evaluation Purposes, *Monthly Weather Review*, 133, 1774–1786. doi.org/10.1175/MWR2939.1.
- Fricke W., & Kaminski, U. (2002). Ist die Zunahme von Starkniederschlägen auf veränderte Wetterlagen zurückzuführen? *GAW Brief des Deutschen Wetterdienstes*, 12, 1-2.
- Gaál, L., Szolgay, J., Kohnová, S., Parajka, J., Merz, R., Viglione, A., & Blöschl, G. (2012). Flood timescales: Understanding the interplay of climate and catchment processes through comparative hydrology. *Water Resources Research*, 48, W04511. doi:10.1029/2011WR011509.
- Gasser, T., & Müller, H. G. (1984). Estimating Regression Functions and Their Derivatives by the Kernel Method. *Scandinavian Journal of Statistics*, 11(3), 171–185.
- Gasser, T., & Müller, H. G. (1979). Kernel estimation of regression functions. In Th. Gasser & M. Rosenblatt (Hrsg.), *Smoothing Techniques for Curve Estimation* (Bd. 757, S. 23–68). Berlin, Heidelberg: Springer Berlin Heidelberg. doi.org/10.1007/BFb0098489
- Godina, R., Lalk, P., Lorenz, P., Müller, G., Weilguni, V. (2006). *Hochwasser 2005 — Ereignisdokumentation: Teilbericht des Hydrographischen Dienstes*. Federal Ministry for Agriculture, Forestry, Environment and Water Management, Sekt. VII, Vienna. 30 pp.
- Grams, C. M., Binder, H., Pfahl, S., Piaget, N., & Wernli, H. (2014). Atmospheric processes triggering the central European floods in June 2013. *Natural Hazards and Earth System Science*, 14(7), 1691–1702. doi.org/10.5194/nhess-14-1691-2014.
- Grazzini, F., & van der Grijn, G. (2002). Central European floods during summer 2002. *ECMWF Newsletter*, 96, 18–28.
- Greatbatch, R. J., Gollan, G., Jung, T., & Kunz, T. (2015). Tropical origin of the severe European winter of 1962/1963: Severe European Winter of 1962/1963. *Quarterly Journal of the Royal Meteorological Society*, 141(686), 153–165. doi.org/10.1002/qj.2346.

-
- Grillakis, M.G., A.G. Koutroulis, J. Komma, I.K. Tsanis, W. Wagner, & Blöschl, G. (2016). Initial soil moisture effects on flash flood generation – A comparison between basins of contrasting hydro-climatic conditions. *Journal of Hydrology*, 541(A), 206–217. doi.org/10.1016/j.jhydrol.2016.03.007.
- Habersack, H.M., & Krapesch, G. (Edts.) (2006). *Hochwasser 2005 – Ereignisdokumentation der Bundeswasserbauverwaltung des Forsttechnischen Dienstes für Wildbach- und Lawinerverbauung und des Hydrographischen Dienstes, Synthesebericht*. Bundesministerium für Land- und Forstwirtschaft, Umwelt und Wasserwirtschaft, Universität für Bodenkultur Wien, 149, Wien.
- Hall J., et al., (2014). Understanding flood regime changes in Europe: a state-of-the-art assessment. *Hydrology and Earth System Sciences*, 18, 2735–2772. doi:10.5194/hess-18-2735-2014.
- Handlos, Z. J., & Martin, J. E. (2016). Composite Analysis of Large-Scale Environments Conducive to Western Pacific Polar/Subtropical Jet Superposition. *Journal of Climate*, 29(19), 7145–7165. doi.org/10.1175/JCLI-D-16-0044.1
- Hanley, J., & Caballero, R. (2012). Objective identification and tracking of multicentre cyclones in the ERA-Interim reanalysis dataset. *Quarterly Journal of the Royal Meteorological Society*, 138, 612–625. doi:10.1002/qj.948.
- Hantel, M. (Ed.) (2005). *Observed Global Climate, Series LandoltBörnstein – Numerical Data and Functional Relationships in Science and Technology. New Series. Vol. 6A: Springer, Berlin.*
- Harada, Y., et al., (2016). The JRA-55 Reanalysis: Representation of atmospheric circulation and climate variability. *Journal of the Meteorological Society of Japan Series II*, 94(3), 269-302. doi:10.2151/jmsj.2016-015.
- Haslinger, K., & Blöschl, G. (2017). Space-time patterns of meteorological drought events in the European Greater Alpine Region over the past 210 years. *Water Resources Research*, 53, 9807–9823. doi.org/10.1002/2017WR020797.
- Hawcroft, M.K., Shaffrey, L.C., Hodges, K.I., & Dacre, H.F. (2012). How much Northern Hemisphere precipitation is associated with extratropical cyclones? *Geophysical Research Letters*, 39, L24809. doi:10.1029/2012GL053866.
- Haylock, M.R., Hofstra, N., Klein Tank, A.M.G., Klok, E.J., Jones, P.D., & New, M. (2008). A European Daily High-Resolution Gridded Data Set of Surface Temperature and Precipitation for 1950–2006. *Journal of Geophysical Research*, 113, D20119. doi:10.1029/2008JD010201.
- Hess P., & Brezowsky, H. (1952). *Katalog der Großwetterlagen Europas (Catalog of the European Large Scale Weather Types)*. *Bericht des Deutschen Wetterdienstes in der US-Zone*, 33, Bad Kissingen, Germany (in German).
- Hewson, T.D., & Titley, H.A. (2010). Objective identification, typing and tracking of the complete life-cycles of cyclonic features at high spatial resolution. *Meteorological Applications*, 17, 355–381. doi:10.1002/mct.204.
- Hodges, K.I., Lee, R.W., & Bengtsson, L. (2011). A comparison of extratropical cyclones in recent reanalyses ERA-Interim, NASA MERRA, NCEP CFSR, and JRA-25. *Journal of Climate*, 24(18), 4888–4906. doi:10.1175/2011JCLI4097.1
- Hofstätter, M., Lexer, A., Homann, M., & Blöschl, G. (2018). Large-scale heavy precipitation over central Europe and the role of atmospheric cyclone track types. *International Journal of Climatology*, 38, e497–e517. doi.org/10.1002/joc.5386.
- Hofstätter, M., Chimani, B., Lexer, A., & Blöschl, G. (2016). A new classification scheme of European cyclone tracks with relevance to precipitation. *Water Resources Research*, 52(9), 7086–7104. doi.org/10.1002/2016WR019146.
- Hofstätter, M., Jucundus, J., Homann, M., Lexer, A., Chimani, B., Philipp, A., Beck, C., & Ganekind, M. (2015). *WETRAX – Weather Patterns, Cyclone Tracks and related Precipitation Extremes. Großflächige Starkniederschläge im Klimawandel in Mitteleuropa* (Bd. 19). Augsburg, Germany: Geographica Augustana. ISBN: 3-923273-96-6.
- Hofstätter, M., & Chimani, B. (2012). Van Bebber’s cyclone tracks at 700 hPa in the Eastern Alps for 1961-2002 and their comparison to Circulation Type Classifications. *Meteorologische Zeitschrift*, 21(5), 459–473. doi.org/10.1127/0941-2948/2012/0473.

-
- Hofstra, N., New, M., & McSweeney, C. (2010). The influence of interpolation and station network density on the distributions and trends of climate variables in gridded daily data. *Climate Dynamics*, 35(5), pp. 841-858.
- Horvath, K., Lin, Y.L., & Ivančan-Picek, B. (2008). Classification of Cyclone Tracks over the Apennines and the Adriatic Sea. *Monthly Weather Review*, 136, 2210–2227. doi.org/10.1175/2007MWR2231.1.
- Hoskins, B.J., & Hodges, K.I. (2002). New Perspectives on the Northern Hemisphere Winter Storm Tracks. *Journal of Atmospheric Science*. 59(6), 1041–1061. doi.org/10.1175/1520-0469(2002)059<1041:NPOTNH>2.0.CO;2.
- Huang Jr, C., Yu, C.K., Lee, J.Y., Cheng, L.W., Lee, T.Y., & Kao, S.J. (2012). Linking typhoon tracks and spatial rainfall patterns for improving flood lead time predictions over a mesoscale mountainous watershed. *Water Resources Research*, 48(9), W09540. doi:10.1029/2011WR011508.
- Hurrell, J. W., Kushnir, Y., Ottersen, G., & Visbeck, M. (2003). An overview of the North Atlantic Oscillation. In James W. Hurrell, Y. Kushnir, G. Ottersen, & M. Visbeck (Eds.), *Geophysical Monograph Series* (Bd. 134, S. 1–35). Washington, D. C.: American Geophysical Union. doi.org/10.1029/134GM01.
- Hurrell, J. W. (2001). CLIMATE: The North Atlantic Oscillation. *Science*, 291(5504), 603–605. doi.org/10.1126/science.1058761.
- Hurrell, J. W. (1995). Decadal Trends in the North Atlantic Oscillation: Regional Temperatures and Precipitation. *Science*, 269(5224), 676–679. doi.org/10.1126/science.269.5224.676
- Iles, C., & Hegerl, G. (2017). Role of the North Atlantic Oscillation in decadal temperature trends. *Environmental Research Letters*, 12(11), 114010. doi.org/10.1088/1748-9326/aa9152
- Ionita, M., et al. (2017). The European 2015 drought from a climatological perspective. *Hydrology and Earth System Sciences*, 21(3), 1397–1419. doi.org/10.5194/hess-21-1397-2017.
- Jacobeit, J., Philipp, A., & Nonnenmacher, M. (2006). Atmospheric circulation dynamics linked with prominent discharge events in Central Europe. *Hydrological Sciences Journal*, 51, 946-965. doi:10.1623/hysj.51.5.946.
- Jacobeit, J. (1993). Regionale Unterschiede im atmosphärischen Zirkulationsgeschehen bei globalen Klimaveränderungen. *Die Erde*, 124, 63-77.
- James, P.M. (2007). An objective classification for Hess and Brezowsky Grosswetterlagen over Europe. *Theoretical and Applied Climatology*, 88, 17-42.
- James P., Stohl, A., Spichtinger, N., Eckhardt, S., & Forster, C. (2004). Climatological aspects of the extreme European rainfall of August 2002 and a trajectory method for estimating the associated evaporative source regions. *Natural Hazards and Earth Systems Sciences*, 4, 733-746. doi:10.5194/nhess-4-733-2004.
- Japanese Meteorological Agency (2013). *JRA-55: Japanese 55-year Reanalysis, daily, 3-hourly and 6-hourly data*. Computational and Information Systems Laboratory, National Center for Atmospheric Research: Tokyo. doi.org/10.5065/D6HH6H41.
- Jones, P. D., Lister, D. H., Osborn, T. J., Harpham, C., Salmon, M., & Morice, C. P. (2012). Hemispheric and large-scale land-surface air temperature variations: An extensive revision and an update to 2010. *Journal of Geophysical Research: Atmospheres*, 117(D5). doi.org/10.1029/2011JD017139
- Kalnay, E., et al. (1996). The NCEP/NCAR 40-year reanalysis project. *Bulletin of the American Meteorological Society*, 77, 437–471. doi.org/10.1175/1520-0477(1996)077<0437:TNYRP>2.0.CO;2.
- Kašpar, M., & Müller, M. (2014). Combinations of large-scale circulation anomalies conducive to precipitation extremes in the Czech Republic. *Atmospheric Research*, 138, 205–212. doi.org/10.1016/j.atmosres.2013.11.014.
- Kašpar M., & Müller, M. (2008): Selection of historic heavy large-scale rainfall events in the Czech Republic. *Natural Hazards and Earth Systems Science*, 8, 1359-1367. doi:10.5194/nhess-8-1359-2008.
- Klein, W. (1957). Principal tracks and mean frequencies of cyclone and anticyclones in the Northern Hemisphere. *Research paper No.40*, U.S. Weather Bureau, Washington DC.
- Kobayashi, S., et al. (2015). The JRA-55 Reanalysis: General Specifications and Basic Characteristics. *Journal of the Meteorological Society of Japan. Ser. II*, 93(1), 5–48. doi.org/10.2151/jmsj.2015-001.

-
- Komma, J., G. Blöschl, & Reszler, C. (2008). Soil moisture updating by Ensemble Kalman Filtering in real-time flood forecasting. *Journal of Hydrology*, 357, 228-242. doi.org/10.1016/j.jhydrol.2008.05.020.
- Kottek, M., Grieser, J., Beck, C., Rudolf, B., & Rubel, F. (2006). World Map of the Köppen-Geiger climate classification updated. *Meteorologische Zeitschrift*, 15, 259-263. doi:10.1127/0941-2948/2006/0130.
- Kummli, C. (2014). *Sensitivity of precipitation to Mediterranean SSTs in the case of the Vb-type cyclone in August 2005 using the regional model WRF*. M.S. thesis, Faculty of Science, University of Bern, 95pp.
- Kundzewicz, Z.W., et al. (2005). Summer Floods in Central Europe – Climate Change Track? *Natural Hazards*, 36(1-2), 165–189. doi:10.1007/s11069-004-4547-6.
- Kundzewicz, Z.W., Szamalek, K., & Kowalczak, P. (1999). The great flood of 1997 in Poland. *Hydrological Sciences Journal*, 44(6), 855-870.
- Lauscher, F. (1985). Klimatologische Synoptik Österreichs mittels der ostalpinen Wetterlagenklassifikation (Synoptic Climatology of Austria based on the Eastern-Alpine Weather Type Classification). *Arbeiten aus der Zentralanstalt für Meteorologie und Geodynamik, Publikation Nr. 302, Heft 64, Austria* (in German).
- Lauscher, F. (1972). 25 Jahre mit täglicher Klassifikation der Wetterlage in den Ostalpenländern. *Wetter und Leben*, 24, 185–189.
- Leckebusch, G.C., Koffi, B., Ulbrich, U., Pinto, J.G., Spangehl, T., & Zacharias, S. (2006). Analysis of frequency and intensity of European winter storm events from a multi-model perspective, at synoptic and regional scales. *Climate Research*, 31(1), 59-74. doi.org/10.3354/cr031059
- Lim, E.P., & Simmonds, I. (2007). Southern Hemisphere winter extratropical cyclone characteristics and vertical organization observed with the ERA-40 data in 1979–2001. *Journal of Climate*, 20(11), 2675–2690. doi: 10.1175/JCLI4135.1
- Lionello, P., et al. (2016). Objective climatology of cyclones in the Mediterranean region: a consensus view among methods with different system identification and tracking criteria. *Tellus A: Dynamic Meteorology and Oceanography*, 68(1), 29391. doi.org/10.3402/tellusa.v68.29391.
- Lionello P., Dalan F., & Elvini, E. (2002). Cyclones in the Mediterranean region: the present and the doubled CO2 climate scenarios. *Climate Research*, 22, 147-159.
- Llasat, M.C., & Puigcerver, M. (1990). Cold Air Pools over Europe. *Meteorology and Atmospheric Physics*, 42(171). doi: 10.1007/BF01314823.
- Lund, I.A., (1963). Map-pattern classification by statistical methods. *Journal of Applied Meteorology*, 2, 56-65.
- Madonna, E., Li, C., Grams, C. M., & Woollings, T. (2017). The link between eddy-driven jet variability and weather regimes in the North Atlantic-European sector: Eddy-driven Jet Variability and Weather Regimes. *Quarterly Journal of the Royal Meteorological Society*, 143(708), 2960–2972. doi.org/10.1002/qj.3155.
- Madonna, E., Wernli, H., Joos, H., & Martius, O. (2014). Warm Conveyor Belts in the ERA-Interim Dataset (1979–2010). Part I: Climatology and Potential Vorticity Evolution. *Journal of Climate*, 27(1), 3–26. doi.org/10.1175/JCLI-D-12-00720.1.
- Maheras, P., Flocas, H. A., Anagnostopoulou, C., & Patrikas, I. (2002). On the vertical structure of composite surface cyclones in the Mediterranean region. *Theoretical and Applied Climatology*, 71(3–4), 199–217. doi.org/10.1007/s007040200005.
- Maheras, P., Flocas, H. A., Patrikas, I., & Anagnostopoulou, C. (2001). A 40 year objective climatology of surface cyclones in the Mediterranean region: spatial and temporal distribution. *International Journal of Climatology*, 21(1), 109–130. doi.org/10.1002/joc.599.
- Mailier, P. J., Stephenson, D. B., Ferro, C. A. T., & Hodges, K. I. (2006). Serial Clustering of Extratropical Cyclones. *Monthly Weather Review*, 134(8), 2224–2240. doi.org/10.1175/MWR3160.1.
- Malitz G., & Schmidt, T. (1997). Hydrometeorologische Aspekte des Sommerhochwassers der Oder 1997. *Wasser und Boden*, 49(9), 9-12, Berlin; zugleich in: Deutscher Wetterdienst (Hrsg.): Klimastatusbericht 1997. 28-36, Offenbach am Main.
- Masato, G., Hoskins, B. J., & Woollings, T. J. (2012). Wave-breaking characteristics of midlatitude blocking. *Quarterly Journal of the Royal Meteorological Society*, 138(666), 1285–1296. doi.org/10.1002/qj.990.

-
- Masson, D., & Frei, C. (2016). Long-term variations and trends of mesoscale precipitation in the Alps: recalculation and update for 1901–2008. *International Journal of Climatology*, *36*, 492–500. doi:10.1002/joc.4343.
- Merz, B., Nguyen, V. D., & Vorogushyn, S. (2016). Temporal clustering of floods in Germany: Do flood-rich and flood-poor periods exist? *Journal of Hydrology*, *541*, 824–838. doi.org/10.1016/j.jhydrol.2016.07.041
- Merz, R., & Blöschl, G. (2003). A process typology of regional floods. *Water Resources Research*, *39*(12): 1340. doi:10.1029/2002WR001951.
- Messmer, M., Gómez-Navarro, J. J., & Raible, C. C. (2017). Sensitivity experiments on the response of Vb cyclones to sea surface temperature and soil moisture changes. *Earth System Dynamics*, *8*, 477–493. doi:10.5194/esd-8-477-2017.
- Messmer, M., Gómez-Navarro, J. J., & Raible, C. C. (2015). Climatology of Vb cyclones, physical mechanisms and their impact on extreme precipitation over Central Europe. *Earth System Dynamics*, *6*(2), 541–553. doi.org/10.5194/esd-6-541-2015.
- Mochizuki, Y., et al. (2016). Similarity in Neuronal Firing Regimes across Mammalian Species. *Journal of Neuroscience*, *36*(21), 5736–5747. doi.org/10.1523/JNEUROSCI.0230-16.2016.
- Morice, C. P., Kennedy, J. J., Rayner, N. A., & Jones, P. D. (2012). Quantifying uncertainties in global and regional temperature change using an ensemble of observational estimates: The HadCRUT4 data set. *Journal of Geophysical Research: Atmospheres*, *117*(D081018). doi.org/10.1029/2011JD017187
- Mudelsee, M. (2014). *Climate time series analysis: classical statistical and bootstrap methods*. New York: Springer.
- Mudelsee, M., Fohlmeister, J., & Scholz, D. (2012). Effects of dating errors on nonparametric trend analyses of speleothem time series. *Climate of the Past*, *8*(5), 1637–1648. doi.org/10.5194/cp-8-1637-2012
- Mudelsee, M. (2009). Break function regression: A tool for quantifying trend changes in climate time series. *The European Physical Journal Special Topics*, *174*(1), 49–63. doi.org/10.1140/epjst/e2009-01089-3.
- Mudelsee, M., Börngen, M., Tetzlaff, G., & Grünewald, U. (2004). Extreme floods in central Europe over the past 500 years: Role of cyclone pathway “Zugstrasse Vb”: EXTREME FLOODS IN CENTRAL EUROPE. *Journal of Geophysical Research: Atmospheres*, *109*(D23). doi.org/10.1029/2004JD005034.
- Mudelsee, M., Börngen, M., Tetzlaff, G., & Grünewald, U. (2003). No upward trends in the occurrence of extreme floods in central Europe. *Nature*, *425*, 166.
- Mudelsee, M. (2002). TAUEST: a computer program for estimating persistence in unevenly spaced weather/climate time series. *Computers & Geosciences*, *28*(1), 69–72. doi.org/10.1016/S0098-3004(01)00041-3.
- Müller, M., Kašpar, M., Valeriánová, A., Crhová, L., Holtanová, E., & Gvoždíková, B. (2015). Novel indices for the comparison of precipitation extremes and floods: an example from the Czech territory. *Hydrology and Earth System Sciences*, *19*, 4641–4652. doi:10.5194/hess-19-4641-2015.
- Müller, M., M. Kašpar, & J. Matschullat (2009). Heavy rains and extreme rainfall-runoff events in Central Europe from 1951 to 2002. *Natural Hazards and Earth System Sciences*, *9*, 441–450. doi:10.5194/nhess-9-441-2009.
- Munich, Re. (1999). Naturkatastrophen in Deutschland: Schadenerfahrungen und Schadenpotentiale. *Publication of the Munich Re*, (Order Number 2798-E-d), www.munichre.com.
- Murray, R., & Simmonds, I. (1991). A numerical scheme for tracking cyclone centres from digital data. Part I: development and operation of the scheme. *Australian Meteorological Magazine*, *39*, 155–166.
- Muskulus M., & Jacob, D. (2005). Tracking cyclones in regional model data: the future of Mediterranean storms. *Advances in Geosciences*, *2*, 13–19. doi.org/10.5194/adgeo-2-13-2005
- Neu, U., et al (2013). IMILAST—A community effort to intercompare extratropical cyclone detection and tracking algorithms. *Bulletin of the American Meteorological Society*, *94*, 529–547.
- Nied, M., Schröter, K., Lüdtke, S., Nguyen, D., & Merz, B. (2017). What are the hydro-meteorological controls on flood characteristics? *Journal of Hydrology*, *545*, 310–326. doi.org/10.1016/j.jhydrol.2016.12.003.

-
- Nied, M., Pardowitz, T., Nissen, K., Ulbrich, U., Hundecha, Y., & Merz, B. (2014). On the relationship between hydro-meteorological patterns and flood types. *Journal of Hydrology*, 519(D), 3249-3262. doi:10.1016/j.jhydrol.2014.09.089.
- Nieto, R., Sprenger, M., Wernli, H., Trigo, R.M., & Gimeno, L. (2008). Identification and climatology of cut-off low near the tropopause. *Annals of the New York Academy of Science*, 1146, 256–290. doi:10.1196/annals.1446.016.
- Nissen, K. M., Leckebusch, G. C., Pinto, J. G., & Ulbrich, U. (2014). Mediterranean cyclones and windstorms in a changing climate. *Regional Environmental Change*, 14(5), 1873–1890. doi.org/10.1007/s10113-012-0400-8.
- Nissen, K.M., U. Ulbrich, & G. Leckebusch (2013). Vb cyclones and associated rainfall extremes over Central Europe under present day and climate change conditions. *Meteorologische Zeitschrift*, 22(6), 649–660. doi:10.1127/0941-2948/2013/0514.
- Nissen, K.M., Ulbrich, U., Leckebusch, G.C., & Becker, N. (2011). Extreme precipitation associated with Vb cyclones under climate change conditions. *EMS Annual Meeting Abstracts Vol. 8*, (ECAM Sept. 12-16, 2011). Berlin, Germany, abstract #EMS2011-341
- Nissen, K. M., Leckebusch, G. C., Pinto, J. G., Renggli, D., Ulbrich, S., & Ulbrich, U. (2010). Cyclones causing wind storms in the Mediterranean: characteristics, trends and links to large-scale patterns. *Natural Hazards and Earth System Science*, 10(7), 1379–1391. doi.org/10.5194/nhess-10-1379-2010.
- O’Gorman, P. A. (2015). Precipitation Extremes Under Climate Change. *Current Climate Change Reports*, 1(2), 49–59. doi.org/10.1007/s40641-015-0009-3.
- Osborn, T. J., & Jones, P. D. (2014). The CRUTEM4 land-surface air temperature data set: construction, previous versions and dissemination via Google Earth. *Earth System Science Data*, 6(1), 61–68. doi.org/10.5194/essd-6-61-2014.
- Panofsky, H.A., & Brier, G.W. (1968). *Some Applications of Statistics to Meteorology*. Pennsylvania State University Press, University Park, pp. 40-45.
- Parajka, J., et al. (2010). Seasonal characteristics of flood regimes across the Alpine–Carpathian range. *Journal of Hydrology*, 394, 78–89. doi:10.1016/j.jhydrol.2010.05.015.
- Pauling, A., Luterbacher, J., Casty, C., Wanner, H. (2006). 500 years of gridded high-resolution precipitation reconstructions over Europe and the connection to large-scale circulation. *Climate Dynamics*, 26, 387-405.
- Peel, M.C., McMahon, T.A., & Finlayson, B.L. (2004). Continental differences in the variability of annual runoff – update and reassessment. *Journal of Hydrology*, 295, 185–197. doi:10.1016/j.jhydrol.2004.03.004.
- Perret R., (1987). Une classification des situations météorologiques à l’usage de la prévision (A classification of meteorological situations for use in prediction). *Schweizerischen Meteorologischen Zentralanstalt, Vol. 46*. Zurich, Switzerland, 124 pp.
- Pfahl, S., & Sprenger, M. (2016). On the relationship between extratropical cyclone precipitation and intensity. *Geophysical Research Letter*, 43, 1752–1758. doi:10.1002/2016GL068018.
- Pfahl, S., Schwierz, C., Croci-Maspoli, M., Grams, C. M., & Wernli, H. (2015). Importance of latent heat release in ascending air streams for atmospheric blocking. *Nature Geoscience*, 8(8), 610–614. doi.org/10.1038/ngeo2487.
- Pfahl, S., & Wernli, H. (2012). Quantifying the Relevance of Cyclones for Precipitation Extremes. *Journal of Climate*, 25(19), 6770–6780. doi.org/10.1175/JCLI-D-11-00705.1.
- Philipp, A.J., et al. (2010). COST733CAT - a database of weather and circulation type classifications. *Physics and Chemistry of the Earth*, 35, 360-373. doi: 10.1016/j.pce.2009.12.010.
- Philipp, A., Della-Marta, P.M., Jacobeit, J., Fereday, D.R., Jones, P.D., Moberg, A., & Wanner, H. (2007). Long term variability of daily North Atlantic–European pressure patterns since 1850 classified by simulated annealing clustering. *Journal of Climate*, 20, 4065-4095.
- Pichler, H., & R. Steinacker (1987). On the synoptics and dynamics of orographically induced cyclones in the Mediterranean. *Meteorology and Atmospheric Physics*, 36(1-4), 108–117. doi:10.1007/BF01045144.

-
- Pichler, H., Steinacker, R., & Lanzinger, A. (1990). Cyclogenesis induced by the Alps. *Meteorology and Atmospheric Physics*, 43(1–4), 21–29. doi.org/10.1007/BF01028106.
- Pinto, J. G., Ulbrich, S., Economou, T., Stephenson, D. B., Karremann, M. K., & Shaffrey, L. C. (2016). Robustness of serial clustering of extratropical cyclones to the choice of tracking method. *Tellus A: Dynamic Meteorology and Oceanography*, 68(1), 32204. doi.org/10.3402/tellusa.v68.32204.
- Pinto, J. G., Gómará, I., Masato, G., Dacre, H. F., Woollings, T., & Caballero, R. (2014). Large-scale dynamics associated with clustering of extratropical cyclones affecting Western Europe. *Journal of Geophysical Research: Atmospheres*, 119(24), 13,704–13,719. doi.org/10.1002/2014JD022305.
- Pinto, J. G., Bellenbaum, N., Karremann, M. K., & Della-Marta, P. M. (2013). Serial clustering of extratropical cyclones over the North Atlantic and Europe under recent and future climate conditions. *Journal of Geophysical Research: Atmospheres*, 118(22), 12,476–12,485. doi.org/10.1002/2013JD020564.
- Pinto, J. G., Spangehl, T., Ulbrich, U., & Speth, P. (2005). Sensitivities of a cyclone detection and tracking algorithm: individual tracks and climatology. *Meteorologische Zeitschrift*, 14(6), 823–838. doi.org/10.1127/0941-2948/2005/0068.
- Raible, C.C., Della-Marta, P., Schwierz, C., Wernli, H., & Blender, R. (2008). Northern Hemisphere extratropical cyclones: A comparison of detection and tracking methods and different reanalyses. *Monthly Weather Review*, 136(3), 880–897. doi:10.1175/2007MWR2143.1.
- Raible, C. C. (2007). On the relation between extremes of midlatitude cyclones and the atmospheric circulation using ERA40. *Geophysical Research Letters*, 34(7). doi.org/10.1029/2006GL029084.
- Rauthe, M., H. Steiner, U. Riediger, A. Mazurkiewicz, & A. Gratzki (2013). A Central European precipitation climatology - Part I: Generation and validation of a high-resolution gridded daily data set (HYRAS), *Meteorologische Zeitschrift*, 22, 235–256. doi:10.1127/0941-2948/2013/0436.
- Reiter, E. R., & Whitney, L. F. (1969). Interaction between subtropical and polar-front jet stream. *Monthly Weather Review*, 97(6), 432–438. doi.org/10.1175/1520-0493(1969)097<0432:IBSAPJ>2.3.CO;2.
- Renard, B., & U. Lall (2014). Regional frequency analysis conditioned on large-scale atmospheric or oceanic fields, *Water Resources Research*, 50(12), 9536–9554. doi:10.1002/2014WR016277.
- Řezáčová, D., Kašpar, M., Müller, M., Zbyněk, S., Kakos, V., Hanslian, D., & Pešice, P. (2005). A comparison of the flood precipitation episode in August 2002 with historic extreme precipitation events on the Czech territory. *Atmospheric Research*, 77(1–4), 354–366. doi: 10.1016/j.atmosres.2004.10.008.
- Richman, M.B. (1986). Rotation of principal components. *International Journal of Climatology*, 6, 293–335. doi:10.1002/joc.3370060305.
- Rimbu, N., Czymzik, M., Ionita, M., Lohmann, G., Brauer, A. (2016). Atmospheric circulation patterns associated with the variability of River Ammer floods: evidence from observed and proxy data. *Climate of the Past*, 12, 377–385. doi: 10.5194/cp-12-377-2016.
- Rimbu, N., Treut, H.L., Janicot, S., Boroneant, C., & Laurent, C. (2001). Decadal precipitation variability over Europe and its relation with surface atmospheric circulation and sea surface temperature. *Quarterly Journal of the Royal Meteorological Society*, 127, 315–329. doi:10.1002/qj.49712757204.
- Roberts, J.F., et al. (2014). The XWS open access catalog of extreme European windstorms from 1979 to 2012, *Natural Hazards and Earth System Sciences*, 14, 2487–2501. doi:10.5194/nhess-14-2487-2014.
- Röckner, E., et al. (2003). *The Atmospheric General Circulation Model ECHAM5. Part 1, Model Description*. Report 349. Max-Planck-Inst. For Meteorology: Hamburg, 127, [Available from Max Planck Institute for Meteorology, Bundesstr. 53, 20146, Hamburg, Germany].
- Rubel, F., & Kottke, M. (2010). Observed and projected climate shifts 1901–2100 depicted by world maps of the Köppen-Geiger climate classification. *Meteorologische Zeitschrift*, 19, 135–141. doi:10.1127/0941-2948/2010/0430.
- Rudari R., Entekhabi D., & Roth, G. (2004). Terrain and multiple-scale interactions as factors in generating extreme precipitation events. *Journal of Hydrometeorology*, 5, 390–404.

-
- Rudolf, B., & Rapp, J. (2003). *Das Jahrhunderthochwasser der Elbe: Synoptische Wetterentwicklung und klimatologische Aspekte*. Klimastatusbericht 2002. Selbstverlag des Deutschen Wetterdienstes, <http://www.ksb.dwd.de>, Offenbach, 172-187.
- Ruiz-Leo, A. M., Hernandez, E., Queralt, S., & G. Maqueda (2013). Convective and stratiform precipitation trends in the Spanish Mediterranean coast. *Atmospheric Research*, *119*, 46-55. doi:10.1016/j.atmosres.2011.07.019.
- Rulfová Z., & Kyselý, J. (2013). Disaggregating convective and stratiform precipitation from station weather data, *Atmospheric Research*, *134*, 100-115. doi:10.1016/j.atmosres.2013.07.015.
- Scherrer, S.C., Begert, M., Croci-Maspoli, M., & Appenzeller, C. (2016). Long series of Swiss seasonal precipitation: regionalization, trends and influence of large-scale flow. *International Journal of Climatology*, *36*, 3673–3689. doi:10.1002/joc.4584.
- Schiemann, R., & Frei, C. (2010). How to quantify the resolution of surface climate by circulation types: An example for Alpine precipitation. *Physics and Chemistry of the Earth*, *35*, 403-410. doi:10.1016/j.pce.2009.09.005.
- Schmidli, J., Schmutz, C., Frei, C., Wanner, H., & Schär, C. (2002). Mesoscale precipitation variability in the region of the European Alps during the 20th century. *International Journal of Climatology*, *22*, 1049–1074. doi:10.1002/joc.769.
- Schneidereit, A., Blender, R., & Fraedrich, K. (2010). A radius-depth model for midlatitude cyclones in reanalysis data and simulations. *Quarterly Journal of the Royal Meteorological Society* *136*(646), 50-60. doi:10.1002/qj.523.
- Schröter, K., Kunz, M., Elmer, F., Mühr, B., & Merz, B. (2015). What made the June 2013 flood in Germany an exceptional event? A hydro-meteorological evaluation. *Hydrology and Earth Systems Sciences*, *19*, 309-327. doi:10.5194/hess-19-309-2015.
- Schröter, K., Kunz, M., Elmer, F., Mühr, B., & Merz, B. (2014). What made the June 2013 flood in Germany an exceptional event? A hydro-meteorological evaluation. *Hydrology and Earth System Science Discussion*, *11*, 8125–8166. doi:10.5194/hess-19-309-2015.
- Schüepp, M., (1979). Witterungsklimatologie – Klimatologie der Schweiz III (Weather Climatology – Climatology of Switzerland III). *Beihefte zu den Annalen der Schweizerischen Meteorologischen Anstalt 1978*. 93 pp (in German).
- Seibert, P., Frank, A., & Formayer, H. (2007). Synoptic and regional patterns of heavy precipitation in Austria. *Theoretical and Applied Climatology*, *87*(139). doi:10.1007/s00704-006-0198-8.
- Seneviratne, S.I., et al. (2012). *Changes in climate extremes and their impacts on the natural physical environment*. In: *Managing the Risks of Extreme Events and Disasters to Advance Climate Change Adaptation* [Field, C.B., V. Barros, T.F. Stocker, D. Qin, D.J. Dokken, K.L. Ebi, M.D. Mastrandrea, K.J. Mach, G.-K. Plattner, S.K. Allen, M. Tignor, & P.M. Midgley (Eds.)]. A Special Report of Working Groups I and II of the Intergovernmental Panel on Climate Change. Cambridge University Press, Cambridge, United Kingdom and New York, NY, USA, pp. 109-230.
- Simmonds, I., Murray, R., & Leighton, R. (1999). A refinement cyclone tracking methods with data from FROST. *Australian Meteorological Magazine, Special edition as part of the Antarctic First Regional Observing Study of the Troposphere (FROST) project*, 35-49.
- Sinclair, M.R. (1997). Objective identification of cyclones and their circulation intensity, and climatology. *Weather Forecasting*, *12*, 595–612. doi.org/10.1175/1520-0434(1997)012<0595:OIOCAT>2.0.CO;2.
- Sinclair, M.R. (1994). An objective cyclone climatology for the southern Hemisphere. *Monthly Weather Review*, *122*, 2239–2256. doi.org/10.1175/1520-0493(1994)122<2239:AOCCT>2.0.CO;2.
- Skublics, D., Blöschl, G., & Rutschmann, P. (2016). Effect of river training on flood retention of the Bavarian Danube. *Journal of Hydrology and Hydromechanics*, *64*(4), 349–356. doi:10.1515/johh-2016-0035.
- Smith, R.B. (1979). The influence of mountains on the atmosphere, *Advances in Geophysics*, *21*, 87–230. doi:10.1016/S0065-2687(08)60262-9.

-
- Stadtherr, L., Coumou, D., Petoukhov, V., Petri, S., & Rahmstorf, S. (2016). Record Balkan floods of 2014 linked to planetary wave resonance. *Science Advances*, 2(4). doi:10.1126/sciadv.1501428.
- Stahl, N., & Hofstätter, M. (2018). Vb-Zugbahnen und deren Auftreten als Serie mit Bezug zu den resultierenden Hochwassern in Bayern und Auswirkungen auf Rückhalteräume im Isareinzugsgebiet. *Hydrologie und Wasserbewirtschaftung / BfG – Jahrgang: 62.2018,2 - ISSN 1439-1783*. doi.org/10.5675/hywa_2018,2_2
- Steinacker R., (2002): Synoptische Beschreibung der Hochwasserkatastrophe vom August 2002. Institut für Meteorologie und Geophysik, Universität Wien. Online from Oct 2003: http://www.univie.ac.at/IMG-Wien/vera/Hochwasser_2002.htm
- Steinschneider, S., & U. Lall (2015). A hierarchical Bayesian regional model for nonstationary precipitation extremes in Northern California conditioned on tropical moisture exports. *Water Resources Research*, 51(3), 1472-1492. doi:10.1002/2014WR016664.
- Stephens, M. A. (1974). EDF Statistics for Goodness of Fit and Some Comparisons. *Journal of the American Statistical Association*, 69(347), 730–737. doi.org/10.1080/01621459.1974.10480196.
- Stohl A., & Paul, J. (2004). A Lagrangian Analysis of the Atmospheric Branch of the Global Water Cycle. Part I: Method Description, Validation, and Demonstration for the August 2002 Flooding in Central Europe. *Journal of Hydrometeorology*, 5,656-678.
- Stucki, P., Rickli, R., Brönnimann, S., Martius, O., Wanner, H., Grebner, D., & Luterbacher, J. (2012). Weather patterns and hydro-climatological precursors of extreme floods in Switzerland since 1868. *Meteorologische Zeitschrift*, 21(6), 531-550(20). doi:10.1127/0941-2948/2012/36.
- Themeßl, M.J., Gobiet, A., & Leuprecht, A. (2011). Empirical-statistical downscaling and error correction of daily precipitation from regional climate models. *International Journal of Climatology*, 31, 1530–1544. doi:10.1002/joc.2168.
- Tilinina, N., Gulev, S.K., Rudeva, I., & Koltermann, P. (2013). Comparing cyclone life cycle characteristics and their interannual variability in different reanalyses. *Journal of Climate*, 26, 6419–6438. doi:10.1175/JCLI-D-12-00777.1.
- Trenberth, K.E., & Stepaniak, D.P. (2004). The flow of energy through the Earth's climate system. *Quarterly Journal of the Royal Meteorological Society*, 130, 2677–2701. doi:10.1256/qj.04.83.
- Trenberth, K. E., Dai, A., Rasmussen, R. M., & Parsons, D. B. (2003). The Changing Character of Precipitation. *Bulletin of the American Meteorological Society*, 84(9), 1205–1218. doi.org/10.1175/BAMS-84-9-1205.
- Trigo, I.F., (2006). Climatology and interannual variability of stormtracks in the Euro-Atlantic sector: a comparison between ERA-40 and NCEP/NCAR reanalyses. *Climate Dynamics*, 26, 127-143.
- Trigo, I. F., Bigg, G. R., & Davies, T. D. (2002). Climatology of Cyclogenesis Mechanisms in the Mediterranean. *Monthly Weather Review*, 130(3), 549–569. doi.org/10.1175/1520-0493(2002)130<0549:COCMIT>2.0.CO;2.
- Trigo, I. F., Davies, T. D., & Bigg, G. R. (1999). Objective Climatology of Cyclones in the Mediterranean Region. *Journal of Climate*, 12(6), 1685–1696. doi.org/10.1175/1520-0442(1999)012<1685:OCOCIT>2.0.CO;2
- Tristan, S., et al. (2015). The Observed State of the Energy Budget in the Early Twenty-First Century. *Journal of Climate*, 28, 8319–8346. doi.org/10.1175/JCLI-D-14-00556.1.
- Ulbrich, U., Leckebusch, G.C., & Pinto, J.G. (2009). Extra-tropical cyclones in the present and future climate: a review. *Theoretical and Applied Climatology*, 96(1-2), 117-131.
- Ulbrich, U., Brücher, T., Fink, A. H., Leckebusch, G. C., Krüger, A., & Pinto, J. G. (2003a). The central European floods of August 2002: Part 1 – Rainfall periods and flood development. *Weather*, 58(10), 371–377. doi.org/10.1256/wea.61.03A
- Ulbrich, U., Brücher, T., Fink, A. H., Leckebusch, G. C., Krüger, A., & Pinto, J. G. (2003b). The Central European floods of August 2002: Part II: Synoptic causes and considerations with respect to climatic change. *Weather*, 58(11), 434-441. doi.org/10.1256/wea.61.03B
- Umlauf F., (1891). *Das Luftmeer: Die Grundzüge der Meteorologie und Klimatologie nach den neuesten Forschungen*. A.Hartleben's Verlag, Wien 1891. 488 pp.

-
- Uppala, S.M., et al. (2005). The ERA-40 re-analysis. *Quarterly Journal of the Royal Meteorological Society*, 131, 2961-3012. doi.org/10.1256/qj.04.176.
- Vitolo, R., Stephenson, D. B., Cook, I. M., & Mitchell-Wallace, K. (2009). Serial clustering of intense European storms. *Meteorologische Zeitschrift*, 18(4), 411–424. doi.org/10.1127/0941-2948/2009/0393.
- Volosciuk, C., Maraun, D., Semenov, V.A., Tilinina, N., Gulev, S.K., & Latif, M. (2016). Rising Mediterranean Sea Surface Temperatures Amplify Extreme Summer Precipitation in Central Europe. *Scientific Reports*, 6, 32450. doi:10.1038/srep32450.
- Wallace, J. M., & Gutzler, D. S. (1981). Teleconnections in the Geopotential Height Field during the Northern Hemisphere Winter. *Monthly Weather Review*, 109(4), 784–812. doi.org/10.1175/1520-0493(1981)109<0784:TITGHF>2.0.CO;2.
- Walz, M. A., Befort, D. J., Kirchner-Bossi, N. O., Ulbrich, U., & Leckebusch, G. C. (2018). Modelling serial clustering and inter-annual variability of European winter windstorms based on large-scale drivers. *International Journal of Climatology*, 2018(38), doi.org/10.1002/joc.5481.
- Werner, P.C., Gerstengarbe, F.W. (2010). Katalog der Großwetterlagen Europas (1881-2009) nach Paul Hess und Helmut Brezowsky - 7. verbesserte und ergänzte Auflage. *PIK Report*, 199, 146 pp.
- Wernli, H., & Schwerz, C. (2006). Surface cyclones in the ERA-40 dataset (1958–2001): Part I: novel identification method and global climatology, *Journal of Atmospheric Science*, 63(10): 2486–2507. doi.org/10.1175/JAS3766.1.
- Westra, S., et al. (2014). Future changes to the intensity and frequency of short-duration extreme rainfall. *Reviews of Geophysics*, 52, 522-555. doi:10.1002/2014RG000464.
- Wettstein, J. J., & Wallace, J. M. (2010). Observed Patterns of Month-to-Month Storm-Track Variability and Their Relationship to the Background Flow (e.g. zonal wind). *Journal of the Atmospheric Sciences*, 67(5), 1420-1437. doi.org/10.1175/2009JAS3194.1.
- Wilks, D.S. (2006). *Statistical Methods in the Atmospheric Sciences*. (2nd ed.). Burlington, MA: Academic Press. ISBN 0-12-751966-1. xvii + 627 pp.
- Woollings, T., et al. (2018). Daily to Decadal Modulation of Jet Variability. *Journal of Climate*, 31(4), 1297–1314. doi.org/10.1175/JCLI-D-17-0286.1.
- Woollings, T., Franzke, C., Hodson, D. L. R., Dong, B., Barnes, E. A., Raible, C. C., & Pinto, J. G. (2015). Contrasting interannual and multidecadal NAO variability. *Climate Dynamics*, 45(1–2), 539–556. doi.org/10.1007/s00382-014-2237-y.
- Woollings, T., & Blackburn, M. (2012). The North Atlantic Jet Stream under Climate Change and Its Relation to the NAO and EA Patterns. *Journal of Climate*, 25(3), 886–902. doi.org/10.1175/JCLI-D-11-00087.1.
- Woollings, T., Hannachi, A., & Hoskins, B. (2010). Variability of the North Atlantic eddy-driven jet stream. *Quarterly Journal of the Royal Meteorological Society*, 136(649), 856–868. doi.org/10.1002/qj.625.
- Woollings, T., Hoskins, B., Blackburn, M., & Berrisford, P. (2008). A New Rossby Wave–Breaking Interpretation of the North Atlantic Oscillation. *Journal of the Atmospheric Sciences*, 65(2), 609–626. doi.org/10.1175/2007JAS2347.1.
- Yarnal, B. (1984). A procedure for the classification of synoptic weather maps from gridded atmospheric pressure surface data. *Computers and Geosciences*, 10, 397-410.
- Zahn, M., & von Storch, H. (2008). Tracking Polar Lows in CLM. *Meteorologische Zeitschrift*, 17(4), 445-453. doi:10.1127/0941-2948/2008/0317.
- Zängl, G. (2004). Numerical simulations of the 12–13 August 2002 flooding events in eastern Germany. *Quarterly Journal of the Royal Meteorological Society*, 130, 1921-1940.
- Zolina, O., Simmer, C., Belyaev, K., Gulev, S.K., & Koltermann, P. (2013). Changes in the duration of European wet and dry spells during the last 60 years. *Journal of Climate*, 26(6). doi:10.1175/JCLI-D-11-00498.1,2022-2047.

Zolina, O., Simmer, C., Kapala, A., Shabanov, P., Becker, P., Maechel, H., Gulev, S.K., & Groisman, P. (2014). Precipitation Variability and Extremes in Central Europe: New View from STAMMEX Results. *Bulletin of the American Meteorological Society*, *95*, 995–1002.

Zolina, O. (2014). Multidecadal trends in the duration of wet spells and associated intensity of precipitation as revealed by very dense observational network. *Environmental Research Letters*, *9*, 025003. doi:10.1088/1748-9326/9/2/025003.

Zveryaev, I.I., & Allan, R.P. (2010). Summertime precipitation variability over Europe and its links to atmospheric dynamics and evaporation. *Journal of Geophysical Research*, *115*, D12102. doi:10.1029/2008JD011213.

Zveryaev, I.I. (2006). Seasonally varying modes in long-term variability of European precipitation during the 20th century. *Journal of Geophysical Research*, *111*, D21116. doi:10.1029/2005JD006821.

Zveryaev, I.I. (2004). Seasonality in precipitation variability over Europe. *Journal of Geophysical Research*, *109*, D05103. doi:10.1029/2003JD003668.